THE ROLE OF MUSCLE DAMAGE ON JOINT TISSUE

by

Logan Nicholas Moore

DISSERTATION

Submitted in partial fulfillment of the requirements

for the degree of Doctor of Philosophy at

The University of Texas at Arlington, December 2022

Arlington, Texas

Supervising Committee:

Marco Brotto, Supervising Professor
Mark Ricard
Rhonda Prisby
Venu Varanasi

ABSTRACT

ROLE OF MUSCLE DAMAGE ON JOINT TISSUE

Logan Moore, PhD

The University of Texas at Arlington

2022

Supervising Professor: Marco Brotto

The musculoskeletal system is a highly diverse network of tissue that operates in conjunction to one other, both mechanically and biochemically. In states of disorder such as musculoskeletal disorders, this cross-communication between tissues is pivotal in the progression of disease state in other tissues, or the prevention and healing of the effected tissue. Musculoskeletal disorders (MSkD) are a broad term encompassing disorders to bones, joints, muscles and connective tissues. These disorders include Osteoarthritis, Osteopenia, Sarcopenia, Tendonitis, Myopathies, and muscle weakness.

Osteoarthritis (OA) is the most common joint disorder, characterized as damage to the articulating cartilage and alterations in other joint tissues such as osteophytes and synovitis. Study 1 (Chapter 2) identifies the current mouse models used in OA studies and explores the advantages and disadvantages of each model. These models include inducing OA by means of genetic alteration, exercise, chemical injection, tibial loading, and the most common surgical induction. Each model has their advantages and disadvantages, and due to the complexities of OA no singular model is best at providing the complete pathophysiology of the disease. The current mouse models explain OA through injury or alteration directly to the joint and lack the

causality of OA through indirect joint injury. Inducing acute muscle damage could provide a physiological and mechanistic causation to indirect joint injury in which OA could develop, study 3 (Chapter 4)

Biomarker analysis is essential in understanding the mechanisms in disorder regulation and provides molecular targets for intervention, therapies, and treatments. A technique for biomarker analysis is RNA sequencing (RNAseq), which provides complete transcriptome analysis in which details the differently expressed genes (DEGs). Synovium is soft tissue that lines the joint cavity, providing nutrients necessary for the joint's health and maintenance. Study 2 (Chapter 3) systematically explores the DEGs in the synovial tissue in subjects that have OA. There were 8 DEGs, MMP13, MMP1, MMP2, APOD, IL6, TNFAIP6, FCER1G, and IGF1 found to overlapped in 4 out of 5 included studies. These genes are related to the inflammatory pathway and regulation of the extracellular matrix. The MMP family, particularly MMP13 was identified by three of the studies, indicating its key role in OA. IL6, a key contributor in the inflammation pathway, was also identified in 3 studies. Further investigation with more clinical gene profiling in synovial tissue of OA subjects is required to reveal the causation and progression and aid in the development of new treatments.

Finally Study 3 (Chapter 4), details the physical, morphological, and biochemical alterations of joint tissues following acute muscle damage. It has been characterized as OA being accompanied by muscle weakness resulting from a lack of physical activity and atrophy. However, muscle weakness causes joint instability and an increased load on the joint. This cause joint alterations in the articular cartilage and in the subchondral bone. It is shown that there changes in peak heights in the Raman spectrum of the articulating cartilage that is indicative of alterations in the collagen composition. The μCT of the subchondral bone revealed increase in

bon volume fraction. In response to muscle damage an inflammatory immune response occurs causing a release of pro-inflammatory molecules, such as cytokines, reactive oxygen species (ROS), and lipid signaling mediators (LMs). The LMs play a vital role in the muscle's ability to regenerate from injury, as well as have downstream effects on other tissues in the musculoskeletal system.

ACKNOWLEDGEMENTS

I would like to express my upmost gratitude to my supervising professor, Dr. Marco Brotto for the continuous support, the endless creativity, passion, and immense knowledge. Without his mentorship none of this work would be possible. I am also grateful for my dissertation committee, Dr. Mark Ricard, Dr. Venu Varanasi, and Dr. Rhonda Prisby. Their guidance and patience allowed me to explore and find my passion.

I would like to express my deepest appreciation to all the members of The Brotto Laboratory both current and past: Dr. Kamal Awad, Dr. Leticia Brotto, Dr. Jian Huang, Dr. Chenglin Mo, Dr. Zhiying Wang, Sarah Nelson, Mathew Fielder, Marlen Hernandez, Lauren Gomez, and Dr. Donnalee Pollack. The Brotto Laboratory has fostered my growth and training, inspired my creativity, and directed me to my goals.

This endeavor would not have been possible without the support from the University of Texas at Arlington College of Nursing and Health Innovations, The Center of Research and Scholarship, and the National Institutes of Health to help fund this work. I would like to thank the Department of Kinesiology, especially Dr. Mathew Brothers, Dr. Paul Fadel, and Dr. David Keller, for acceptance into the program, the opportunity to hold positions of Graduate Teaching Assistant and Graduate Research Assistant.

I would like to recognize the members of the Bone Muscle Research Center (BMRC) at UTA especially Dr. Zui Pan, Dr. Jingsong Zhou, The Pan Laboratory, and the Zhou Laboratory for their collaboration and extension of resources, and the BMRC Core Facility. I would also like to recognize all my fellow students, who have pushed me and supported me through all our highs and lows.

Finally, I would like to acknowledge my family. My wife, Allie, my parents, Greg and Michelle Moore, my in-laws, John, and Annette Cawyer, and all my siblings, nieces, and nephews; Megan and Payton Northrup, Macy and Bailey Pickering, Jeff, Jamie, Merritt and Sloane Cawyer, and Jay, Tannah, Reece, and Reagan Cawyer. They have all encouraged me to dream big and to follow my passion. Their constant support and belief in me are evident throughout my journey.

DEDICATION

This work is dedicated to my wife, Allie Moore. Allie challenges me to be my best self every day. She is the reason I embarked on this journey and the reason I have been able to finish. Her unconditional love, patience and support was my source of inspiration through the challenges of graduate school and life.

TABLE OF CONTENTS

LIST OF FIGURES

LIST OF TABLES

CHAPTER 1

Introduction

Osteoarthritis

Musculoskeletal disorders (MSkD) are a wide range of debilitating disorders that affect bone, muscle, and or tendon (National Academies of Sciences, 2020). These disorders include Osteoarthritis, Osteopenia, Sarcopenia, Tendonitis, Myopathies, and muscle weakness. These disorders often manifest in multiple musculoskeletal tissues, and through the progression the MSkD can lead to comorbidities and the development of other MSkDs.

Osteoarthritis (OA) is manifested by damage to the articulating cartilage and alterations in other joint tissues. These alterations can be shown as osteophyte formation and synovitis. OA is the most common of joint disorders, defined as chronic arthropathy (Glyn-Jones et al., 2015; Kontzias, 2020; National Academies of Sciences, 2020). This is a progressive disease shown in symptoms of pain, stiffness, and swelling of the joint (Kontzias, 2020). These clinical manifestations place OA as the leading form of workplace disability in the US (Glyn-Jones et al., 2015; National Academies of Sciences, 2020). OA places a major financial burden on the patient and healthcare system. (Glyn-Jones et al., 2015). The development of OA is multifactorial and not limited to a certain subgroup. Risk factors contributing to OA development include age, obesity, history of injury and genetic disposition (Glyn-Jones et al., 2015). The damage to the joint is irreversible, as there is currently no cure for OA. Treatment protocols are limited to management of the disease's progression. Common treatments are rehabilitation or exercise, lifestyle changes, pain medication, and in most severe cases surgery (Glyn-Jones et al., 2015; Kontzias, 2020).

Small animal models have provided invaluable information on the manifestation and development of OA. In a systematic review of the literature on the current OA mouse models

(Chapter 2), we found a wide range of mouse models used. These models include inducing OA by means of genetic alteration, exercise, injection (MIA, CIOA (Collagenase induced OA), or Papain), tibial loading, and the most common surgical induction. However, each of these models demonstrate OA through primary damage to the joint, as the manifestation of OA is multifactorial the examination of the joint tissue in different states of MSkD is pivotal in understanding the underlining mechanism of disease progression in OA.

Musculoskeletal cross-communication:

The Musculoskeletal system is a diverse network of tissues working in synchrony to provide stability and locomotion (Brotto & Bonewald, 2015; Villa-Forte, 2019). This network of tissues not only includes the major contributors: bone and muscle, but also tendons, ligaments, cartilage, joints, and the connective tissue. It is well known that mechanically these tissues operate in conjunction to provide movement, however these tissues also work on a biochemical and cellular level. This is an emerging topic in research known as the "Bone-Muscle Crosstalk". Bone and muscle have both been established to have secretory and endocrine functions (Allen et al., 2008; Brotto & Bonewald, 2015; Brotto & Johnson, 2014; Dallas et al., 2013; Isaacson & Brotto, 2014; Kurek et al., 1997; Pedersen, 2013).

Skeletal muscle is the largest organ in the body and plays a vital role in functionality. Mechanically, it maintains posture and stability, locomotion, and aids in breathing through contraction of the muscle fibers (Pedersen, 2013). Furthermore, skeletal muscle serves a role in its endocrine capabilities by secreting cytokines, peptides, and lipids deemed as "myokines."(Brotto & Bonewald, 2015; Brotto & Johnson, 2014; Huang et al., 2017; Kojouharov et al., 2021; Pedersen, 2013; Pedersen & Febbraio, 2012) The secretome produced

by skeletal muscle provides communication with other tissues in the body such as bone, adipose, liver, and brain. A major emphasis has been placed on understanding the regulatory effects these myokines have on tissues. These myokines have been shown to change through exercise, injury, and disease (Brotto & Bonewald, 2015; Brotto & Johnson, 2014; Kojouharov et al., 2021; Pedersen & Febbraio, 2012). Myokines also contribute to the regulation of bone reabsorption and bone remodeling, pro-inflammatory effects, conversion of adipose tissue, protection of cell death in osteocytes, and many more yet to be discovered (Brotto & Bonewald, 2015; Pedersen, 2013; Pedersen & Febbraio, 2012). Through understanding the production of myokines and their effects on other tissues, we will be able to devise new treatments and therapies for patients that suffer from MSD and improve the daily functionality of all.

Muscle Weakness and Damage Effecting the Joint

Previously it has been thought that muscle weakness is a side effect of joint degeneration. That the pain caused by the increased load on the joint encourages lower levels of activity, which therefore causes atrophy due to disuse (Brandt, 2006). However, the question of if muscle weakness or damage could be a primary causation to joint damage or if it is a secondary contributing factor has yet to be fully determined.

Mechanically periarticular muscle weakness causes instability to the joint and causes increased joint loading (Brandt, 1997; Rehan Youssef et al., 2009; Slemenda, 1997). In human subjects that already have diagnosed knee OA, they have been shown to have significant muscle weakness in their hip musculature (Brandt, 1997, 2006; Hinman et al., 2010; Slemenda, 1997). However, since these patients already had OA at the time of the study it could not be determined if the muscle weakness occurred before or after joint damage. In 1-year-old New Zealand white

rabbits, it was shown that induced muscle weakness by intramuscular injection of botulinum toxin type-A (BTX-A) induced significant weakness in the quadriceps and showed disruption in the articulating cartilage (Egloff et al., 2014; Rehan Youssef et al., 2009). This shows evidence that muscle weakness could be a primary causation to joint damage and the onset of OA, but before a definitive causality linkage can be made more research into the effect muscle weakness and damage has on adjacent tissues needs to be done.

Lipids are small, hydrophobic molecules with important roles in nutrition, health, and disease. Bioactive lipids act as important intra- and inter-cellular signaling molecules, usually referred to as lipid signaling mediators (LMs). LMs can exert their effects as ligands to G-protein-coupled receptors (GPCRs) and transcription factors, as allosteric modulators, and by direct covalent modification of proteins where heterogeneity of acyl chains within general classes of lipids can result in distinct cellular signaling properties, thus play a significant role on the regulation of pathophysiological states such as inflammation, metabolic syndrome, and cancer (Brotto & Johnson, 2014). Currently much work is needed to identify the lipid molecules and the pathways responsible for their production and modes of action during muscle damage and their effects in adjacent tissue.

Barium Chloride Injury Model

Barium Chloride ($BaCl_2$) is a common and well-known chemical used to induce muscle damage (Jung et al., 2019; Morton et al., 2019). $BaCl_2$ is a potassium (K^+) ion channel inhibitor (Morton et al., 2019). This results in the depolarization of the sarcolemma, inducing transient calcium (Ca^{2+}) overload. This disrupts the motor intervention of the myofiber and causes proteolysis and membrane rupture (Morton et al., 2019). The benefit of using $BaCl_2$ over other

chemical reagents to induce muscle damage, such as notexin or freeze injury is that $BaCl_2$ does not disrupt the function of satellite cells (Hardy et al., 2016; Jung et al., 2019; Morton et al., 2019). As the satellite cells are not disrupted, they can be activated and proliferated into new muscle fibers. Jung et al. demonstrates the regenerative compacity of skeletal muscle in response to $BaCl_2$ (Jung et al., 2019). It was shown that at day 7 there are small myofibers and the immune response has been cleared. These results are congruent and follow the process of muscle regeneration in the established model with the model of muscle regeneration set forth by Kojouharov et al (Kojouharov et al., 2021). After muscle injury through $BaCl_2$, the ruptured myofibers will initiate an inflammatory immune response to begin the destructive phase of muscle regeneration. This phase is controlled through the release of pro-inflammatory molecules, such as cytokines, reactive oxygen species (ROS), and lipid signaling mediators (LMs, i.e. leukotrienes and prostaglandins [PGs]) (Kojouharov et al., 2021). We hypothesize that through the circulation of the pro-inflammatory molecules it will affect the adjacent joint tissue, causing inflammation which leads to synovitis and potential damage to the articulating cartilage.

There are multiple reasons in which the Tibialis Anterior (TA) muscle has been chosen for this proposed study. The TA originates at multiple sites: the lateral tibial condyle, the lateral surface of the tibia, and the anterior surface of the interosseous membrane, and inserts on the medial cuneiform (Moore et al., 2014). The origin and insertion points create a periarticular connection between the knee and the ankle joint. It is easily identifiable and accessible for intramuscular injection, and congruent with previous methodology using $BaCl_2$ (Hardy et al., 2016; Jung et al., 2019; Morton et al., 2019). The TA functions to produce dorsiflexion of the foot and stability to the ankle and lower limb (Moore et al., 2014). The muscle damage caused by

the $BaCl_2$ injection will cause mechanical instability of the lower limb and incite a biochemical response of the musculoskeletal system.

References

Allen, D. L., Cleary, A. S., Speaker, K. J., Lindsay, S. F., Uyenishi, J., Reed, J. M., Madden, M. C., & Mehan, R. S. (2008). Myostatin, activin receptor IIb, and follistatin-like-3 gene expression are altered in adipose tissue and skeletal muscle of obese mice. American Journal of Physiology-Endocrinology and Metabolism, 294(5), E918–E927. https://doi.org/10.1152/ajpendo.00798.2007

Brandt, K. D. (1997). Putting Some Muscle into Osteoarthritis. Annals of Internal Medicine, 127(2), 155–156. https://doi.org/https://doi.org/10.7326/0003-4819-127-2-199707150-00011

Brandt, K. D. (2006). Yet more evidence that osteoarthritis is not a cartilage disease. Annals of the Rheumatic Diseases, 65(10), 1261–1264. https://doi.org/10.1136/ard.2006.058347

Brotto, M., & Bonewald, L. (2015). Bone and muscle: Interactions beyond mechanical. Bone, 80. https://doi.org/10.1016/j.bone.2015.02.010

Brotto, M., & Johnson, M. L. (2014). Endocrine Crosstalk Between Muscle and Bone. Current Osteoporosis Reports, 12(2). https://doi.org/10.1007/s11914-014-0209-0

Dallas, S. L., Prideaux, M., & Bonewald, L. F. (2013). The Osteocyte: An Endocrine Cell … and More. Endocrine Reviews, 34(5), 658–690. https://doi.org/10.1210/er.2012-1026

Egloff, C., Sawatsky, A., Leonard, T., Hart, D. A., Valderrabano, V., & Herzog, W. (2014). Effect of muscle weakness and joint inflammation on the onset and progression of osteoarthritis in the rabbit knee. Osteoarthritis and Cartilage, 22(11), 1886–1893. https://doi.org/10.1016/j.joca.2014.07.026

Glyn-Jones, S., Palmer, A. J. R., Agricola, R., Price, A. J., Vincent, T. L., Weinans, H., & Carr, A. J. (2015). Osteoarthritis. The Lancet, 386(9991). https://doi.org/10.1016/S0140-6736(14)60802-3

National Academies of Sciences, Engineering, and Medicine; Health and Medicine Division; Board on Health Care Services; Committee on Identifying Disabling Medical Conditions Likely to Improve with Treatment. Selected Health Conditions and Likelihood of Improvement with Treatment. Washington (DC): National Academies Press (US); 2020 Apr 21. 5, Musculoskeletal Disorders. Available from: https://www.ncbi.nlm.nih.gov/books/NBK559512/

Hardy, D., Besnard, A., Latil, M., Jouvion, G., Briand, D., Thépenier, C., Pascal, Q., Guguin, A., Gayraud-Morel, B., Cavaillon, J.-M., Tajbakhsh, S., Rocheteau, P., & Chrétien, F. (2016). Comparative Study of Injury Models for Studying Muscle Regeneration in Mice. PLOS ONE, 11(1), e0147198. https://doi.org/10.1371/journal.pone.0147198

Hinman, R. S., Hunt, M. A., Creaby, M. W., Wrigley, T. v., McManus, F. J., & Bennell, K. L. (2010). Hip muscle weakness in individuals with medial knee osteoarthritis. Arthritis Care & Research, 62(8), 1190–1193. https://doi.org/10.1002/acr.20199

Hoff, J. (2000). Methods of Blood Collection in the Mouse. Lab Animal, 29(10), 47–53.

Huang, J., Romero-Suarez, S., Lara, N., Mo, C., Kaja, S., Brotto, L., Dallas, S. L., Johnson, M. L., Jähn, K., Bonewald, L. F., & Brotto, M. (2017). Crosstalk Between MLO-Y4 Osteocytes and C2C12 Muscle Cells Is Mediated by the Wnt/β-Catenin Pathway. JBMR Plus, 1(2). https://doi.org/10.1002/jbm4.10015

Huang, J., Wang, K., Shiflett, L. A., Brotto, L., Bonewald, L. F., Wacker, M. J., Dallas, S. L., & Brotto, M. (2019). Fibroblast growth factor 9 (FGF9) inhibits myogenic differentiation of

C2C12 and human muscle cells. Cell Cycle, 18(24). https://doi.org/10.1080/15384101.2019.1691796

Isaacson, J., & Brotto, M. (2014). Physiology of Mechanotransduction: How Do Muscle and Bone "Talk" to One Another? Clinical Reviews in Bone and Mineral Metabolism, 12(2). https://doi.org/10.1007/s12018-013-9152-3

Jung, H.-W., Choi, J.-H., Jo, T., Shin, H., & Suh, J. M. (2019a). Systemic and Local Phenotypes of Barium Chloride Induced Skeletal Muscle Injury in Mice. Annals of Geriatric Medicine and Research, 23(2), 83–89. https://doi.org/10.4235/agmr.19.0012

Kojouharov, H. v., Chen-Charpentier, B. M., Solis, F. J., Biguetti, C., & Brotto, M. (2021a). A simple model of immune and muscle cell crosstalk during muscle regeneration. Mathematical Biosciences, 333. https://doi.org/10.1016/j.mbs.2021.108543

Kontzias, A. (2020, May). Osteoarthritis (OA). Merck Manual.

Kurek, J. B., Bower, J. J., Romanella, M., Koentgen, F., Murphy, M., & Austin, L. (1997). The role of leukemia inhibitory factor in skeletal muscle regeneration. Muscle & Nerve, 20(7), 815–822. https://doi.org/10.1002/(SICI)1097-4598(199707)20:7<815::AID-MUS5>3.0.CO;2-A

Mo, C., Wang, Z., Bonewald, L., & Brotto, M. (2019). Multi-Staged Regulation of Lipid Signaling Mediators during Myogenesis by COX-1/2 Pathways. International Journal of Molecular Sciences, 20(18). https://doi.org/10.3390/ijms20184326

Moore, K., Agur, A. M. R., & Dalley, A. F. , I. (2014). Essential Clinical Anatomy (5th ed.). Lippincott Williams & Wilkins.

Morton, A. B., Norton, C. E., Jacobsen, N. L., Fernando, C. A., Cornelison, D. D. W., & Segal, S. S. (2019a). Barium chloride injures myofibers through calcium-induced proteolysis

with fragmentation of motor nerves and microvessels. Skeletal Muscle, 9(1), 27. https://doi.org/10.1186/s13395-019-0213-2

Movasaghi, Z., Rehman, S., & Rehman, I. U. (2007a). Raman Spectroscopy of Biological Tissues. Applied Spectroscopy Reviews, 42(5), 493–541. https://doi.org/10.1080/05704920701551530

Pedersen, B. K. (2013a). Muscle as a Secretory Organ. In Comprehensive Physiology (pp. 1337–1362). Wiley. https://doi.org/10.1002/cphy.c120033

Pedersen, B. K., & Febbraio, M. A. (2012). Muscles, exercise and obesity: skeletal muscle as a secretory organ. Nature Reviews Endocrinology, 8(8), 457–465. https://doi.org/10.1038/nrendo.2012.49

Plesia, M., Stevens, O. A., Lloyd, G. R., Kendall, C. A., Coldicott, I., Kennerley, A. J., Miller, G., Shaw, P. J., Mead, R. J., Day, J. C. C., & Alix, J. J. P. (2021). In Vivo Fiber Optic Raman Spectroscopy of Muscle in Preclinical Models of Amyotrophic Lateral Sclerosis and Duchenne Muscular Dystrophy. ACS Chemical Neuroscience, 12(10), 1768–1776. https://doi.org/10.1021/acschemneuro.0c00794

Pritzker, K. P. H., Gay, S., Jimenez, S. A., Ostergaard, K., Pelletier, J.-P., Revell, P. A., Salter, D., & van den Berg, W. B. (2006). Osteoarthritis cartilage histopathology: grading and staging. Osteoarthritis and Cartilage, 14(1). https://doi.org/10.1016/j.joca.2005.07.014

Qi, Y., Yang, L., Liu, B., Liu, L., Liu, Y., Zheng, Q., Liu, D., & Luo, J. (2021). Accurate diagnosis of lung tissues for 2D Raman spectrogram by deep learning based on short-time Fourier transform. Analytica Chimica Acta, 1179. https://doi.org/10.1016/j.aca.2021.338821

Rehan Youssef, A., Longino, D., Seerattan, R., Leonard, T., & Herzog, W. (2009). Muscle weakness causes joint degeneration in rabbits. Osteoarthritis and Cartilage, 17(9), 1228–1235. https://doi.org/10.1016/j.joca.2009.03.017

Rutgers, M., van Pelt, M. J. P., Dhert, W. J. A., Creemers, L. B., & Saris, D. B. F. (2010). Evaluation of histological scoring systems for tissue-engineered, repaired and osteoarthritic cartilage. Osteoarthritis and Cartilage, 18(1). https://doi.org/10.1016/j.joca.2009.08.009

Slemenda, C. (1997). Quadriceps Weakness and Osteoarthritis of the Knee. Annals of Internal Medicine, 127(2), 97. https://doi.org/10.7326/0003-4819-127-2-199707150-00001

Villa-Forte, A. (2019, December). Introduction to the Biology of the Musculoskeletal System. Merck Manual. https://www.merckmanuals.com/home/bone,-joint,-and-muscle-disorders/biology-of-the-musculoskeletal-system/introduction-to-the-biology-of-the-musculoskeletal-system

Wang, Z., Bian, L., Mo, C., Kukula, M., Schug, K. A., & Brotto, M. (2017). Targeted quantification of lipid mediators in skeletal muscles using restricted access media-based trap-and-elute liquid chromatography-mass spectrometry. Analytica Chimica Acta, 984. https://doi.org/10.1016/j.aca.2017.07.024

CHAPTER 2

Systematic Review: Advantages and Disadvantages of Current Osteoarthritis Mouse Models

Logan Moore[1], Marco Brotto[1*]

Bone Muscle Research Center, College of Nursing and Health, University of Texas at Arlington, Arlington, TX, USA

*Correspondence:

Marco Brotto

Marco.brotto@uta.edu

Abstract:

Osteoarthritis (OA), the most common joint disease, usually becomes symptomatic in people aged 40-50s. OA is a chronic degenerative arthropathy, characterized by substantial disruption and the loss of cartilage. The prevalence of OA is only rising with the manifestation and progression being multifactorial. Currently, there is no known cure. The use of animal models, such as mice, allows researchers to investigate the disease in a controlled environment, and attempt to determine signaling pathways that could lead to new therapies. However due to the multifactorial nature of OA, animal models are limited in scope. The purpose of this review was to investigate the current preclinical OA mouse models used and find the advantages and disadvantages of found models. Following PRISMA guidelines, this review systematically searched three electronic, online databases (PubMed, CINHAL, and Academic Search Complete). Using the following inclusion criteria: 1) Dated between 2019 and 2022, 2) Published in a peer-reviewed journal, with full free text and abstracts available, 3) Mouse model with osteoarthritis was the focus of the study. 18 articles were included in this review of the 44 found. The most common methodology of inducing OA in mice was through surgical approaches (n = 14), and of those articles' the most frequent was destabilization of the medial meniscus (DMM, n = 12). Other forms of inducing OA included Tibial Plateau Compression, injection based, genetic manipulation, and exercise induced. Each model has their advantages and disadvantages, and due to the complexities of OA no singular model is best at providing the complete pathophysiology of the disease. As research continues to develop in OA, the researchers need to carefully select their model based on their research question. Conducting studies in multiple model types may prove beneficial in providing key insights into the

complexities of OA. Continued work in developing study protocols to induce OA in small animal models needs to commence to further provide all intricacies of the disease.

Introduction

Osteoarthritis (OA) is the leading form of disability in the US, and one of the most common bone joint diseases (Arden et al., 2006; Johnson et al., 2014; Neogi et al., 2012; Glynn-Jones et al., 2015). This disease poses as a major public health problem, as OA has been estimated to affect 10% of the male population and 18% of the female population over the age of 60 (Glynn-Jones et al., 2015). With the continued aging population, the prevalence of OA is expected to continue to rise (Johnson et al., 2014). This places a financial strain not only on the patient, but the healthcare system as well, as shown in 2015 with the annual indirect cost ranging from $1,442 to $21,335 (Glyn-Jones et al., 2015; Xie et al., 2016).

OA can be defined as a degenerative joint disease, which can be characterized by the disruption and potential loss of joint cartilage (Stiffel et al., 2019; Merck Manual, Professional Version). The reason for the development of the disease is multifactorial, and it has been shown that age, obesity, history of injury, and genetic disposition are all risk factors in the development (Glyn-Jones et al., 2015; Johnson et al., 2014). There is no known cure, but common treatments for the disease include lifestyle changes, exercise, pain medication, and in the most severe cases surgery (Glyn-Jones et al., 2015; Flannery, 2018).

Research into OA needs to continue to develop to better understand the pathophysiology of the disease. This will allow for new treatment protocols, prevention mechanisms can be put into action, and a cure could be developed. Research on human subjects can be costly, timely, and inefficient therefore the use of animal models can circumvent the problems using human subjects. The goal for animal models is that they are able to mimic aspects of the disease ("Animal Model"). Small animal models such as the mouse have provided invaluable information on OA (Mailhiot et al., 2015; Stiffell et al., 2020; Pitcher et al., 2016). Using the

mouse as the model, researchers can implement their research protocol in a cheaper and more time efficient manner, compared to other models (Stiffell et al., 2020).

Currently there are multiple methodologies in which OA can be induced in mice. The purpose of this literature review and analysis is to find the current preclinical mouse models used for osteoarthritis studies and compare the models to find the best available model for future research.

Methods

Following the guidelines set forth by the Preferred Reporting Items for Systematic Reviews and Meta-analysis (PRISMA), three electronic, online databases where chosen to conduct this systematic review: PubMed, CINHAL, and Academic Search Complete (Moher et al., 2015). The initial search was conducted at the conception of this study in October of 2021, and a final, updated search was completed in December of 2022. The systematic search strategy used for each database can be found in table _.

Table 2-1: Systematic Search Strategy

Database	Search String	Filters
PubMed	"Osteoarthritis, Mouse, Model, Preclinical"	Results by year: 2019-2022 Text Availability: Abstract, Free Full Text
CINHAL	Osteoarthritis AND Mouse AND Model	Results by year: 2019-2022 Abstract Available, English Language
Academic Search Complete	Osteoarthritis AND Mouse AND Model and Preclinical	Results by year: 2019-2022

For inclusion in this study, the articles had to meet the following eligibility criteria: 1) published between 2019 and 2022, 2) Published in a peer reviewed journal, with full free text and abstracts available, 3) Mouse model with osteoarthritis was the focus of the study. Articles that did not meet the prescribed inclusion criteria were excluded.

Articles were excluded if they were non-peer-reviewed articles, abstracts, study protocols, newspapers, or editorials, as it was deemed a priori that the caliber and rigor of the research needed to be validated by a peer review process. Systematic reviews were also excluded, as the goal was to find original research articles. For continuity in the reviewing process, only articles in the English language were included.

The search results from each database were downloaded into a .bib format, for upload into a reference manager. Using the reference manager, duplicate articles were removed. The resulting articles' titles and abstracts were scanned for broad inclusion. Articles were removed if they did not meet the inclusion and exclusion criteria stated above. The full text of the articles was then reviewed by the inclusion and exclusion criteria. For quality control the results were also download in a .csv and uploaded to a separate spreadsheet.

To ensure the quality of studies included, all studies were subjected to risk of bias assessment. The studies were evaluated biased on the Revised Cochrane risk-of-bias tool for randomized trials (RoB 2) for the assessment of biases for randomized control studies (Sterne et al., 2019). For visualization of the resulting bias found in the seven domains, the tool robvis was used (McGuinness, 2020).

The systematic review was conducted by a singular reviewer (LM), and the results were then validated and confirmed by a second reviewer (MB). There were no discrepancies in results, or questions on inclusion/exclusion of an article.

Results

44 articles were found in the initial search in October 2021 (see Figure 1.). Through duplicate removal and title scan, 9 articles were removed. Thirty-five articles were then subjected to full abstract scans. 28 articles met the broad inclusion criteria, and 7 were excluded.

These articles were excluded for being review articles and for the study being not a mouse with OA. After full text review of the 28 articles, 10 articles were excluded for either the article not focusing on OA or not having the correct subject. A final, updated search was conducted in December of 2022, and it yielded 6 new articles. Of these 6 articles, 3 of them met the inclusion/exclusion criteria. 18 articles met the full criteria set and were included for this review.

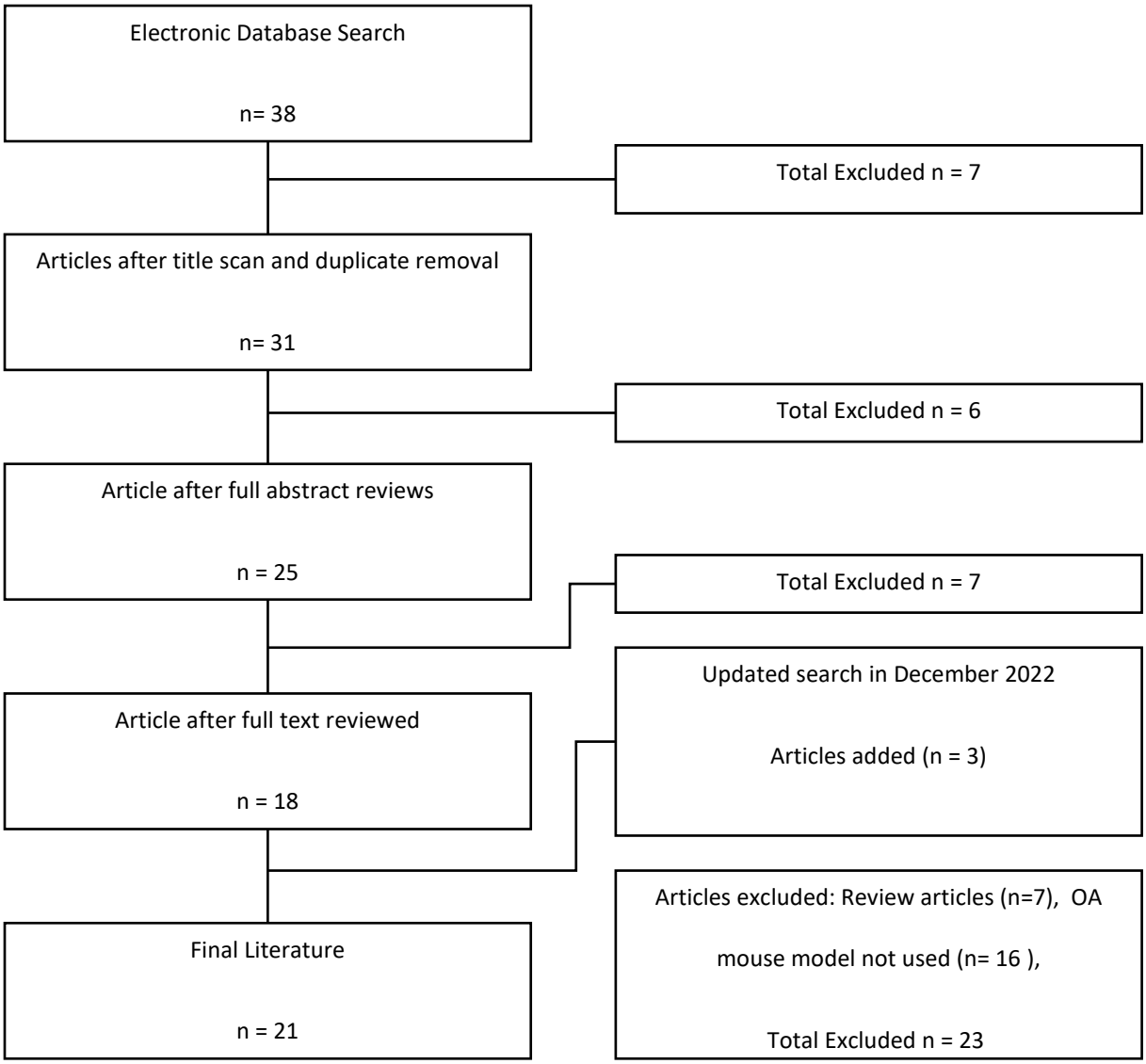

Figure 2-1: Flow Diagram of Article Selection

To ensure the quality of the articles chosen for inclusion in this literature review, bias reporting was conducted. The 21 articles were analyzed for the 5 domains of bias according to

the ROB2 scale (see **Figure 2.)**. 3 articles were found to have bias concerns (O-Sullivan et al., 2022; Armstrong et al., 2021; Wegner et al., 2019). This was due to concerns in which the authors did not report if the measurement out comes where blinded. Having non-blinded reporting outcomes in analyzing graded outcomes could influence the grade given to

experimental and control groups, as the reported outcomes are consistent with the current literature only some concerns were raised. All other articles were shown to have low bias.

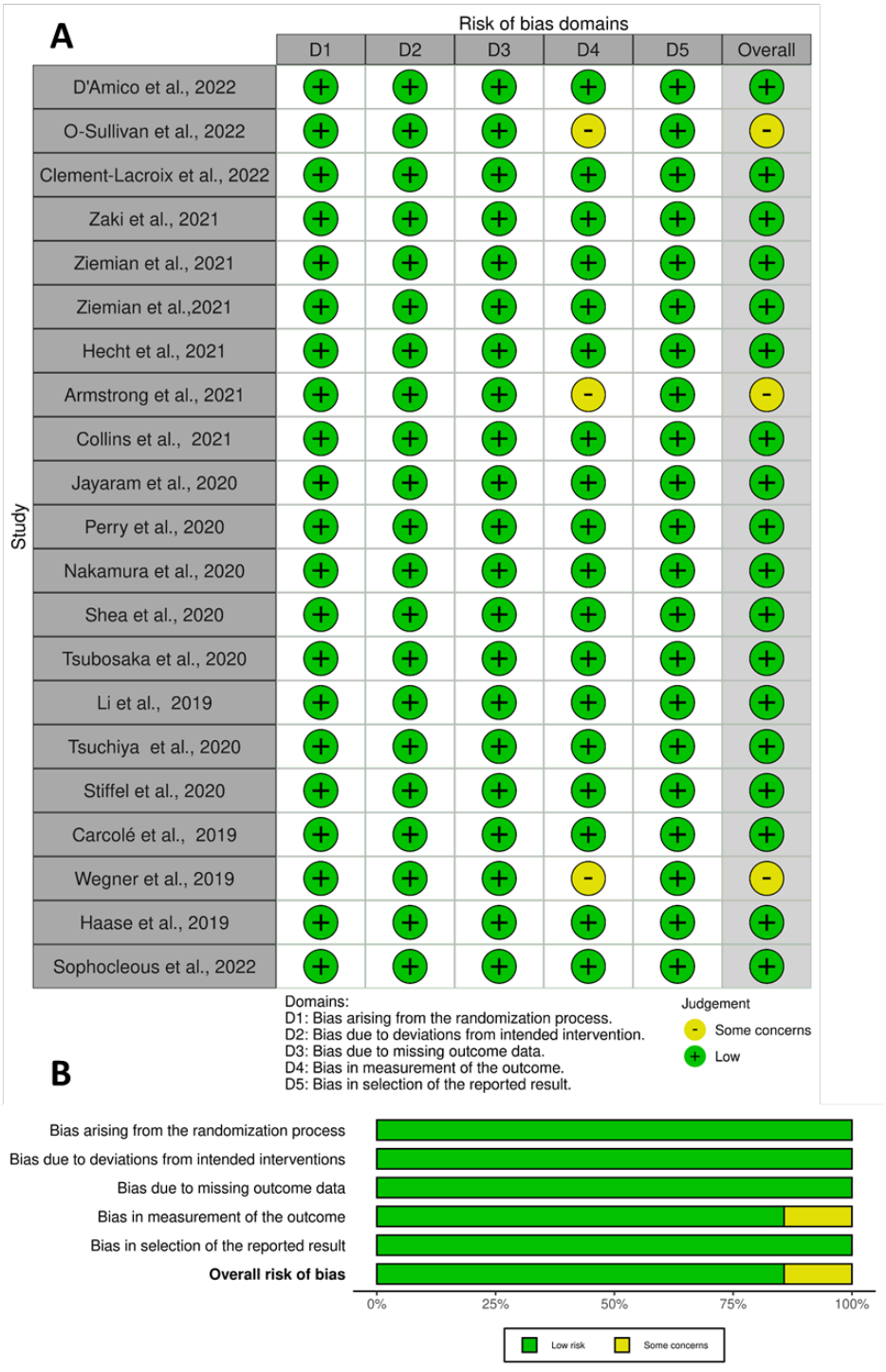

Figure 2-2: Risk of bias for randomized control studies (RoB2 scale). A) Each studies individual bias assessment. B) Summary of bias according to individual domains.

Surgical Induction

There were 8 differing types of methodologies reported in which OA could be induced in a mouse model from 2019 to 2022. The most common category in inducing OA was through surgical intervention (see **Table 2**.). Of the 21 articles that used surgical intervention, 14 of them used the destabilization of the medial meniscus (DMM) (D'Amico et al., 2022 Clement-Lacroix et al., 2022; Zaki et al., 2021; Collins et al., 2021; Jayaram et al., 2020; Nakamura et al., 2020; Tsubosaka et al., 2020; Li et al., 2019; Tsuchiya et al., 2020; Haase et al., 2019; Sophocleous et al., 2022; Armstrong et al., 2021; Perry et al., 2020; O-Sullivan et al., 2022). One article the Medial Cruciate Ligament – Medial Meniscus (MCL-MM) model along with the DMM model (Haase et al., 2019).

Table 2-2: Type of Mouse Models Found

OA Induced		Total Articles
Surgical		
	Destabilization of the medial meniscus (DMM)	n = 14
	Medial Curiate Ligament – Medial Meniscus (MCL-MM)	n = 1
Injection		
	Monoiodeacete (MIA) injections	n = 1
Genetic		
	I-ER Stress	n = 4
Load		n = 1
	Tibia Plataue Compressive Load	n = 1
	Tibia Cyclic Load	n = 2
Aging		n =2

DMM was first established by Glasson et al. in 2007 (See **Figure 3**.), through this procedure the Medial Meniscus Tibial Ligament (MMTL) is transected. Transection on the MMTL leads to increased mechanical stress on the posterior femur and central tibia. This model closely resembles post-traumatic OA in human subjects (Leahy et al., 2015; Shu et al., 2016; Haase et al. 2019; Wang et al., 2014; Das Neves Borges et al., 2017). Although DMM is considered to be a post-traumatic model for OA, it has been noted that the tearing the Anterior

Cruciate Ligament (ACL) during physical activity can be more traumatic as compared to DMM surgery (Thomas et al. 2015).

The Osteoarthritis Research Society International (OARSI) developed the Osteoarthritis cartilage histopathology grading system (Prizker et al., 2006; Glasson et al., 2010). The OARSI cartilage histopathology grading system is a universally used and accepted methodology to report the stage and progression of OA. This method can define OA in early development stages and can be used with novice histological researchers. The grading system ranges from 0, no evidence of alteration in cartilage or development of OA, to 1, the threshold of OA, to 6, deformation and changes in contour of the articular surface (Prizker et al., 2006,; Glasson et al., 2010). In the DMM model OA scores reaching above the threshold of 1 occur as early as one week post induction and progressively rise throughout the disease (Tsubosaka et al., 2020; Haase et al., 2019; Tsuchiya et al., 2020). Characteristics of DMM are cartilage degeneration, proteoglycan loss, chondrocyte hypertrophy, structural damage (D'Amico et al., 2022; Clement-Lacroix et al; 2022; Tsubosaka et al., 2020; Haase et al., 2019; Tsuchiya et al., 2020; Kung et. al 2016, Das Neves Borges et al., 2017; Leahy et al., 2015; Shu et al., 2016). It has been shown that as early as 4-weeks post DMM, there are structural changes in the subchondral bone and osteophyte formation that continue to progress throughout disease state (Das Neves Borges et al., 2017; Sophocleous et al., 2022). A limitation to the DMM model or a surgical methodology, is that the

induction of OA is too controlled and does not replicate that natural development of OA in humans (Wang et al., 2014).

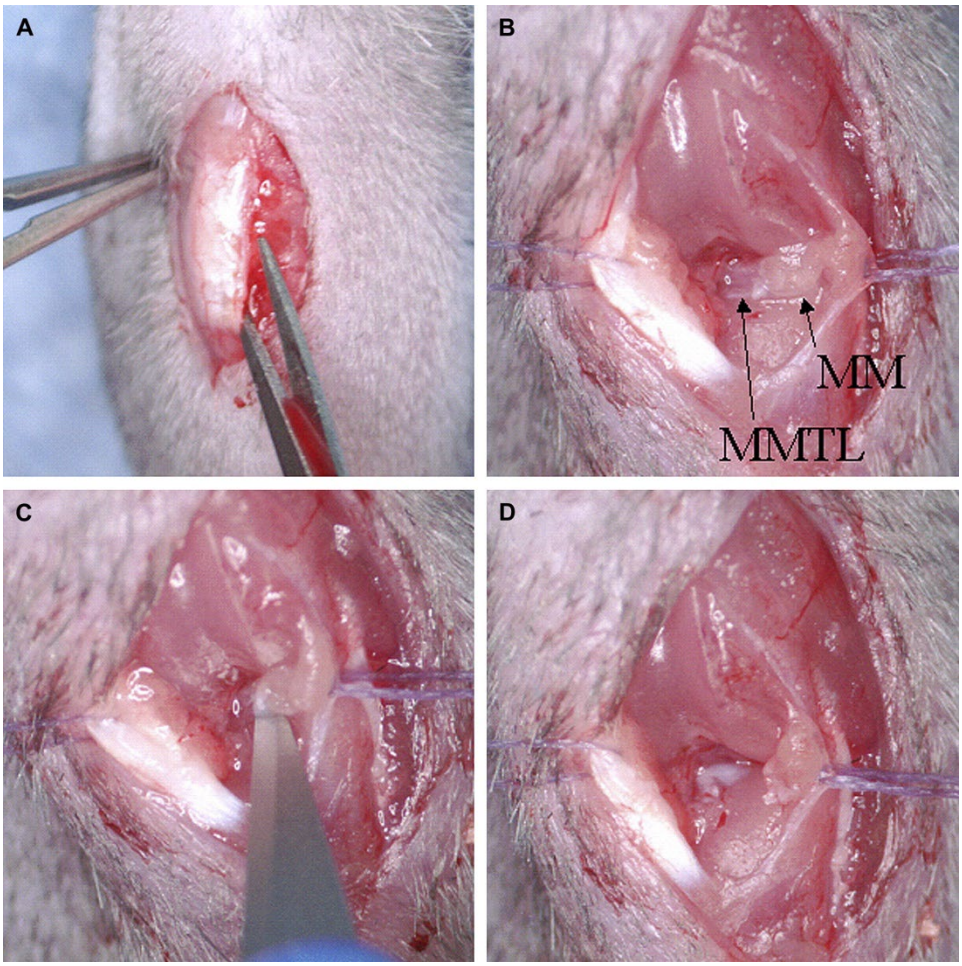

Figure 2-3: Example of DMM Surgery. Images taken from Glasson et al., 2007 illustrating the procedure of DMM. A) Initial incision (incision larger for better imaging) B) Dissection of Fat pad and identification of Medial Meniscus (MM) and Medial Meniscus Tibial Ligament (MMTL) C) Transection of the MMTL D) Completed transection

Medial Collateral Ligament – Medial Meniscus Transection (MCL-MM) was established by Kamekura et al. in 2005. In this method the Medial Collateral Ligament is transected, and the medial meniscus is removed. In this method there is rapid loss in proteoglycan and depletion in chondrocytes (Haase et al., 2019). Osteocyte changes can be seen in 2-4 weeks and osteophyte formation occurs at 12 weeks (Kamekura et al., 2005). It was shown that the destabilization of

the medial meniscus alone had a slower OA progression as compared to the MCL-MM transection (Haase et al., 2019). A limitation to the MCL-MM and DMM is that the progressive cellular lose in the weight bearing area, targeted cellular therapy becomes time sensitive, and results may vary if administered too late after induction of OA (Haase et. al, 2019)

Table 2-3: Key Findings of the 21 included articles

Authors	Model	Group Sample Size	Weeks Post Induction	Age at Induction	Mouse line	Key Findings
D'Amico et al., 2022	DMM	12	8 Weeks	4 month	C57BL/6	There is a dose dependent protection of cartilage degradation, when mice are given Urolithin A (UA) supplementation in their diets post DMM. The DMM control resulted in a significantly higher OARSI score as compared to the sham, and dosage of 250 mpk significantly reduced the OARSI score compared to the DMM control.
Clement-Lacroix et al., 2022	DMM	20	8 weeks	10 week	C57BL/6	Oral supplementation of GLPG197 had a dose dependent protective effect on cartilage pathology. DMM showed an increased proteoglycan loss, fibrillation, and full-thickness erosion of non-calcified cartilage.
Zaki et al., 2021	DMM	10	1, 2, 4, 8, 12 weeks	11 week	C57BL/6	DMM showed a reduction in affected limb stride length in early-stage OA (4-8 weeks), and a reduction in weight-bearing in the affected limb at late-stage OA (12-16 weeks). DMM had a progressive degradation in cartilage, increased subchondral bone sclerosis and osteophyte size.
Collins et al., 2021	DMM	7 to 16	12 weeks	16 weeks	C57BL/6 and lipodystrophy	Lipodystrophy (LD) mice completely lack adipose tissue, and after DMM it was shown to have a protection from cartilage damage. When adipose tissue is reintroduced through transplantation to the LD mice, it no longer has protective effects and has similar cartilage damage as compared to WT C57BL/6 mice.

Jayaram et al., 2020	DMM	10 to 12	3.5 months	Three Month	FVB/N	Following DMM, mice were treated with intra-articular injections of either leukocyte rich - platelet rich plasma (PRP) or leucocyte poor - PRP. The PRP therapy provided mild protection against OA development, however showed significant protection in cartilage volume and cartilage surface as compared to the DMM control group.
Nakamura et al., 2020	DMM	15 to 40	4 and 8 weeks	10 week	TIMP3 transgenic WT and KO	Transgenic [-1A} TIMP3 mice have selective inhibition of ADAMTS. The inhibition of ADAMTS provides a significant protection in the cartilage degradation as compared to TIMP3 WT mice following DMM.
Tsubosaka et al., 2020	DMM	6	1 week and 8 weeks	10 week	C57BL/6	DMM showed early onset of OA from alterations in the articular cartilage at one-week post-surgical induction. The supplementation of EPA through intraarticular injection immediately after DMM had a significant decrease in the development of OA through cartilage degradation and synovitis.
Li et al., 2019	DMM	15	8 Weeks	10 week	C57Bl/6	Mangiferin was administered intra-gastrically for 8 weeks after DMM. The treatment of Mangiferin resulted in a smoother appearance of the articulating cartilage resulting in a significantly lower OA score as compared to the DMM control group.
Tsuchiya et al., 2020	DMM	12	2, 4, and 8 weeks	12 Week	C57Bl/6	Mice chow was supplemented with 4-methylumbelliferone (4-MU) after DMM. The control DMM showed progressive deterioration in the articular cartilage beginning at 2-week post-surgical induction. The 4-MU chow mice showed a significant reduction in OA progression

						resulting in a decreased amount of articular cartilage damage and osteophyte size.
Haase et al., 2019	DMM and MCL-MM	3	1, 2, 4, 6, 8, and 12 weeks	11 weeks	C57BL/6	Transection of the medial cruciate ligament and destabilization of the medial meniscus (MCL-MM) rapidly form OA as compared to the destabilization of the medial meniscus alone. The MCL-MM model showed a significantly higher OA score, depletion of chondrocytes, and proteoglycan loss as early as 1 - 2 weeks compared to the DMM. This showed that time dependent studies are critical in targeting the loss of chondrocytes, as there may be no chondrocytes to target in longer experimental protocols.
Sophocleous et al., 2022	DMM	10 to 11	8 weeks	8 weeks	C57BL/6	The mice intestinal microbiome was depleted 1 week before birth and reconstituted at 6-weeks of age. At 8-weeks of age the mice were subjected to DMM and were given probiotics of glycerol in their drinking water. The probiotic treatment only showed a significant decrease in articular cartilage damage at the medial femoral condyle. The probiotic treatment significantly increased the bone volume and trabecular thickness in the femoral epiphyseal trabecular bone.
Armstrong et al., 2021	DMM and Aged	10 to 15	8 weeks	12 weeks 18 months		The OA grading systems from OARSI and ACS perform similarly, and it is shown that H&E-stained mid-coronal sections are effective to determine OA severity alone.
Perry et al., 2020	PMM	6 to 12	8 to 12 weeks	10 week	C57BL/6	Following PMM, the mice received an intra-articular injection of human umbilical cord-derived mesenchymal stromal cells (hUC-MSCS). The treatment of hUC-MSCS showed no alterations in the OA pathophysiology developed in control PMM

						shown in subchondral bone volume, synovitis, and articular cartilage degeneration.
O-Sullivan et al., 2022	PMM	6	12 Weeks	11 Weeks	C57BL/6	There was a significant increase in OARSI score in the PMM control as compared to the sham, and treatment with Lactobacillus acidophilus showed significant protection of damage to the articulating cartilage along with decreased levels of MMP-13 and RUNX2.
Stiffel et al., 2020	Tibial Plataue Compression	16		12 Week	C57Bl/6	Tibial Plateau compression caused erosion of the articular cartilage alterations in the bone thickness of the subchondral bone, and osteophyte formation.
Wegner et al., 2019	Tibial compression	7	7 Days	10 weeks	C57BL/6 and Nox4 KO	Tibial compression loading of 14N was applied until the Anterior Cruciate Ligament ruptured causing a boney avulsion. The genetic knock down of Nox4 showed a significant reduction in bone volume and bone density in the subchondral bone.
Ziemian et al., 2021	Cyclic load	6 to 8	2 Weeks	26 week	pOC-ERαKO	pOC-ERαKO mice display a phenotype of subchondral bone osteoporosis without altered cartilage due to the lack of estrogen. After two weeks of cyclic loading of the tibia, there is a load dependent (6.5 -9 N) increase in cartilage damage shown by a higher OARSI score. Loaded pOC-ERαKO mice showed thinner articular cartilage as compared to the control.
Ziemian et al., 2021	Cyclic load	7 to 8	3 Weeks and 6 weeks	26 week	C57BL/6	Cyclic loading of 9 N created cartilage damage in all groups. Daily treatment

						of alendronate (ALN) preserved the subchondral bone volume and reduced the amount of cartilage degeneration as compared to vehicle control.
Hecht et al., 2021	I-ER Stress	10	4 weeks	16 week	I-ER Stress	I-ERS is a biogenic mouse strain causing ER stress in the articular cartilage. This line was generated by using two plasmids: Cartilage oligomeric matrix protein and reverse tetracycline, and through the administration of DOX mutant-COMP is expressed in cartilage. the combination of ER stress and treadmill running induced higher levels of articular cartilage damage.
Shea et al., 2020	Aging	22 to 27	6 months	11 month	C57BL/6	The control group aged mice showed natural-occurring OA demonstrated by articular cartilage damage, however showed a high variability in the onset and severity of disease. Mice that had been supplemented with a low vitamin K diet, articular cartilage damage and subchondral bone thickness were similar. The low vitamin K diet promoted
Carcolé et al., 2019	MIA Injection	5 to 6	1 or 15 days	8 to 12 Week	Swiss Albino	Mice receive an intra-articular injection of 10 µL of Monioacetate, however confirmation of OA development was not confirmed. Intra-peritoneal injection of selective σ1 receptor antagonist E-52862 and µ receptor agonist inhibited the mechanical hypersensitivity seen in the MIA control group.

Non-Surgical Induction

In the non-surgical approach, inducing OA by form of joint loading was the most common (n = 4). There were 3 articles that chose to induce OA through means of the Tibial Compression Loading (Wegner et al., 2019; Ziemain et al., 2021; Zeimian et al., 2021), and one article used Tibial Plateau Compression Loading Induced Injury Model (Stiffel et al., 2020).

There is a variety of loads that can be applied of the tibia to cause joint alterations. Tibial Plateau Compression Loading Induced Injury Model was developed by Stiffel et al. (see **Figure 4**). The conception of this model was to develop a non-invasive method in inducing post-traumatic OA (PTOA) (Stiffel et al. 2019). This method depends on the precise placement of the indenter to apply the proper amount of load on the tibial plateau. If the load calculation or placement is off fractures could occur and the results of developing PTOA are diminished. However, under the right guidelines it was illustrated that this methodology manifested characteristics of PTOA, such as erosion of articular cartilage thickening of the trabecular plate, formation of osteocytes, and remodeling of the subchondral bone (Stiffel et al. 2019).

Tibial compression loading of the entire joint is also used in inducing OA. This methodology would require less precision in the placement of the joint, as the entire joint is loaded. In Wegner et al., they used a single dynamic load of 14 N. This resulted in the Anterior Cruciate Ligament (ACL) to rupture creating the joint instability much like the surgical models. The single bout of compression loading leads to consistent OA within a 4-to-8-week period, and modification in subchondral bone thickness can be observed within a week of injury (Wegner et al., 2019). A single bout of cyclic mechanical loading of 1200 cycles at 4 hz producing a

maximum of 9 N was shown to cause significantly elevated OA scores with in 3 weeks post induction (Ziemain et al., 2021 Ziemain et al., 2021).

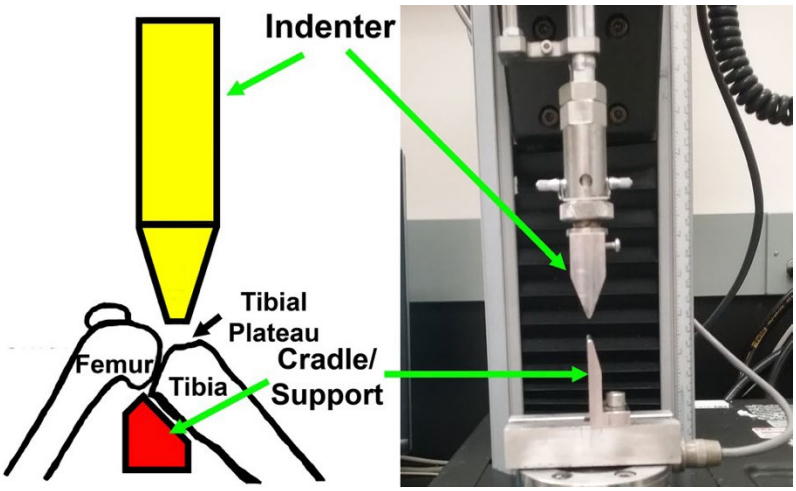

Figure 2-4: Tibial Plateau Loading. Image from Stiffel et al. demonstrating the schematic in which the tibial plateau is loaded.

Monoiodeacete (MIA) injections were used by Carcolé et al., 2019. The methodology for inducing OA through MIA is explained in Pitcher et al. MIA is an intra-articular injection which causes a rapid pain response. The MIA disrupts chondrocyte glycolysis, resulting in chondrocyte death, neovascularization, subchondral bone necrosis and collapse, as well as inflammation (Carcolé et al., 2019; Pitcher et al 2016). These are all clinical pathologies of OA. MIA injections are not complex, but there can be complications in which they are not contained in the joint capsule resulting in failure (Pitcher et al., 2016).

OA can be induced through genetic manipulation as seen in I-ERS mouse strain (Hect et al., 2021). The I-ERS mouse strain is bigenic mouse that induces ER stress in the articular cartilage. The mouse strain was generated using two plasmids: cartilage oglimeric matrix protein [pTRE-COMP] and reverse tetracycline-controlled transactivator [rtTA]. The ER stress is inducible by administration of DOX. Hect et al., 2021 showed that along with exercise the I-ERS

mouse strain had elevated OA score, resulted from articular cartilage damage, and loss of proteoglycans.

Aging is another factor in the development and progression of osteoarthritis. In Shea et al., C57BL/6 wildtype mice were aged to either 14.5 months or 17 months. The C57BL/6 mice showed OA development through articular cartilage damage and modification to the subchondral bone thickness (Shea et al., 2020) Aged C57BL/6 mice showed a variable and inconsistent development as compared to other experimental OA induction approaches. Armstrong et al., used the aging methodology along with DMM, and it was shown that the aged model had similar articular cartilage damage to the medial tibial plateau as the DMM (Armstrong et al., 2021). The Age mice also had a higher OA score on the lateral tibial plateau as compared to the DMM.

Discussion

This review aimed to discover the currently used preclinical osteoarthritis mouse models and analyze the benefits and limitations of each model. Not only are there advantages and disadvantages to each model, but there are also advantages and disadvantages in using small animal subjects in general. A limitation in all mouse models or small animal models is the amount of cartilage that can be harvested for processing and imaging (Li et al., 2015; Marenzana et al. 2014). However, through advancements in imaging techniques it has been demonstrated that mouse articular cartilage can be viewed using high-resolution micro-CT (Marenzana et al., 2014). A limitation that could arise in any experimental protocol is the use of the contralateral limb as the control (Wu et al., 2017). In using the contralateral limb as a control there is no way to calculate the effect the involved limb has on it unless a priori testing is completed.

It was evident that the most common methodology in inducing OA was through surgical intervention, such as DMM. A clear advantage in using this methodology is that there is

development of OA in 4 to 12 weeks post-surgery depending on the method. This method closely resembles PTOA in humans. However, there are limitations as this procedure is dependent on the skill of the surgeon to repeatedly perform the same outcome on multiple mice. There is an increased risk of the mouse developing an infection in the involved limb. Finally, there is a higher cost in materials and personnel, as the mouse must be anesthetized and undergo surgery.

The induction of OA through injection-based methodology, such as MIA, has benefits and limitations. Injections allow for rapid and controlled development of OA based on the dosage and concentration. The technique is limited, making the procedure to be easier. As this does not ideally model slow, natural progressive OA, it does allow for time efficient experiments testing the effects on drugs. These protocols then can be replicated using a model in which OA is induced at a more progressive rate. Previous methodologies using other chemicals or reagents have also been used to develop OA, such as Collagenase or Papain (Cosenza et al., 2017; Toupet et al., 2015 Delgado-Enciso et al., 2018). However, these methodologies were not found in our systematic search.

Tibial Plateau Compression Loading Induced Injury Model and Tibial Compression Loading is a non-invasive way in which researchers can model PTOA. This model eliminates the use of a surgeon and chances of the mouse developing an infection. However, without careful calculations of the amount of load and the placement of in the indenter this method can cause multiple fractures and injury resulting with PTOA not being able to develop.

Aging and genetic manipulation such as the I-ER stress model do not require surgery as compared to the surgical models. Aging presents natural OA, but the housing and maintenance of the colonies to reach the age of disease state can be costly and demanding and there is substantial variability between animals. The inconsistency makes it challenging to control treatment and

therapy outcomes. Genetic modification can create a specific pathway or mechanism of disease, which can be beneficial in targeted gene therapy development. However, these models lack the ability to show the multifactorial manifestation of OA. Previously, other genetically modified mice were used too, such as the SRT/ort mice strains (Mason et al., 2001; Wei et al., 2014; Chiusaroli et al., 2011; Chiusaroli et al., 2013).

Conclusion

Osteoarthritis is a multifactorial disease, with risk factors including age, obesity, history of injury, and genetic disposition. Each of these mice models in this review brings special characteristics to the study of OA in which researchers can gain valuable insights. However, each of these models do have their flaws and do not model all the pathophysiological manifestations of OA. Therefore, currently there is not a "best model" for OA, but researchers can advance the science of OA and treatments with this diversity of models.

In future studies, researchers may find it beneficial to use multiple models for the same research question. Having multiple models could fill in the gaps in which the other model may have limited the research or outreach. Furthermore, it will be important to develop new ways in which OA can be induced in small animals needs to be conducted, therefore a model could show the complete pathophysiological characteristics of human OA.

References

Animal Model. (n.d.). Retrieved January 08, 2021, from https://www.genome.gov/genetics-glossary/Animal-ModelArden, N., & Nevitt, M. C. (2006). Osteoarthritis: Epidemiology. Best Practice & Research Clinical Rheumatology, 20(1), 3–25. https://doi.org/10.1016/j.berh.2005.09.007

Armstrong, A. R., Carlson, C. S., Rendahl, A. K., & Loeser, R. F. (2021). Optimization of histologic grading schemes in spontaneous and surgically-induced murine models of osteoarthritis. *Osteoarthritis and cartilage*, *29*(4), 536–546. https://doi.org/10.1016/j.joca.2021.01.006

Butler, R. K., Knapp, D. J., Ulici, V., Longobardi, L., Loeser, R. F., & Breese, G. R. (2017). A mouse model for chronic pain-induced increase in ethanol consumption. *Pain* (03043959), 158(3), 457–462. https://doi.org/10.1097/j.pain.0000000000000780

Carcolé, M., Kummer, S., Gonçalves, L., Zamanillo, D., Merlos, M., Dickenson, A. H., Fernández-Pastor, B., Cabañero, D., Maldonado, R., & Fernández-Pastor, B. (2019). Sigma-1 receptor modulates neuroinflammation associated with mechanical hypersensitivity and opioid tolerance in a mouse model of osteoarthritis pain. *British Journal of Pharmacology*, *176*(20), 3939–3955. http://10.0.4.87/bph.14794

Chiusaroli, R., Piepoli, T., Zanelli, T., Ballanti, P., Lanza, M., Rovati, L. C., & Caselli, G. (2011). Experimental Pharmacology of Glucosamine Sulfate. *International Journal of Rheumatology*, 2011, 1–8. http://10.0.4.131/2011/939265

Chiusaroli, R., Visentini, M., Galimberti, C., Casseler, C., Mennuni, L., Covaceuszach, S., Lanza, M., Ugolini, G., Caselli, G., Rovati, L. C., & Visintin, M. (2013). Targeting of ADAMTS5's ancillary domain with the recombinant mAb CRB0017 ameliorates disease

progression in a spontaneous murine model of osteoarthritis. *Osteoarthritis & Cartilage*, 21(11), 1807–1810. https://doi.org/10.1016/j.joca.2013.08.015

Collins, K. H., Lenz, K. L., Pollitt, E. N., Ferguson, D., Hutson, I., Springer, L. E., Oestreich, A. K., Tang, R., Choi, Y. R., Meyer, G. A., Teitelbaum, S. L., Pham, C. T. N., Harris, C. A., & Guilak, F. (2021). Adipose tissue is a critical regulator of osteoarthritis. *Proceedings of the National Academy of Sciences of the United States of America*, *118*(1), e2021096118. https://doi.org/10.1073/pnas.2021096118

Cosenza, S., Ruiz, M., Toupet, K., Jorgensen, C., & Noël, D. (2017). Mesenchymal stem cells derived exosomes and microparticles protect cartilage and bone from degradation in osteoarthritis. *Scientific Reports*, 7(1), 16214. https://doi.org/10.1038/s41598-017-15376-8

Clement-Lacroix, P., Little, C. B., Smith, M. M., Cottereaux, C., Merciris, D., Meurisse, S., Mollat, P., Touitou, R., Brebion, F., Gosmini, R., De Ceuninck, F., Botez, I., Lepescheux, L., van der Aar, E., Christophe, T., Vandervoort, N., Blanqué, R., Comas, D., Deprez, P., & Amantini, D. (2022). Pharmacological characterization of GLPG1972/S201086, a potent and selective small-molecule inhibitor of ADAMTS5. *Osteoarthritis and cartilage*, *30*(2), 291–301. https://doi.org/10.1016/j.joca.2021.08.012

D'Amico, D., Olmer, M., Fouassier, A. M., Valdés, P., Andreux, P. A., Rinsch, C., & Lotz, M. (2022). Urolithin A improves mitochondrial health, reduces cartilage degeneration, and alleviates pain in osteoarthritis. *Aging cell*, *21*(8), e13662. https://doi.org/10.1111/acel.13662

Das Neves Borges, P., Vincent, T. L., & Marenzana, M. (2017). Automated assessment of bone changes in cross-sectional micro-CT studies of murine experimental osteoarthritis. *PLoS*

ONE, 12(3), 1–22. http://10.0.5.91/journal.pone.0174294

Delgado-Enciso, I., Paz-Garcia, J., Rodriguez-Hernandez, A., Madrigal-Perez, V. M., Cabrera-Licona, A., Garcia-Rivera, A., Soriano-Hernandez, A. D., Cortes-Bazan, J. L., Galvan-Salazar, H. R., Valtierra-Alvarez, J., Guzman-Esquivel, J., Rodriguez-Sanchez, I. P., Martinez-Fierro, M. L., & Paz-Michel, B. (2018). A promising novel formulation for articular cartilage regeneration: Preclinical evaluation of a treatment that produces SOX9 overexpression in human synovial fluid cells. *Molecular Medicine Reports*, 17(3), 3503–3510. https://doi.org/10.3892/mmr.2017.8336

Ezaki, J., Hashimoto, M., Hosokawa, Y., Ishimi, Y., Ezaki, J., Hashimoto, M., Hosokawa, Y., & Ishimi, Y. (2013). Assessment of safety and efficacy of methylsulfonylmethane on bone and knee joints in osteoarthritis animal model. *Journal of Bone & Mineral Metabolism*, 31(1), 16–25. https://doi.org/10.1007/s00774-012-0378-9

Flannery, W. (2018, November 13). You have Osteoarthritis...What's Next? - OSMS - Orthopedic and Rheumatology Services in Wisconsin. Retrieved November 30, 2020, from https://osmsgb.com/rheum/you-have-osteoarthritis-whats-next/

Glasson, S. S., Chambers, M. G., Van Den Berg, W. B., & Little, C. B. (2010). The OARSI histopathology initiative - recommendations for histological assessments of osteoarthritis in the mouse. *Osteoarthritis and cartilage*, 18 Suppl 3, S17–S23. https://doi.org/10.1016/j.joca.2010.05.025

Glasson, S. S., Blanchet, T. J., & Morris, E. A. (2007). The surgical destabilization of the medial meniscus (DMM) model of osteoarthritis in the 129/SvEv mouse. *Osteoarthritis and cartilage*, 15(9), 1061–1069. https://doi.org/10.1016/j.joca.2007.03.006

Glyn-Jones, S., Palmer, A. J. R., Agricola, R., Price, A. J., Vincent, T. L., Weinans, H., & Carr,

A. J. (2015). Osteoarthritis. *The Lancet,* 386(9991), 376–387. DOI: 10.1016/S0140-6736(14)60802-3

Greenblatt, M. B., Ritter, S. Y., Wright, J., Tsang, K., Hu, D., Glimcher, L. H., & Aliprantis, A. O. (2013). NFATc1 and NFATc2 repress spontaneous osteoarthritis. P*roceedings of the National Academy of Sciences of the United States of America*, 110(49), 19914–19919. http://10.0.4.49/pnas.1320036110

Haase, T., Sunkara, V., Kohl, B., Meier, C., Bußmann, P., Becker, J., Jagielski, M., von Kleist, M., & Ertel, W. (2019). Discerning the spatio-temporal disease patterns of surgically induced OA mouse models. *PLoS ONE*, 14(4), 1–19. http://10.0.5.91/journal.pone.0213734

Hayami, T., Zhuo, Y., Wesolowski, G. A., Pickarski, M., & Duong, L. T. (2012). Inhibition of cathepsin K reduces cartilage degeneration in the anterior cruciate ligament transection rabbit and murine models of osteoarthritis. *BONE*, 50(6), 1250–1259. http://10.0.3.248/j.bone.2012.03.025

Hecht, J. T., Veerisetty, A. C., Wu, J., Coustry, F., Hossain, M. G., Chiu, F., Gannon, F. H., & Posey, K. L. (2021). Primary Osteoarthritis Early Joint Degeneration Induced by Endoplasmic Reticulum Stress Is Mitigated by Resveratrol. *The American journal of pathology*, *191*(9), 1624–1637. https://doi.org/10.1016/j.ajpath.2021.05.016

Jayaram, P., Liu, C., Dawson, B., Ketkar, S., Patel, S. J., Lee, B. H., & Grol, M. W. (2020). Leukocyte-dependent effects of platelet-rich plasma on cartilage loss and thermal hyperalgesia in a mouse model of post-traumatic osteoarthritis. *Osteoarthritis & Cartilage*, 28(10), 1385–1393. https://doi.org/10.1016/j.joca.2020.06.004

Johnson, V. L., & Hunter, D. J. (2014). The epidemiology of osteoarthritis. Best practice &

research. Clinical rheumatology, 28(1), 5–15. https://doi.org/10.1016/j.berh.2014.01.004

Kamekura, S., Hoshi, K., Shimoaka, T., Chung, U., Chikuda, H., Yamada, T., Uchida, M., Ogata, N., Seichi, A., Nakamura, K., & Kawaguchi, H. (2005). Osteoarthritis development in novel experimental mouse models induced by knee joint instability. *Osteoarthritis and cartilage*, 13(7), 632–641. https://doi.org/10.1016/j.joca.2005.03.004

Kerckhofs, G., Sainz, J., Wevers, M., Van de Putte, T., & Schrooten, J. (2013). Contrast-enhanced nanofocus computed tomography images the cartilage subtissue architecture in three dimensions. *European Cells & Materials*, 25, 179–189. https://doi.org/10.22203/ecm.v025a13

Kerckhofs, G., Sainz, J., Maréchal, M., Wevers, M., Van de Putte, T., Geris, L., & Schrooten, J. (2014). Contrast-Enhanced Nanofocus X-Ray Computed Tomography Allows Virtual Three-Dimensional Histopathology and Morphometric Analysis of Osteoarthritis in Small Animal Models. *Cartilage*, 5(1), 55–65. https://doi.org/10.1177/1947603513501175

Kotwal, N., Li, J., Sandy, J., Plaas, A., & Sumner, D. R. (2012). Initial application of EPIC-μCT to assess mouse articular cartilage morphology and composition: effects of aging and treadmill running. Osteoarthritis and Cartilage, 20(8), 887–895. https://doi.org/10.1016/j.joca.2012.04.012

Kung, L. H. W., Zaki, S., Ravi, V., Rowley, L., Smith, M. M., Bell, K. M., Bateman, J. F., & Little, C. B. (2017). Utility of circulating serum miRNAs as biomarkers of early cartilage degeneration in animal models of post-traumatic osteoarthritis and inflammatory arthritis. *Osteoarthritis & Cartilage*, 25(3), 426–434. https://doi.org/10.1016/j.joca.2016.09.002

Leahy, A. A., Esfahani, S. A., Foote, A. T., Hui, C. K., Rainbow, R. S., Nakamura, D. S.,

Tracey, B. H., Mahmood, U., & Zeng, L. (2015). Analysis of the Trajectory of Osteoarthritis Development in a Mouse Model by Serial Near-Infrared Fluorescence Imaging of Matrix Metalloproteinase Activities. *Arthritis & Rheumatology*, *67*(2), 442–453. http://10.0.3.234/art.38957

Li, Y., Wu, Y., Jiang, K., Han, W., Zhang, J., Xie, L., Liu, Y., Xiao, J., & Wang, X. (2019). Mangiferin Prevents TBHP-Induced Apoptosis and ECM Degradation in Mouse Osteoarthritic Chondrocytes via Restoring Autophagy and Ameliorates Murine Osteoarthritis. *Oxidative Medicine and Cellular Longevity*, 2019, 8783197. https://doi.org/10.1155/2019/8783197

Li, W., Cai, L., Zhang, Y., Cui, L., & Shen, G. (2015). Intra-articular resveratrol injection prevents osteoarthritis progression in a mouse model by activating SIRT1 and thereby silencing HIF-2α. *Journal of Orthopaedic Research* : Official Publication of the Orthopaedic Research Society, 33(7), 1061–1070. https://doi.org/10.1002/jor.22859

Mailhiot, S. E., Zignego, D. L., Prigge, J. R., Wardwell, E. R., Schmidt, E. E., & June, R. K. (2015). Non-Invasive Quantification of Cartilage Using a Novel In Vivo Bioluminescent Reporter Mouse. *PLoS ONE*, 10(7), 1–16. http://10.0.5.91/journal.pone.0130564

Marenzana, M., Hagen, C. K., Borges, P. D. N., Endrizzi, M., Szafraniec, M. B., Vincent, T. L., Rigon, L., Arfelli, F., Menk, R.-H., & Olivo, A. (2014). Synchrotron- and laboratory-based X-ray phase-contrast imaging for imaging mouse articular cartilage in the absence of radiopaque contrast agents. *Philosophical Transactions.* Series A, Mathematical, Physical, and Engineering Sciences, 372(2010), 20130127. https://doi.org/10.1098/rsta.2013.0127

Mason, R. M., Chambers, M. G., Flannelly, J., Gaffen, J. D., Dudhia, J., & Bayliss, M. T. (2001).

The STR/ort mouse and its use as a model of osteoarthritis. *Osteoarthritis and cartilage*, 9(2), 85–91. https://doi.org/10.1053/joca.2000.0363

McGuinness, LA, Higgins, JPT. Risk-of-bias VISualization (robvis): An R package and Shiny web app for visualizing risk-of-bias assessments. *Res Syn Meth*. 2020; 1- 7. https://doi.org/10.1002/jrsm.1411

Miyagi, M., Ishikawa, T., Kamoda, H., Suzuki, M., Inoue, G., Sakuma, Y., Oikawa, Y., Orita, S., Uchida, K., Takahashi, K., Takaso, M., Ohtori, S., Miyagi, M., Ishikawa, T., Kamoda, H., Suzuki, M., Inoue, G., Sakuma, Y., Oikawa, Y., & Orita, S. (2017). Efficacy of nerve growth factor antibody in a knee osteoarthritis pain model in mice. *BMC Musculoskeletal Disorders*, 18, 1–8. https://doi.org/10.1186/s12891-017-1792-x

Moher, D., Shamseer, L., Clarke, M., Ghersi, D., Liberati, A., Petticrew, M., Shekelle, P., Stewart, L. A., & Group, P.-P. (2015). Preferred reporting items for systematic review and meta-analysis protocols (PRISMA-P) 2015 statement. *Systematic Reviews*, *4*(1), 1. https://doi.org/10.1186/2046-4053-4-1

Nakamura, H., Vo, P., Kanakis, I. et al. Aggrecanase-selective tissue inhibitor of metalloproteinase-3 (TIMP3) protects articular cartilage in a surgical mouse model of osteoarthritis. *Sci Rep* 10, 9288 (2020). https://doi.org/10.1038/s41598-020-66233-0

Neogi, T., & Zhang, Y. (2013). Epidemiology of osteoarthritis. Rheumatic diseases clinics of North America, 39(1), 1–19. https://doi.org/10.1016/j.rdc.2012.10.004

O-Sullivan, I., Natarajan Anbazhagan, A., Singh, G., Ma, K., Green, S. J., Singhal, M., Wang, J., Kumar, A., Dudeja, P. K., Unterman, T. G., Votta-Velis, G., Bruce, B., van Wijnen, A. J., & Im, H. J. (2022). *Lactobacillus acidophilus* Mitigates Osteoarthritis-Associated Pain, Cartilage Disintegration and Gut Microbiota Dysbiosis in an Experimental Murine OA

Model. *Biomedicines*, *10*(6), 1298. https://doi.org/10.3390/biomedicines10061298

Perry, J., McCarthy, H. S., Bou-Gharios, G., van 't Hof, R., Milner, P. I., Mennan, C., & Roberts, S. (2020). Injected human umbilical cord-derived mesenchymal stromal cells do not appear to elicit an inflammatory response in a murine model of osteoarthritis. *Osteoarthritis and Cartilage Open*, 2(2), 100044. https://doi.org/10.1016/j.ocarto.2020.100044

Pitcher, T., Sousa-Valente, J., & Malcangio, M. (2016). The Monoiodoacetate Model of Osteoarthritis Pain in the Mouse. *Journal of Visualized Experiments* : JoVE, 111. https://doi.org/10.3791/53746

Pritzker, K. P., Gay, S., Jimenez, S. A., Ostergaard, K., Pelletier, J. P., Revell, P. A., Salter, D., & van den Berg, W. B. (2006). Osteoarthritis cartilage histopathology: grading and staging. *Osteoarthritis and cartilage*, 14(1), 13–29. https://doi.org/10.1016/j.joca.2005.07.014

Sampson, E. R., Hilton, M. J., Tian, Y., Chen, D., Schwarz, E. M., Mooney, R. A., Bukata, S. V, O'Keefe, R. J., Awad, H., Puzas, J. E., Rosier, R. N., & Zuscik, M. J. (2011). Teriparatide as a chondroregenerative therapy for injury-induced osteoarthritis. *Science Translational Medicine*, 3(101), 101ra93. https://doi.org/10.1126/scitranslmed.3002214

Shea, M. K., Booth, S. L., Harshman, S. G., Smith, D., Carlson, C. S., Harper, L., Armstrong, A. R., Fang, M., Cancela, M. L., Márcio Simão, & Loeser, R. F. (2020). The effect of vitamin K insufficiency on histological and structural properties of knee joints in aging mice. *Osteoarthritis and cartilage open*, *2*(3), 100078. https://doi.org/10.1016/j.ocarto.2020.100078

Shu, C. C., Jackson, M. T., Smith, M. M., Smith, S. M., Penm, S., Lord, M. S., Whitelock, J. M.,

Little, C. B., & Melrose, J. (2016). Ablation of Perlecan Domain 1 Heparan Sulfate Reduces Progressive Cartilage Degradation, Synovitis, and Osteophyte Size in a Preclinical Model of Posttraumatic Osteoarthritis. *Arthritis & Rheumatology*, 68(4), 868–879. https://doi.org/10.1002/art.39529

Sophocleous, A., Azfer, A., Huesa, C. et al. Probiotics Inhibit Cartilage Damage and Progression of Osteoarthritis in Mice. *Calcif Tissue Int* (2022). https://doi-org.ezproxy.uta.edu/10.1007/s00223-022-01030-7

Sousa-Valente, J., Calvo, L., Vacca, V., Simeoli, R., Arévalo, J. C., & Malcangio, M. (2018). Role of TrkA signalling and mast cells in the initiation of osteoarthritis pain in the monoiodoacetate model. *Osteoarthritis & Cartilage*, 26(1), 84–94. https://doi.org/10.1016/j.joca.2017.08.006

Sterne JAC, Savović J, Page MJ, Elbers RG, Blencowe NS, Boutron I, Cates CJ, Cheng H-Y, Corbett MS, Eldridge SM, Hernán MA, Hopewell S, Hróbjartsson A, Junqueira DR, Jüni P, Kirkham JJ, Lasserson T, Li T, McAleenan A, Reeves BC, Shepperd S, Shrier I, Stewart LA, Tilling K, White IR, Whiting PF, Higgins JPT. RoB 2: a revised tool for assessing risk of bias in randomised trials. *BMJ* 2019; 366: l4898

Sterne JAC, Hernán MA, Reeves BC, Savović J, Berkman ND, Viswanathan M, Henry D, Altman DG, Ansari MT, Boutron I, Carpenter JR, Chan AW, Churchill R, Deeks JJ, Hróbjartsson A, Kirkham J, Jüni P, Loke YK, Pigott TD, Ramsay CR, Regidor D, Rothstein HR, Sandhu L, Santaguida PL, Schünemann HJ, Shea B, Shrier I, Tugwell P, Turner L, Valentine JC, Waddington H, Waters E, Wells GA, Whiting PF, Higgins *JPT*. ROBINS-I: a tool for assessing risk of bias in non-randomized studies of interventions. BMJ 2016; 355; i4919.

Stiffel, V., Rundle, C. H., Sheng, M. H.-C., Das, S., & Lau, K.-H. W. (2020). A Mouse Noninvasive Intraarticular Tibial Plateau Compression Loading-Induced Injury Model of Posttraumatic Osteoarthritis. *Calcified Tissue International*, *106*(2), 158–171. https://doi.org/10.1007/s00223-019-00614-0

Thomas, N. P., Li, P., Fleming, B. C., Chen, Q., Wei, X., Xiao-Hua, P., Li, G., & Wei, L. (2015). Attenuation of cartilage pathogenesis in post-traumatic osteoarthritis (PTOA) in mice by blocking the stromal derived factor 1 receptor (CXCR4) with the specific inhibitor, AMD3100. *Journal of Orthopaedic Research* : Official Publication of the Orthopaedic Research Society, 33(7), 1071–1078. https://doi.org/10.1002/jor.22862

Toupet, K., Maumus, M., Luz-Crawford, P., Lombardo, E., Lopez-Belmonte, J., van Lent, P., Garin, M. I., van den Berg, W., Dalemans, W., Jorgensen, C., & Noël, D. (2015). Survival and biodistribution of xenogenic adipose mesenchymal stem cells is not affected by the degree of inflammation in arthritis. *PloS One*, 10(1), e0114962. https://doi.org/10.1371/journal.pone.0114962

Tsuchiya, S., Ohashi, Y., Ishizuka, S., Ishiguro, N., O'Rourke, D. P., Knudson, C. B., & Knudson, W. (2020). Suppression of murine osteoarthritis by 4-methylumbelliferone. *Journal of orthopaedic research : official publication of the Orthopaedic Research Society*, *38*(5), 1122–1131. https://doi.org/10.1002/jor.24541

van der Kraan, P. M., Vitters, E. L., van de Putte, L. B., & van den Berg, W. B. (1989). Development of osteoarthritic lesions in mice by "metabolic" and "mechanical" alterations in the knee joints. *The American journal of pathology*, 135(6), 1001–1014.

Veronesi, F., Giavaresi, G., Maglio, M., Scotto d'Abusco, A., Politi, L., Scandurra, R., Olivotto, E., Grigolo, B., Borzì, R. M., & Fini, M. (2017). Chondroprotective activity of N-acetyl

phenylalanine glucosamine derivative on knee joint structure and inflammation in a murine model of osteoarthritis. *Osteoarthritis and Cartilage*, 25(4), 589–599. https://doi.org/10.1016/j.joca.2016.10.021

Wang, Q., Pan, X., Wong, H. H., Wagner, C. A., Lahey, L. J., Robinson, W. H., & Sokolove, J. (2014). Oral and topical boswellic acid attenuates mouse osteoarthritis. *Osteoarthritis & Cartilage*, 22(1), 128–132. https://doi.org/10.1016/j.joca.2013.10.012

Wegner, A. M., Campos, N. R., Robbins, M. A., Haddad, A. F., Cunningham, H. C., Yik, J. H. N., Christiansen, B. A., & Haudenschild, D. R. (2019). Acute Changes in NADPH Oxidase 4 in Early Post-Traumatic Osteoarthritis. *Journal of Orthopaedic Research* : Official Publication of the Orthopaedic Research Society, 37(11), 2429–2436. https://doi.org/10.1002/jor.24417

Wei, W., Clockaerts, S., Bastiaansen-Jenniskens, Y. M., Gierman, L. M., Botter, S. M., Bierma-Zeinstra, S. M. A., Weinans, H., Verhaar, J. A. N., Kloppenburg, M., Zuurmond, A.-M., & van Osch, G. J. V. M. (2014). Statins and fibrates do not affect development of spontaneous cartilage damage in STR/Ort mice. *Osteoarthritis & Cartilage*, 22(2), 293–301. https://doi.org/10.1016/j.joca.2013.11.009

Wu, C.-L., Kimmerling, K. A., Little, D., & Guilak, F. (2017). Serum and synovial fluid lipidomic profiles predict obesity-associated osteoarthritis, synovitis, and wound repair. *Scientific Reports*, 7, 44315. https://doi.org/10.1038/srep44315

Xia, Q., Zhu, S., Wu, Y., Wang, J., Cai, Y., Chen, P., Li, J., Heng, B. C., Ouyang, H. W., & Lu, P. (2015). Intra-articular transplantation of atsttrin-transduced mesenchymal stem cells ameliorate osteoarthritis development. *Stem Cells Translational Medicine*, 4(5), 523–531. https://doi.org/10.5966/sctm.2014-0200

Xie, F., Kovic, B., Jin, X., He, X., Wang, M., & Silvestre, C. (2016). Economic and Humanistic Burden of Osteoarthritis: A Systematic Review of Large Sample Studies. PharmacoEconomics, 34(11), 1087–1100. https://doi.org/10.1007/s40273-016-0424-x

Yotsuya, M., Iriarte-Diaz, J., & A Reed, D. (2020). Temporomandibular Joint Hypofunction Secondary to Unilateral Partial Discectomy Attenuates Degeneration in Murine Mandibular Condylar Cartilage. *The Bulletin of Tokyo Dental College*, 61(1), 9–19. https://doi.org/10.2209/tdcpublication.2019-0008

Zaki, S., Smith, M. M., & Little, C. B. (2021). Pathology-pain relationships in different osteoarthritis animal model phenotypes: it matters what you measure, when you measure, and how you got there. *Osteoarthritis and cartilage*, *29*(10), 1448–1461. https://doi.org/10.1016/j.joca.2021.03.023

Ziemian, S. N., Ayobami, O. O., Rooney, A. M., Kelly, N. H., Holyoak, D. T., Ross, F. P., & van der Meulen, M. C. H. (2021). Low bone mass resulting from impaired estrogen signaling in bone increases severity of load-induced osteoarthritis in female mice. *Bone*, *152*, 116071. https://doi.org/10.1016/j.bone.2021.116071

Ziemian, S. N., Witkowski, A. M., Wright, T. M., Otero, M., & van der Meulen, M. C. H. (2021). Early inhibition of subchondral bone remodeling slows load-induced posttraumatic osteoarthritis development in mice. *Journal of bone and mineral research : the official journal of the American Society for Bone and Mineral Research*, *36*(10), 2027–2038. https://doi.org/10.1002/jbmr.4397

CHAPTER 3

(Published Article in Frontiers of Aging)

RNAseq of Osteoarthritic Synovial Tissues: Systematic Literary Review

Logan Moore[1], Zui Pan[1], Marco Brotto[1*]

Bone Muscle Research Center, College of Nursing and Health, University of Texas at Arlington, Arlington, TX, USA

*Correspondence:

Marco Brotto

Marco.brotto@Uta.edu

A version of this chapter has been published: Moore, L., Pan, Z., & Brotto, M. (2022). RNAseq of Osteoarthritic Synovial Tissues: Systematic Literary Review [Systematic Review]. *Frontiers in Aging*, *3*. https://doi.org/10.3389/fragi.2022.836791

Abstract

Osteoarthritis (OA) is one of the most common causes of disability in aged people, and it is defined as a degenerative arthropathy, characterized by the disruption in joint tissue. The synovium plays a vital role in maintaining the health of the joint by supplying the nutrients to the surrounding tissues and the lubrication for joint movement. While it is well known that all the joint tissues are communicating and working together to provide a functioning joint, most studies on OA have been focused on bone and cartilage but much less about synovium have been reported. The purpose of this review was to investigate the current literature focused on RNA sequencing (RNAseq) of osteoarthritic synovial tissues to further understand the dynamic transcriptome changes occurring in this pivotal joint tissue. A total of 3 electronic databases (PubMed, CINHAL Complete, and Academic Complete) were systematically searched following PRISMA guidelines. The following criteria was used for inclusion: English language, free full text, between the period 2011 – 2022, size of sample (n>10), study design being either retrospective or prospective, and RNAseq data of synovial tissue from OA subjects. From the initial search, 174 articles, 5 met all of our criteria and were selected for this review. The RNAseq analysis revealed several differentially expressed genes (DEGs) in synovial tissue. These genes are related to the inflammatory pathway and regulation of the extracellular matrix. The MMP family, particularly MMP13 was identified by three of the studies, indicating its important role in OA. IL6, a key contributor in the inflammation pathway, was also identified in 3 studies. There was a total of 8 DEGs, MMP13, MMP1, MMP2, APOD, IL6, TNFAIP6, FCER1G, and IGF1 that overlapped in 4 out of the 5 studies. One study focused on microbial RNA in the synovial tissue found that the microbes were differentially expressed in OA subjects too. These differentially expressed microbes have also been linked to the inflammatory pathway.

Further investigation with more clinical gene profiling in synovial tissue of OA subjects is required to reveal the causation and progression, as well as aid in the development of new treatments.

Introduction

Osteoarthritis (OA) is a chronic, debilitating joint disease. It is clinically defined as disruption and potential loss of joint cartilage, as well as changes to other joint tissues (Glyn-Jones et al. 2015; Johnson and Hunter 2014; Neogi and Zhang 2013; Vina and Kwoh 2018). OA can occur in any population, and the causation is multifactorial such as age, sex, obesity, previous history of injury, and genetic disposition (Johnson and Hunter 2014; Glyn-Jones et al. 2015; Blagojevic et al. 2010). As a painful disease, OA is one of the most common causes of disability, especially in aged people (Johnson and Hunter 2014; Glyn-Jones et al. 2015; Neogi and Zhang 2013). Currently, there is no known cure and limited treatments for OA patients, including lifestyle changes, exercise, pain medication, and in the most severe cases surgery Click or tap here to enter text.(Johnson and Hunter 2014; Bannuru et al. 2019). The prevalence of this disease is predicted rising due to the rise of obesity rates and the aging population (Johnson and Hunter 2014; Blagojevic et al. 2010). The CDC estimates by the year of 2040 78 million US adults will be affected by OA, an increase by 20 million as compared to now (Barbour et al. 2017). This places a major public health burden with annual indirect cost ranging from approximately 1,400 to 22,000 USD per patient (Johnson and Hunter 2014; Xia et al. 2015).

It is well established that all the joint tissues are communicating and working together to provide a functioning joint. Hyaline cartilage is the dense connective tissue that forms a smooth articulating surface for joints (Goldring 2020; Rovenský and Payer 2009). The hyaline cartilage is avascularized and is dependent on the nutrients provided by the synovium (Rovenský and Payer 2009; Smith and Wechalekar 2015). The synovium is a soft tissue that lines the joint cavity except for the cartilage (Smith and Wechalekar 2015; Veale and Firestein 2017). It contains a rich network of blood and lymphatic vessels in which provide the nutrients for

homeostasis in the joint (Veale and Firestein 2017). It also secretes synovial fluid, comprised of hyaluronan, lubricin, lactoferrin and proinflammatory and anti-inflammatory cytokines (Veale and Firestein 2017; Smith and Wechalekar 2015; Petty and Cassidy 2005; Stark, Grzelak, and Hadfield 2019; Guilen et al., 1998). The synovial fluid is a highly viscous material that aids in the lubrication of the joint space for smooth articulation (Stark, Grzelak, and Hadfield 2019; Petty and Cassidy 2005). Thus, the synovial tissues are vitally important in protection, maintenance, and homeostasis of the joint. While hyaline cartilage is typically at the forefront of OA research as it is seen as the most effected joint tissue, yet, much less about synovium have been reported.

Comparing the gene expression pattern in synovial cells from OA patients to that from healthy subjects can provide important information to understand the cellular mechanism underlying the pathology of OA, which may shed light to identification of new therapeutic targets. The complete set of gene expression pattern, i.e., transcriptome ("Transcriptome" 2014), can be obtained by high-throughput techniques such as microarrays and RNA sequencing (RNAseq) (O'Leary et al. 2016). RNAseq was first introduced over a decade ago and is still considered the next generation of transcriptome analysis (Z. Wang, Gerstein, and Snyder 2009; Kukurba and Montgomery 2015). Due to the development of faster and cheaper sequencing technique, RNAseq becomes to be a standard research tool to provide whole transcriptome-wide analysis (Kukurba and Montgomery 2015; Z. Wang, Gerstein, and Snyder 2009; Stark, Grzelak, and Hadfield 2019). It allows researchers to investigate the regulation of genes by their level of expression, also if there are changes or mutations in a certain transcriptome (Kukurba and Montgomery 2015).

This review is to collect and analyze the current literature on the dynamic transcriptional changes occurring in osteoarthritic synovial tissue, which may assist to identify the potential causation of OA and to provide targets for therapies.

Methods

Three electrotonic online databases, PubMed, CINHAL Complete, and Academic Search Complete, were systematically searched using the guidelines set forth by the Preferred Reporting Items for Systematic Reviews and Meta-analysis (PRISMA) (Moher et al. 2015). The initial, investigatory search was completed at the conception of this study, February 2021. The final systematic search was conducted in May 2022. The following key words were used for the search string: “Osteoarthritis”, “RNA sequencing”, “RNAseq”, “RNA-seq”, “Synovial”, Synovium”. The key words were joined by either “AND” or “OR”.

For inclusion in this review articles needed to meet the following criteria: 1) English Language, 2) Free full text available, 3) Study design followed either retrospective or prospective design, 4) between the period 2011 and 2022, 5) sample population groups greater than 10 samples, 6) RNAseq performed on osteoarthritic synovial tissue.

Articles were excluded if they did not meet the stated inclusion criteria. A priori to the search it was deemed the articles needed to be of the utmost caliber and rigor, therefore non-peer-reviewed articles, newspapers, and editorials were excluded. Only articles of the English language were included, to ensure proper interpretation from the reviewer. Since the review is a systematic review, all systematic reviews, narrative reviews, or meta-analysis were excluded. All abstracts, study protocols, and pilot data were excluded. A prior it was determined only completed articles with groups larger than 10 participants per group were included, to ensure precision of results.

Following each search, the results were downloaded for importation into a reference manager. The results were downloaded in two formats .bib and .csv. The reference manager was used for duplicate removal and storage of full text. To ensure the reference manager was correct, all resulting articles were also managed in a separate spreadsheet. After duplicate removal, a broad scan of titles and abstracts was conducted eliminating any articles that were obviously not meeting the inclusion/exclusion criteria. The resulting full text of the articles was reviewed for inclusion.

The final studies were assessed for bias. The resulting bias assessment did not dictate inclusion or exclusion in this review, but rather serves as further information on the quality of the articles included. Either the Revised Cochrane risk-of-bias tool for randomized trials (RoB2) or The Risk of Bias in Non-randomized Studies of Interventions (ROBINS-I) were used to determine bias based on their classification type of clinical study either being retrospective, clinical case series, prospective or randomized control trials as indicated by The National Health and Medical Research Council (NHMRC. 2000) (Sterne et al. 2019; 2016). RoB2 was used for randomized control studies and ROBINS-I was used for non-randomized control studies. The tool robvis was used for the visualization of the results (McGuinness and Higgins 2021).

Results

Through the initial search, a total of 174 articles were found (see **figure 1**.). Duplicate removal removed 100 articles. This shows that there was consistent overlap in the literature between search strings and without variation of the search string articles may have been missed. The titles and abstracts were broadly reviewed. A total of 46 articles were removed for not meeting inclusion/exclusion criteria. The remaining articles (n=28) had the full text reviewed. After full text review, 5 articles met the inclusion/exclusion criteria set a priori. Exclusion from this review mainly resulted from RNAseq not being performed on osteoarthritic synovial tissue, incomplete data, or not enough samples per group. The search was updated periodically throughout the drafting of this manuscript and the final literature search was in02

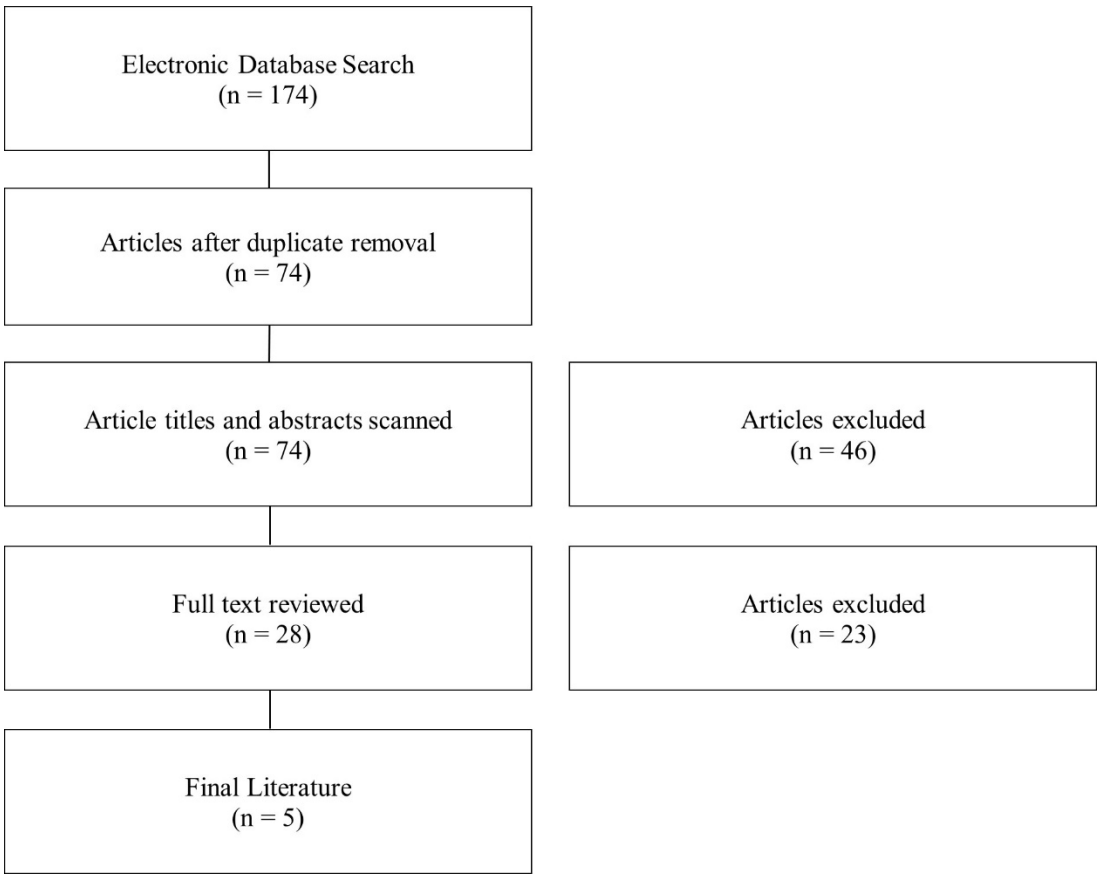

Figure 3-1: Flow Diagram of literary search strategy and eligibility

The 5 studies included in this review were all published between 2020 and 2022 (see Table 1.). Three articles were published from the United States (USA) (Tsai et al. 2020; Li and Zheng 2020; McCoy et al. 2020), one article was jointly published from Germany and the UK (Steinberg et al. 2021), and one article jointly published from China and the USA (Huang et al., 2021). The articles were either defined as a retrospective or prospective. The two retrospective studies obtained their RNAseq data from the NCBI GEO DataSets (https://www.ncbi.nlm.nih.gov/gds), in which one used the data from USA Human OA subjects (Li and Zheng 2020) and the other used Australian Human OA subjects (Tsai et al. 2020). In the three prospective studies, one used a post-traumatic equine model, and two used synovial tissue obtained prior to arthroplasty of either the hip or knee in human subjects (Steinberg et al. 2021; Huang et al., 2021).

Table 3-1: Data summary of the 5 selected articles for review

Authors	Year	Country	Type of study	Sample Composition
Tsai et al.	2020	USA	Retrospective	14 Human OA
Li et al.	2020	USA	Retrospective	20 Human Knee OA
McCoy et al.	2020	USA	Prospective	11 Post-traumatic OA equine
Steinberg et al.	2021	Germany, UK	Prospective	90 Human knee OA
Huang et al.	2021	China, USA	Prospective	14 Human Knee OA

When the synovium from the OA patients (n=20) were compared to that from the healthy controls, 372 genes were identified as differential expression genes (DEG) (Li and Zheng 2020). Of those genes 188 had increased expression and 184 had decreased levels of expression (Li and Zheng 2020). Using the UniProt system, the authors identified 10 DEGs related to the

inflammatory pathway that were significantly altered (Li and Zheng 2020). These DEG are: Apolipoprotein D (APOD), Complement CLq subcomponent subunit B (C1QB), N-formyl peptide receptor 3 (FPR3), Histone cluster 1 H3 family member b (HIST1H3B), Interferon epsilon (IFNE), Macrophage scavenger receptor type I (MSR1), Lymphokine-activated killer T-cell-originated protein kinase (PBK), Tumor necrosis factor-inducible gene 6 protein (TNFAIP6), Triggering receptor expressed on myeloid cells I (TREM1), and V-set and immunoglobulin domain-congaing protein 4 (VSIG4). Li et al. also found there are 7 genes that were significantly altered that contribute to the functionality of the Extracellular Matrix (ECM). Those 7 genes are Myocilin (MYOC), Amelotin (AMTN), Chitinase-3-like protein 2 (CHI3L2), Prolyl endopeptidase Fibroblast activation protein alpha (FAP), Leucine-rich repat-containing protein 15 (LRRC15), Matrix Metallopeptidase-13 (MMP13), TNFAIP6 (C. Li and Zheng 2020).

In single cell RNAseq conducted by Huang et al. they profiled over 93,000 synovial cells from 14 knee OA individuals (female, age: 70.7±5.9 years; BMI: 25.9±4.4 kg/m^2). They were able to identify 7 distinct cell types: fibroblasts (59%), antigen presenting cells (APCs) (13.6%), T cells (11.4%), endothelial cells (ECs) (10%), mural cells (3%), B cells (1.8%) and mast cells (1%) along with 43 DEGS. The APCs had 4 cell subtypes: Transitional macrophages, fibrotic immune regulated macrophages, interferon stimulated macrophages, and S100A8/9^{hi} macrophages. These macrophage cell types showed high expression in genes related to inflammation and the inflammatory pathway, such as IL6 (Interterluekin-6), CCL3 (C-C Motif Chemokine Ligand 3), CCL3L1 (C-C Motif Chemokine Ligand 3 Like 1), IL1A (Interleukin-1 alpha) IL1B (Interleukin-1 Beta), TLR2 (Toll-like receptor 2). However, transitional

macrophages also showed high expression in inflammation resolving genes IGF1 (Insulin Like Growth Factor 1) and MRC1 (Mannose receptor C-type 1).

McCoy et al. used a post-traumatic OA equine model (n=11) to demonstrate the effects of OA on the synovium (McCoy et al. 2020). In this study, a larger amount of DEGs was reported as compared to Li et al. It was found that there were 397 genes that had been upregulated, and 365 genes down regulated (McCoy et al. 2020). Using a Markov clustering algorithm 213 DEGs were able to be assigned to 28 unique clusters. Nine of the clusters had equal to or greater than 10 DEGs, detailed in the Supplementary Table. There were significant alterations in gene expression pathways for ECM organization and protein metabolism (McCoy et al. 2020).

Based upon RNAseq data from the synovial lining of OA patients (n=90), Steinberg et al. identified two groups of OA patients, low-grade and high-grade OA (Steinberg et al. 2021). Steinberg et al. defined low-grade OA as having largely intact cartilage as compared to the degraded tissue in the high-grade group. The authors showed that there are DEGs in the inflammatory pathway between high-grade OA and low-grade OA. Furthermore, the low-grade OA group can be subdivided into two subgroups based on the changes in transcription in the ECM pathway. The authors developed a predictive tool to detect low-grade OA in the knee based on 7 DEGs (MMP1, MMP2, MMP13, APOD, IL6, CYTL1 (Cytokine-like 1), C15orf48 (Chromosome 15 open reading frame 48)) related to the inflammatory pathway (Steinberg et al. 2021).

Using GEO RNAseq data, Tsai et al. found 299 bacterial species in OA synovial biopsies (n=14) (Tsai et al. 2020). A total of 84 bacterial species were found in healthy synovial biopsies, however not all the microbial species were found in the synovium of OA samples. There were 43 microbes to be found differentially abundant in the OA samples as compared to the healthy,

detailed in the Supplementary Table. Of the 43 differentially abundant microbes, 27 of them were species of Pseudomonas. The bacterium found in OA synovial biopsies can be linked to immune signatures and immune cell types (Tsai et al. 2020)

Comparing the 5 studies selected there were only 8 DEGs that were represented in multiple studies, with 2 DEGs being represented in 3 of the 5 studies (see. Figure 2). Tsai et al. had no overlapping DEGs as this study analyzed microbial RNA as compared to the others. The 8 DEGs that were represented in at least 2 studies were: MMP1, MMP2, MMP13, APOD, TNFAIP6, IL6, FCER1G, and IGF1. Three of the overlapping DEGs, APOD, TNFAIP6, and IL6 are all genes that have been found to regulate the pro-inflammatory pathway (Li and Zheng 2020; McCoy et al. 2020; Steinberg et al. 2021, Huang et al., 2021). IL6 was differently expressed in 3 of the 5 studies and is a key contributor to modulating inflammation in both acute and chronic inflammation (McCoy et al. 2020; Huang et al. 2021; Steinburg et al. 2021; Safran et al., 2022). IL6 has a crucial role in the pathology of OA, as it induces MMP13 and through pathway signaling reduces the sensitization of IGF1 (Wiegertjes et al. 2020). IGF1 was shown to be highly expressed having a role in the inflammation resolving pathway, as well as having a role in enhanced extracellular matrix production and inhibition of apoptosis in chondrocytes. (McCoy et al. 2020; Huang et al. 2021; Wen et al. 2021). The gene MMP13 was represented in 3 of the 5 studies included. MMP13 is a gene that encodes a peptidase in the matrix metalloproteinases (MMP) family (Safran et al., 2022). MMP13 when synthesized must be proteolytically processed to become a matured protease (Salerno et al. 2020). This activated protease is known to cleave type II collagen (Garnero 2007; Salerno et al. 2020; O'Leary et al. 2016). The MMP family of genes has been shown to be upregulated in OA patients and linked to the cartilage destruction through the breakdown of collagen fibers (Davidson et al. 2006; McCoy

et al. 2020). In OA samples the MMP family was seen to be upregulated by 8.5 to 12.7fold (McCoy et al. 2020).

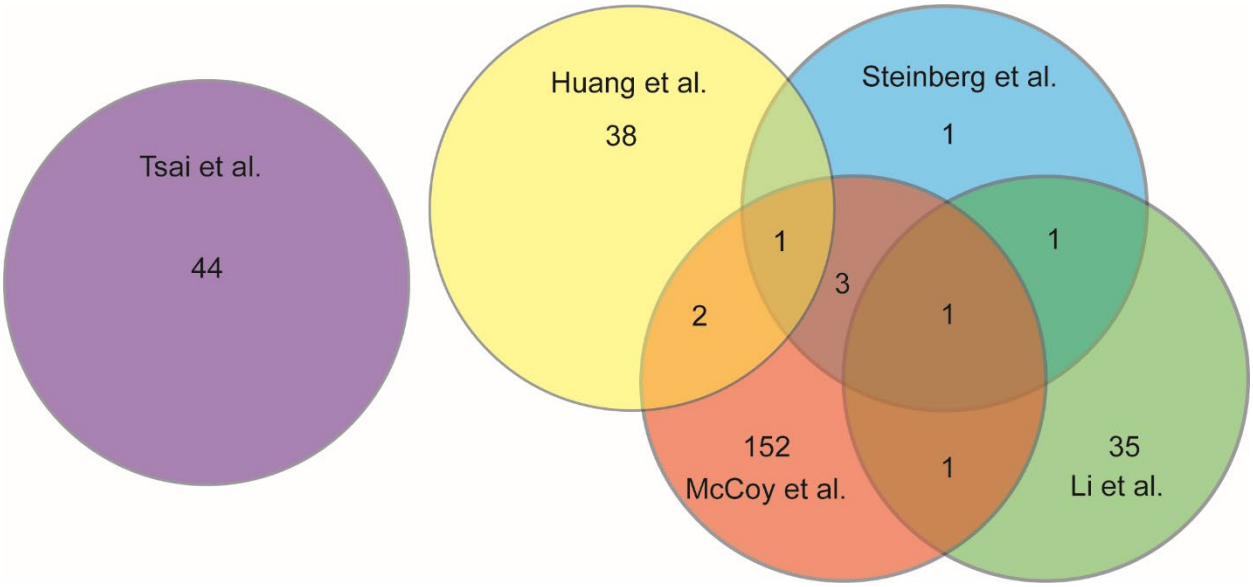

Figure 3-2: Venn diagram analyzing the overlap of DEGs discussed in each study chosen for this review

Risk of bias was assessed for each included article. All remaining articles were determined to be non-randomized control trials. Therefore, only the ROBIN-1 assessment tool was used. A priori to assessing the articles it was determined that the confounding domains were gender, age, previous history of injury, and intervention pre-sampling of the synovial tissue. Of the 5 articles selected for this review two articles scored a low risk of bias (see. Figure 3.) (Tsai et al. 2020; Huang et al. 2021). The remaining 3 articles were found to have a serious risk of bias due to confounding domains (C. Li and Zheng 2020a; McCoy et al. 2020; Steinberg et al. 2018). To

score a serious risk of bias in domain 1, the articles either did not account or report gender differences, previous history of injury, or intervention pre-sampling.

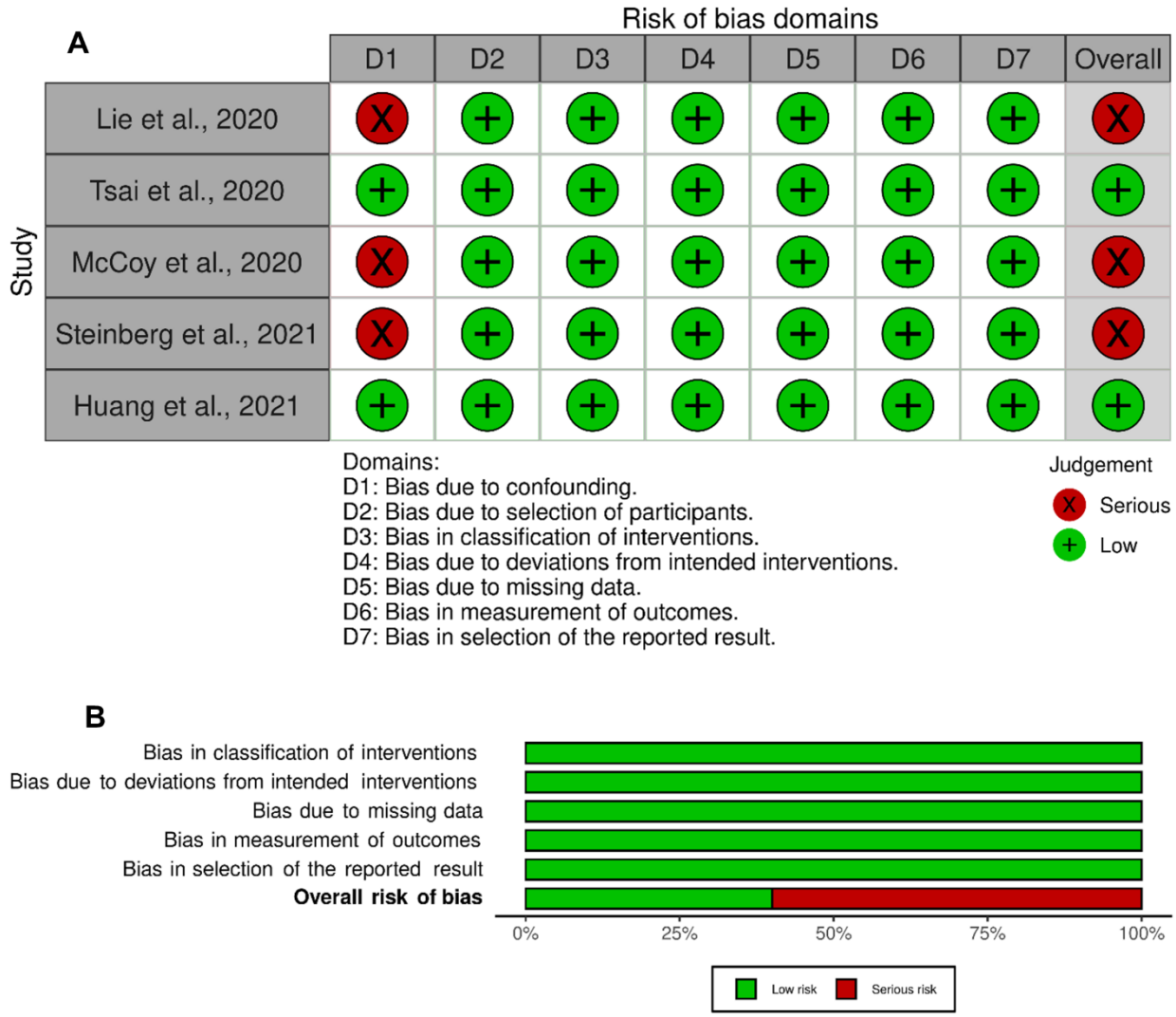

Figure 3-3: Bias Reporting, (A) Bias domains for ROBINS-I for the included studies. (B) Total Score for each ROBINS-I score.

Discussion

It is evident that the RNAseq is a relative new technique in the field of OA research, as all the articles selected for this study are between 2020 and 2021, and only 4 articles met the

inclusion/exclusion criteria. In the 4 articles, each showed significant alterations in gene expression in the synovial tissue of OA subjects. The genes shown to be differentially expressed have contributing roles in the destruction of collagen fibers and inflammation of the joint. The understanding of the mechanisms and pathways which contribute to the progression of OA will aid in the development of new therapies, interventions, and detection methods.

Synovial tissue plays a pivotal role in the causality and progression of OA. This is illustrated by the dynamic changes found in the transcriptome produced through RNAseq. Each study selected for this review showed significant DEGs as compared to the healthy controls. In a PTOA equine model it showed that there were as many as 762 changes in the transcriptome, and in a human OA model there were as many as 372 DEGs. There was 8 DEGs that were discussed in 2 or more of the studies included, and 2 DEGs that was discussed in 3 out of the 5 studies. The 8 DEGs (MMP1, MMP2, MMP13, FAPOD, IL6, TNFAIP6, FCER1G, IGF1) require future investigation as potential biomarkers in the onset or progression of OA (see Table 2.).

Table 3-2: The 8 DEGS found to overlap in the 5 studies (Safran et al., 2022)

Gene		Article Found	Description
MMP13	Matrix Metallopeptidase 13	Li et al., McCoy et al., Steinberg et al.	Associated with the breakdown of the extracellular matrix. Member of the M10 family of matrix metalloproteinases. The associated mature protease cleaves type II collagen and is involved in the turnover of articular cartilage.
MMP1	Matrix Metallopeptidase 1	McCoy et al., Steinberg et al.	Associated with the breakdown of the extracellular matrix. Member of the M10 family of matrix metalloproteinases. The associated mature protease breakdown interstitial collagens (type I, II, and II).
MMP2	Matrix Metallopeptidase 2	McCoy et al., Steinberg et al.	Associated with the breakdown of the extracellular matrix. The associated protease differs from other MMP family members as it is activated on the cell membrane either extracellularly or intracellularly. It is responsible for the breakdown of collagen type IV and V and elastin.
APOD	Apolipoprotein D	Li et al., Steinberg et al.	Encodes for a high-density lipoprotein, which is a family member of the lipocalins. The associated lipoprotein is involved in the binding and transport of bilin.
IL6	Interleukin 6	McCoy et al., Steinberg et al., Huang et al.	Encodes for a pro-inflammatory cytokine, and the protein is produced at sites of acute and chronic inflammation. It is associated with inducing the acute phase immune response.
TNFAIP6	Tumor Necrosis Factor Alpha-Inducible Protein 6	Li et al., McCoy et al.	Associated with the maintenance of the extracellular matrix and can be induced through pro-inflammatory cytokines. The associated secretory protein is a member of the hyaluronan-binding protein family.
FCER1G	Fc Epsilon Receptor IG	McCoy et al., Huang et al.	Encodes for an adaptor protein which produces activation signaling in immunoreceptors. Contributes to the cell differentiation of T-cells
IGF1	Insulin Like Growth Factor 1	McCoy et al., Huang et al.	Associated with mediating growth and development. The associated protein activates tyrosine kinase activity, and downstream activates the P13K-AKT/PKB and the Ras-MAPK pathways.

The regulation of the MMP family and more specifically MMP13 has already become a topic of interest as seen in recent studies (Salerno et al. 2020; Bai et al. 2020; M. Wang et al. 2013; H. Li et al. 2017; Murphy and Lee 2005). Cells found in the synovium and in cartilage both are found to express MMP13 (Murphy and Lee 2005; Davidson et al. 2006). In the Biological Process (GO) found in the STRING network, the terms related to MMP13 are extracellular matrix organization, extracellular matrix disassembly, collagen catabolic process, skeletal system development, and multicellular organismal process ("Mmp13 Protein (Human)"). Davidson et al. confirms the results of these studies by showing a significant upregulation in both synovium and cartilage using quantitative PCR (Davidson et al. 2006). MMP13 plays a central role in the degradation of extracellular matrix by degrading collagen type I, II, III, IV, XIV, and X, with its highest activity being collagen type II (Murphy and Lee 2005; "MMP13 Gene"). MMP13 is thought to be an important factor in the early onset and progression of OA (Davidson et al. 2006; M. Wang et al. 2013; Sato et al. 2006). MMP13 is now a targeted gene in potential therapies (Salerno et al. 2020; M. Wang et al. 2013). In a study conducted by Wang et al., MMP13 is shown be a significant regulator in OA progression (M. Wang et al. 2013). Using a MMP13 knock out mouse, after OA induction by meniscal-ligamentous injury the knockout (Mmp13Col2ER) mice showed significant decrease in degeneration of cartilage/OA progression at 8, 12, and 16 weeks (M. Wang et al. 2013). The potential of being able decrease or eliminate the destruction of cartilage through regulating MMP13 and the MMP family, could provide clinical and preventative treatments of OA. This implication would have a major impact on the future of OA research and most importantly the wellbeing of the effected patients. While in cartilage the down regulating the production of the MMP family and MMP13 may have beneficial effects to the development of OA it may have detrimental effects in other joint tissues.

It was shown recently that MMP13 plays a vital role in osteogenic differentiation and by knocking out MMP13 osteogenic differentiation decreased (Arai et al 2021). This presents problems in global inhibition of MMP13, and the need to create tissue specific genetic inhibitors.

Inflammation of synovium or synovitis is a common pathology in OA patients (Wiegertjes et al. 2020; Ayral et al. 2005; Tsuchida et al. 204). Of the 8 overlapping DEGs found, 3 DEGs (APOD, TNFAIP6, and IL6) had roles in the pro-inflammatory pathway. IL6 is a common cytokine found in the pathogenesis of various inflammatory diseases, and recently has been a target in the treatment of OA (Laavola et al. 2018; Wiegertjes et al. 2020). In addition to the pro-inflammatory effects, IL6 has been shown to contribute to the disruption in the extracellular matrix in the cartilage of OA subjects. IL6 induces A Disintegrin and Metalloproteinase (ADAMTS) and the MMP family including MMP13, which degrades the extracellular matrix and collagen in the cartilage (Wiegertjes et al. 2020; Laavola et al 2018). In a study conducted by Laavola et al., they examined the effect of inhibition of IL6 through the treatment with stilbenoids. It was shown that stilbenoids inhibits the expression of IL6 and reduce the levels of MMPs (Laavola et al. 2018). Increased expression of IL6 can also lead to IGF-1 desensitization (Wiegertjes et al. 2018). IGF-1 is critical to the repair of the cartilage, as IGF-1 inhibits cartilage catabolism and promotes cartilage regeneration. (Wen et al. 2021). More research is needed, however the inhibition of IL6 has potential in being a superb mechanism in the treatment of OA, through the decreasing MMP and potentially restoring the sensitivity of IGF-1.

The linkage between the gut microbiome and gut permeability leading to musculoskeletal disease has been widely researched. It has been shown that gut permeability is increased in obese and aging populations, which are both predisposed to OA (Nagpal et al., 2018; Portincasa et al., 2021). There is a possible linkage between pathogenic bacteria leaking from the gut migrates

into the synovium to create systemic inflammation leading to the onset of OA (Collins et al., 2019; Tsai et al., 2020; Ulici et al., 2018). The 8 overlapping DEGs that were found have a pivotal role in modulating inflammation and degradation of cartilage, and more so the inflammatory pathway was discussed to be differently expressed in all 5 articles chosen for this review. Interestingly, the differentially abundant bacteria found by Tsai et al. were majority from the species Pseudomonas (Tsai et al. 2020). There were also E. Coli differentially expressed. Both are gram-negative bacterium, which produces lipopolysaccharide (LPS). LPS has been identified as an important factor in the development of OA, for the proinflammatory response (Huang and Kraus 2016). It was shown recently by Mendez et al. that in a post-traumatic OA mouse model given the mouse an injection of LPS prior to injury increased the development of OA (Mendez et al. 2020). The hypothesis that bacteria can increase the risk and development of OA can be shown by Ulici et al., who showed that in germ-free mice the development of OA was reduced (Ulici et al. 2018). Tsai et al. showed that 299 bacterial species were in synovial biopsies. Being able to limit the leakage of bacteria from the gut and the type of species could modulate the inflammation and progression of OA. Further research is required to illustrate the relationship between bacteria, bacterial components, and the development of OA.

OA is a chronic joint arthropathy disrupting multiple joint tissues, and the disruption in the transcriptome in the synovium plays a significant role in the onset and progression of this disease. As discussed earlier synovial tissue provides cartilage with nutrients, as well as regulates the synovial fluid. Through understanding the many dynamic changes in the transcriptome of the synovial tissue, researchers will have a greater level of discernment on the mechanisms of OA. The 5 articles that were selected in this review showed transcriptional changes in the inflammatory pathway as well as the extracellular matrix pathway. These two pathways have

been a common focus in OA research, and still more research into how modulating these pathways can decrease and prevent the detrital, and painful effects of OA is needed.

There were 2 studies selected for this review that passed all seven domains in the bias assessment. The three other articles had a high risk of bias due to confounding variables. In future research, confounding variables need to be considered, as the causation of OA is multifactorial. Accounting for these variables, such as age, gender, ethnicity, or history of injury could provide insights into new genetic links and the identification of new biomarkers for a certain subset of OA patients. Each of these studies had the samples taken at a singular time point, further research needs to be developed in longitudinal studies to show the changes in transcriptional factors over the progression of the disease.

Transcriptional analysis is important in understanding disease mechanisms, as it gives information on the amplification of genes. The regulation of these genes affects the quality, composition, and number of certain proteins in the body. Furthermore, it is important to correlate the transcriptional profile with proteomic, lipidomic, and metabolic profiles to encompass the entire mechanistic effect of the disease. In a proteomic analysis of human OA synovial fluid 677 proteins were identified. Forty percent of the proteins were extracellular, 12% had a molecular function of extracellular matrix structural constituent, and 13% of the biological processes were involved in the immune response (Balakrishnan et al., 2014) In a recent lipidomic profile and metabolomic analysis of OA synovial membrane it was found that there were 53 significantly modulated lipids (Rocha et al., 2021). Glycerophospholipids (GP) were shown to be significantly elevated and have been correlated in articular inflammation and joint degeneration (Brouwers et al., 2016; Rocha et al., 2021). Rocha et al also showed an increase in metabolomics associated with oleic acid, arachidonic acid, and lysophosphatidic acid. Arachidonic acid has been linked to

the recruitment and activation of immune cells in the early phase of inflammation (Lawrence et al., 2002; Rocha et al 2021). These results are congruent with the findings in the 5 selected articles in which there were a significant change in genes responsible for regulating the extracellular matrix and inflammatory pathway.

It has already been shown that the prevalence of OA is on the rise; the COVID-19 pandemic situation could increase the OA prevalence to an even higher level (Johnson and Hunter 2014; Blagojevic et al. 2010). Sedentary behavior and the level of sedentariness has been directly linked to the onset and severity of OA symptoms (Daste et al., 2021). Through the global shut down physical activity levels have decreased, and sedentary behavior increased (Stockwell et al. 2021). This decrease in physical activity will have adverse effects in years to come placing a greater public health need, therefore continued investments in research efforts into understanding the mechanisms and pathways of OA is urgent.

Conclusion

OA is a multi-faceted disease in which causation and progression depends not only on a single joint tissue, but all joint tissues and body as a whole. Through the understanding that there are significant transcriptional changes occurring in the synovium and synovial tissues, further research can be developed to identify potential biomarkers for detection and for treatments. There were 8 DEGS (MMP13, MMP1, MMP2, APOD, IL6, TNFAIP6, FCER1G, IGF1) that overlapped in 3 out of the 5 articles selected for this review. These 8 genes offer great potential in being recognized as biomarkers in OA, as these genes play a significant role in the regulation of the extracellular matrix and the inflammatory pathway. The creation of longitudinal studies that have a direct focus on how these genes are differently expressed will aid in creation of early detection screens and targets in gene therapy. The role in which the microbiome plays by

inspiring inflammation and causing alterations in the synovium and joint tissues needs to be further explored. Through understanding the dynamic changes in the differentially expressed bacteria the onset and progression of disease may be describe through environmental or dietary elements. The study of RNAseq of OA synovial tissue is relatively scarce but is desperately needed. More RNAseq datasets of synovial tissues during the progression of OA and among different subsets of OA patients will provide molecular mechanisms and identify genetic links to the causation and progression of OA.

References

Arai, Y., Choi, B., Kim, B. J., Park, S., Park, H., Moon, J. J., & Lee, S. H. (2021). Cryptic ligand on collagen matrix unveiled by MMP13 accelerates bone tissue regeneration via MMP13/Integrin α3/RUNX2 feedback loop. Acta biomaterialia, 125, 219–230. https://doi.org/10.1016/j.actbio.2021.02.042

Ayral, X., Pickering, E.H., Woodworth, T.G., Mackillop, N., Dougados, M., 2005. Synovitis: a potential predictive factor of structural progression of medial tibiofemoral knee osteoarthritis – results of a 1 year longitudinal arthroscopic study in 422 patients. Osteoarthritis and Cartilage 13, 361–367. doi: 10.1016/j.joca.2005.01.005

Bai, Z.-M., M.-M Kang, X.-F. Zhou, and D Wang. 2020. "CircTMBIM6 Promotes Osteoarthritis-Induced Chondrocyte Extracellular Matrix Degradation via MiR-27a/MMP13 Axis." European Review for Medical and Pharmacological Sciences 24 (15): 7927–36. https://doi.org/10.26355/eurrev_202008_22475.

Bannuru, R, M C Osani, E Vaysbrot, N K Arden, K Bennell, S M A Bierma-Zeinstra, V B Kraus, et al. 2019. "OARSI Guidelines for the Non-Surgical Management of Knee, Hip, and Polyarticular Osteoarthritis." Osteoarthritis and Cartilage 27 (11): 1578–89. https://doi.org/https://doi.org/10.1016/j.joca.2019.06.011.

Blagojevic, M., C. Jinks, A. Jeffery, and K.P. Jordan. 2010. "Risk Factors for Onset of Osteoarthritis of the Knee in Older Adults: A Systematic Review and Meta-Analysis." Osteoarthritis and Cartilage 18 (1). https://doi.org/10.1016/j.joca.2009.08.010.

Brouwers, H., Von Hegedus, J., Toes, R., Kloppenburg, M., Ioan-Facsinay, A., 2015. Lipid mediators of inflammation in rheumatoid arthritis and osteoarthritis. Best Practice & Research Clinical Rheumatology 29, 741–755. doi: 10.1016/j.berh.2016.02.003

Collins, K.H., Paul, H.A., Reimer, R.A., Seerattan, R.A., Hart, D.A., Herzog, W., 2015. Relationship between inflammation, the gut microbiota, and metabolic osteoarthritis development: studies in a rat model. Osteoarthritis and Cartilage 23, 1989–1998. doi: 10.1016/j.joca.2015.03.014

Daste, C., Kirren, Q., Akoum, J., Lefèvre-Colau, M.-M., Rannou, F., Nguyen, C., 2021. Physical activity for osteoarthritis: Efficiency and review of recommendations. Joint Bone Spine 88, 105207. doi: 10.1016/j.jbspin.2021.105207

Davidson, Rose K, Jasmine G Waters, Lara Kevorkian, Clare Darrah, Adele Cooper, Simon T Donell, and Ian M Clark. 2006. “Expression Profiling of Metalloproteinases and Their Inhibitors in Synovium and Cartilage.” Arthritis Research & Therapy 8 (4). https://doi.org/10.1186/ar2013.

Garnero, Patrick. 2007. “Chapter 8 - Biochemical Markers of Osteoarthritis.” In Osteoarthritis, edited by Leena Sharma and Francis Berenbaum, 113–30. Philadelphia: Mosby. https://www.sciencedirect.com/science/article/pii/B9780323039291500136.

Glyn-Jones, S, A J R Palmer, R Agricola, A J Price, T L Vincent, H Weinans, and A J Carr. 2015. “Osteoarthritis.” The Lancet 386 (9991): 376–87. https://doi.org/https://doi.org/10.1016/S0140-6736(14)60802-3.

Goldring, Mary B. 2020. “Cartilage Biology: Overview.” In Encyclopedia of Bone Biology, edited by Mone Zaidi, 521–34. Oxford: Academic Press. https://doi.org/10.1016/B978-0-12-801238-3.62211-0.

Guillen, C., Mcinnes, I.B., Kruger, H., Brock, J.H., 1998. Iron, lactoferrin and iron regulatory protein activity in the synovium; relative importance of iron loading and the inflammatory response. Annals of the Rheumatic Diseases 57, 309–314. doi:10.1136/ard.57.5.309

Huang, Z.Y., Luo, Z.Y., Cai, Y.R., Chou, C.-H., Yao, M.L., Pei, F.X., Kraus, V.B., Zhou, Z.K., 2022. Single cell transcriptomics in human osteoarthritis synovium and in silico deconvoluted bulk RNA sequencing. Osteoarthritis and Cartilage 30, 475–480. doi: 10.1016/j.joca.2021.12.007

Huang, Zeyu, and Virginia Byers Kraus. 2016. “Does Lipopolysaccharide-Mediated Inflammation Have a Role in OA?” Nature Reviews Rheumatology 12 (2): 123–29. https://doi.org/10.1038/nrrheum.2015.158.

Johnson, Victoria L., and David J. Hunter. 2014. “The Epidemiology of Osteoarthritis.” Best Practice & Research Clinical Rheumatology 28 (1). https://doi.org/10.1016/j.berh.2014.01.004.

Kamil E. Barbour, C. G. H., Michael Boring, Teresa J. Brady (2017). "Vital Signs: Prevalence of Doctor-Diagnosed Arthritis and Arthritis-Attributable Activity Limitation — United States, 2013–2015." Morbidity and Mortality Weekly Report 66: 246-253.

Kukurba, Kimberly R, and Stephen B Montgomery. 2015. “RNA Sequencing and Analysis.” Cold Spring Harbor Protocols 2015 (11): 951–69. https://doi.org/10.1101/pdb.top084970.

Laavola, M., Leppänen, T., Hämäläinen, M., Vuolteenaho, K., Moilanen, T., Nieminen, R., Moilanen, E., 2018. IL-6 in Osteoarthritis: Effects of Pine Stilbenoids. Molecules 24, 109. doi:10.3390/molecules24010109

Lawrence, T., Willoughby, D.A., Gilroy, D.W., 2002. Anti-inflammatory lipid mediators and insights into the resolution of inflammation. Nature Reviews Immunology 2, 787–795. doi:10.1038/nri915

Li, Chenshuang, and Zhong Zheng. 2020. "Identification of Novel Targets of Knee Osteoarthritis Shared by Cartilage and Synovial Tissue." International Journal of Molecular Sciences 21 (17). https://doi.org/10.3390/ijms21176033.

Li, Heng, Dan Wang, Yongjian Yuan, and Jikang Min. 2017. "New Insights on the MMP-13 Regulatory Network in the Pathogenesis of Early Osteoarthritis." Arthritis Research & Therapy 19 (1): 248. https://doi.org/10.1186/s13075-017-1454-2.

McCoy, Annette M, Ann M Kemper, Mary K Boyce, Murray P Brown, and Troy N Trumble. 2020. "Differential Gene Expression Analysis Reveals Pathways Important in Early Post-Traumatic Osteoarthritis in an Equine Model." BMC Genomics 21 (1): 843. https://doi.org/10.1186/s12864-020-07228-z.

McGuinness, Luke A, and Julian P T Higgins. 2021. "Risk-of-Bias VISualization (Robvis): An R Package and Shiny Web App for Visualizing Risk-of-Bias Assessments." Research Synthesis Methods 12 (1): 55–61. https://doi.org/https://doi.org/10.1002/jrsm.1411.

Mendez, Melanie E, Aimy Sebastian, Deepa K Murugesh, Nicholas R Hum, Jillian L McCool, Allison W Hsia, Blaine A Christiansen, and Gabriela G Loots. 2020. "LPS-Induced Inflammation Prior to Injury Exacerbates the Development of Post-Traumatic Osteoarthritis

in Mice." Journal of Bone and Mineral Research: The Official Journal of the American Society for Bone and Mineral Research 35 (11): 2229–41. https://doi.org/10.1002/jbmr.4117.

"MMP13 Gene." n.d. Gene Cards. Accessed November 9, 2021. https://www.genecards.org/cgi-bin/carddisp.pl?gene=MMP13.

"Mmp13 Protein (Human) ." n.d. String Interaction Network. . Accessed November 9, 2021. https://version11.string-db.org/cgi/network.pl?taskId=Yvg0dqJ8CO2Q.

Moher, David, Larissa Shamseer, Mike Clarke, Davina Ghersi, Alessandro Liberati, Mark Petticrew, Paul Shekelle, Lesley A Stewart, and PRISMA-P Group. 2015. "Preferred Reporting Items for Systematic Review and Meta-Analysis Protocols (PRISMA-P) 2015 Statement." Systematic Reviews 4 (1): 1. https://doi.org/10.1186/2046-4053-4-1.

Murphy, G, and M H Lee. 2005. "What Are the Roles of Metalloproteinases in Cartilage and Bone Damage?" Annals of the Rheumatic Diseases 64 (suppl 4): iv44–iv47. https://doi.org/10.1136/ard.2005.042465.

Nagpal, R., Mainali, R., Ahmadi, S., Wang, S., Singh, R., Kavanagh, K., Kitzman, D. W., Kushugulova, A., Marotta, F., & Yadav, H. (2018). Gut microbiome and aging: Physiological and mechanistic insights. Nutrition and healthy aging, 4(4), 267–285. https://doi.org/10.3233/NHA-170030

Neogi, Tuhina, and Yuqing Zhang. 2013. "Epidemiology of Osteoarthritis." Rheumatic Disease Clinics of North America 39 (1). https://doi.org/10.1016/j.rdc.2012.10.004.

O'Leary, Nuala A, Mathew W Wright, J Rodney Brister, Stacy Ciufo, Diana Haddad, Rich McVeigh, Bhanu Rajput, et al. 2016. "Reference Sequence (RefSeq) Database at NCBI: Current Status, Taxonomic Expansion, and Functional Annotation." Nucleic Acids Research 44 (D1): D733–45. https://doi.org/10.1093/nar/gkv1189.

Petty, Ross E, and James T Cassidy. 2005. "CHAPTER 2 - STRUCTURE AND FUNCTION." In Textbook of Pediatric Rheumatology (Fifth Edition), edited by James T Cassidy, Ross E Petty, Ronald M Laxer, and Carol B Lindsley, Fifth Edit, 9–18. Philadelphia: W.B. Saunders. https://doi.org/https://doi.org/10.1016/B978-1-4160-0246-8.50008-5.

Portincasa, P., Bonfrate, L., Khalil, M., Angelis, M.D., Calabrese, F.M., D'Amato, M., Wang, D.Q.-H., Di Ciaula, A., 2021. Intestinal Barrier and Permeability in Health, Obesity and NAFLD. Biomedicines 10, 83.. doi:10.3390/biomedicines10010083

Rocha, B., Cillero-Pastor, B., Ruiz-Romero, C., Paine, M.R.L., Cañete, J.D., Heeren, R.M.A., Blanco, F.J., 2021. Identification of a distinct lipidomic profile in the osteoarthritic synovial membrane by mass spectrometry imaging. Osteoarthritis and Cartilage 29, 750–761. doi: 10.1016/j.joca.2020.12.025

Rovenský, J, and J Payer. 2009. "Hyaline Cartilage." In Dictionary of Rheumatology, 82–82. Vienna: Springer Vienna. https://doi.org/10.1007/978-3-211-79280-3_455.

Safran M, Rosen N, Twik M, BarShir R, Iny Stein T, Dahary D, Fishilevich S, and Lancet D. The GeneCards Suite Chapter, Practical Guide to Life Science Databases (2022) pp 27-56 [PDF]

Salerno, Anna, Kyla Brady, Margot Rikkers, Chao Li, Eva Caamaño-Gutierrez, Francesco Falciani, Ashley W. Blom, Michael R. Whitehouse, and Anthony P. Hollander. 2020. "MMP13 and TIMP1 Are Functional Markers for Two Different Potential Modes of Action

by Mesenchymal Stem/Stromal Cells When Treating Osteoarthritis." STEM CELLS, July. https://doi.org/10.1002/stem.3255.

Sato, Tomoo, Koji Konomi, Satoshi Yamasaki, Satoko Aratani, Kaneyuki Tsuchimochi, Masahiro Yokouchi, Kayo Masuko-Hongo, et al. 2006. "Comparative Analysis of Gene Expression Profiles in Intact and Damaged Regions of Human Osteoarthritic Cartilage." Arthritis & Rheumatism 54 (3): 808–17. https://doi.org/https://doi.org/10.1002/art.21638.

Smith, Malcolm D, and Mihir D Wechalekar. 2015. "4 - The Synovium." In , edited by Marc C Hochberg, Alan J Silman, Josef S Smolen, Michael E Weinblatt, and Michael H B T - Rheumatology (Sixth Edition) Weisman, 27–32. Philadelphia: Mosby. https://doi.org/https://doi.org/10.1016/B978-0-323-09138-1.00004-8.

Stark, Rory, Marta Grzelak, and James Hadfield. 2019. "RNA Sequencing: The Teenage Years." Nature Reviews Genetics 20 (11): 631–56. https://doi.org/10.1038/s41576-019-0150-2.

Steinberg, Julia, Roger A Brooks, Lorraine Southam, Sahir Bhatnagar, Theodoros I Roumeliotis, Konstantinos Hatzikotoulas, Eleni Zengini, et al. 2018. "Widespread Epigenomic, Transcriptomic and Proteomic Differences between Hip Osteophytic and Articular Chondrocytes in Osteoarthritis." Rheumatology (Oxford, England) 57 (8): 1481–89. https://doi.org/10.1093/rheumatology/key101.

Steinberg, Julia, Lorraine Southam, Andreas Fontalis, Matthew J Clark, Raveen L Jayasuriya, Diane Swift, Karan M Shah, et al. 2021. "Linking Chondrocyte and Synovial Transcriptional Profile to Clinical Phenotype in Osteoarthritis." Annals of the Rheumatic Diseases 80 (8): 1070–74. https://doi.org/10.1136/annrheumdis-2020-219760.

Sterne, Jonathan A C, Miguel A Hernán, Barnaby C Reeves, Jelena Savović, Nancy D Berkman, Meera Viswanathan, David Henry, et al. 2016. "ROBINS-I: A Tool for Assessing Risk of Bias in Non-Randomized Studies of Interventions." BMJ 355. https://doi.org/10.1136/bmj.i4919.

Sterne, Jonathan A C, Jelena Savović, Matthew J Page, Roy G Elbers, Natalie S Blencowe, Isabelle Boutron, Christopher J Cates, et al. 2019. "RoB 2: A Revised Tool for Assessing Risk of Bias in Randomized Trials." BMJ 366. https://doi.org/10.1136/bmj.l4898.

Stockwell, Stephanie, Mike Trott, Mark Tully, Jae Shin, Yvonne Barnett, Laurie Butler, Daragh McDermott, Felipe Schuch, and Lee Smith. 2021. "Changes in Physical Activity and Sedentary Behaviors from before to during the COVID-19 Pandemic Lockdown: A Systematic Review." BMJ Open Sport & Exercise Medicine 7 (1). https://doi.org/10.1136/bmjsem-2020-000960.

"Transcriptome." 2014. Citable by Nature Education. 2014. https://www.nature.com/scitable/definition/transcriptome-296/.

Tsai, Joseph C, Grant Casteneda, Abby Lee, Kypros Dereschuk, Wei Tse Li, Jaideep Chakladar, Alecio F Lombardi, Weg M Ongkeko, and Eric Y Chang. 2020. "Identification and Characterization of the Intra-Articular Microbiome in the Osteoarthritic Knee." International Journal of Molecular Sciences 21 (22). https://doi.org/10.3390/ijms21228618.

Tsuchida, A.I., Beekhuizen, M., `T Hart, M.C., Radstake, T.R., Dhert, W.J., Saris, D.B., Van Osch, G.J., Creemers, L.B., 2014. Cytokine profiles in the joint depend on pathology, but are different between synovial fluid, cartilage tissue and cultured chondrocytes. Arthritis Research & Therapy 16. doi: 10.1186/s13075-014-0441-0

Ulici, V, K L Kelley, M A Azcarate-Peril, R J Cleveland, R B Sartor, T A Schwartz, and R F Loeser. 2018. “Osteoarthritis Induced by Destabilization of the Medial Meniscus Is Reduced in Germ-Free Mice.” Osteoarthritis and Cartilage 26 (8): 1098–1109. https://doi.org/10.1016/j.joca.2018.05.016.

Veale, Douglas J, and Gary S Firestein. 2017. “Chapter 2 - Synovium.” In Kelley and Firestein’s Textbook of Rheumatology (Tenth Edition), edited by Gary S Firestein, Ralph C Budd, Sherine E Gabriel, Iain B McInnes, and James R O’Dell, Tenth Edit, 20–33. Elsevier. https://doi.org/https://doi.org/10.1016/B978-0-323-31696-5.00002-4.

Vina, Ernest R., and C. Kent Kwoh. 2018. “Epidemiology of Osteoarthritis: Literature Update.” Current Opinion in Rheumatology 30 (2). https://doi.org/10.1097/BOR.0000000000000479.

Wang, Meina, Erik R Sampson, Hongting Jin, Jia Li, Qiao H Ke, Hee-Jeong Im, and Di Chen. 2013. “MMP13 Is a Critical Target Gene during the Progression of Osteoarthritis.” Arthritis Research & Therapy 15 (1): R5. https://doi.org/10.1186/ar4133.

Wang, Zhong, Mark Gerstein, and Michael Snyder. 2009. “RNA-Seq: A Revolutionary Tool for Transcriptomics.” Nature Reviews Genetics 10 (1): 57–63. https://doi.org/10.1038/nrg2484.

Wen, C., Xu, L., Xu, X., Wang, D., Liang, Y., Duan, L., 2021. Insulin-like growth factor-1 in articular cartilage repair for osteoarthritis treatment. Arthritis Research & Therapy 23. doi:10.1186/s13075-021-02662-0

Wiegertjes, R., Van De Loo, F.A.J., Blaney Davidson, E.N., 2020. A roadmap to target interleukin-6 in osteoarthritis. Rheumatology 59, 2681–2694. doi:10.1093/rheumatology/keaa248

Xia, Qingqing, Shouan Zhu, Yan Wu, Jiaqiu Wang, Youzhi Cai, Pengfei Chen, Jie Li, Boon Chin Heng, Hong Wei Ouyang, and Ping Lu. 2015. “Intra-Articular Transplantation of Atsttrin-Transduced Mesenchymal Stem Cells Ameliorate Osteoarthritis Development.” STEM CELLS Translational Medicine 4 (5): 523–31. https://doi.org/10.5966/sctm.2014-0200.

Supplementary Material

Table 3-3: Details on the DEGs Discussed in each study chosen for this review.

Study	Genes	Description	
Tsai et al.	Aeromans hydrophila, Azotobacter vinelandii, Burkholderia sp LCSAOTU14, Cupriavidus necator, Escherichia coli, Escherichia coli DSM 30083 = JCM 1649 = ATCC 11775, obligately oligotrophic bacterium POCPN-83, Pseudomonas aeruginosa, Pseudomonas baetica, Pseudomonas nitroreducens, Pseudomonas sp. HHS 16, Pseudomonas stutzeri, Pseudomonas taetrolens, Pseudomonas veronii, Psuedomonas arsenicoxydans, Psuedomonas azotoformans, Psuedomonas filiscindens, Psuedomonas fluorescens, Psuedomonas gessardii, Psuedomonas kilonensis, Psuedomonas Koreenis, Psuedomonas lini, Psuedomonas miguelae, Psuedomonas plecoglossicida, Psuedomonas putida, Psuedomonas sp, Psuedomonas sp. A_wp02223, Psuedomonas sp. BB2-1-31, Psuedomonas sp. BSR1-2-20, Psuedomonas sp. K1/KB1, Psuedomonas sp. Ps6, Psuedomonas syringae, Psuedomonas tolaasii, Serratia marcescens, uncultured bacterium, uncultured Bradyrhizobium sp., uncultured Firmicutes Bacterium, uncultured Marinobacter sp., uncultured Pseudomonas sp., uncultured sulfur-oxidizing symbiont bacterium, uncultured Gammaproteobacteria bacterium, unidentified eubacterium clone ESH20b-4, unidentified eubacterium clone ESH21b-4	The 43 differentially abundant microbes found in OA samples compared to healthy samples	
Li et al.	APOD, C1QB, FPR3, HIST1H3B, IFNE, MSR1, PBK, TNFAIP6, TREM1, VSIG4	Inflammation modulating	DEGs found in two of the main

	MYOC, AMTN, CHI3L2, FAP, LRRC15, MMP13, TNFAIP6	Extracellular matrix (ECM) Binding	contributing pathways in OA

Study	Genes	Description	
McCoy et al.	TBXA2R, FZD6, GPER1, GPSM2, CD247, CACNA1D, PTH2R, GPR68, S1PR3, ADRA1B, CYSLTR2, QRFPR, NTS, GNA15, CD8A, PRKAR1B, ADCY5, MC4R, GPR31, PTGER3, GNGT2, GPR4, LAT, DRD2, ADCY7, HTR1D, ADRA1D, VIPR1, EDNRA, CARD11, APLNR, PRKCQ, GNAO1	Smooth muscle contraction, blood pressure regulation, cell signaling	The nine gene clusters with greater than 10 DEGs along with their respected associated pathway
	ANGPT1, B3GNT3, COMP, UST, EPHB4, LRMP, MMP9, B4GALT1, CHST1, MMP11, TNFAIP6, CHIT1, CHST2, TNN, TEK, MMP2, ACAN, DCN, MMP16, B3GALNT1, NID1, CNN2, MMP13, CTSH, QPCT, MMP1, MMP3	Extracellular matrix organization, aminoglycan metabolism	
	IGF1, IGFBP7, PRSS23, IGFBP5, ALB, ABCA7, VWF, DMP1, SERPINF2, IL6, IGFBP4, SPARC, GRB10, LAMB1, LAMA2, ACTN1, STC2, APOA1	Protein and growth factor binding, signaling and structural receptors	
	P4HA3, COL4A1, COL5A1, COL1A2, COL6A6, COL1A1, COL6A3, COL23A1, COL9A2, PCOLCE2, COL6A5, FLT4, COL12A1, PDGFB, SERPINH1, COL4A4, COL4A2	Structural growth and development, collagen and extracellular matrix organization	
	GSN, SNAP91, SH3GL3, SH3GL2, BIN2, SYNJ2, PTEN, ARRB2, DAB2, TRIP10, GJA1, HSPH1, AMPH, HSPA8, RPS6KA1, DNM1	Vesicle formation and transport, response to cell stimulus	
	DES, MYLK, ACTA2, ITGB7, TNNC2, CALD1, TNNI3, TPM1, ACTG2, MYH11, TPM2, ITGA1, TPM4	Cytoskeletal organization	
	CLEC12A, FCER1G, CD93, DYNLL1, ANK3, CD53, CHRNB4, KIF1A, FRMPD3, KLC3, SPTB, ATP8B4	Signal transduction and cellular component localization	
	RDH12, ALDH1A3, CDO1, AOC3, ALDH1A1, GAD2, ABAT, ALDH1A2, AOX1, GGT7, SDR16C5	Cellular metabolic processes and response to cell stimulus	

	ADAMTS18, ADAMTS15, ADAMTS12, SBSPON, THBS2, ADAMTS9, SPON2, THBS1, ADAMTS16, THSD4	Angiogenesis	
Steinberg et al.	MMP1, MMP2, MMP13, APOD, IL6, CYTL1, C15orf48	The seven gene classifier	

Study	Genes	Description	
Huang et al.	FCER1G, KlRb1, AHR, GATA3, HLA-DRA, IL1R1, IL23R, IL2RA, NFKB1, NFKBIA	Cell differentiation-related genes	Cell Type: Th17
	Il-2, IL1JA, GATA3, IL4R, FOXP3, IL21R, TBX21, IL12RB1	Cell signaling related genes	Cell Type: CD4+T
	CTLA4, IFI2J	Proliferating related genes	Cell Type: CD8+T
	GZMB, NKGj, CCL5, TCFJ	Cytotoxic related	
	CCL3, CCL3L1	Proinflammatory related genes	Cell Type: T-Mφ,
	IGF1, MRC1	Inflammation resolving genes	
	FN1, SPP1	Fibrosis related genes	Cell Type: IR-Mφ
	ESPTI1, STAT1, MX1, IFI44L, ISG15	Interferon-induced genes	
	IL6, IL1A, IL1B, TLR2 and TNF	Inflammation related genes	
	FGCR3A, CD163, MRC1	Inflammation resolving genes	

CHAPTER 4

The Systemic Physical, Morphological, and Biochemical Effects of Muscle Damage

Logan Moore[1], Kamal Awad[1], Jian Huang[1], Leticia Brotto[1], Rhonda Prisby[12], Mark Ricard[3], Venu Varanasi[1], Marco Brotto[1*]

[1]Bone Muscle Research Center, College of Nursing and Health, University of Texas at Arlington, Arlington, TX, USA

[2]Bone Vascular and Microcirculation Laboratory, Department of Kinesiology, University of Texas at Arlington

[3]Biomechanics Laboratory, Department of Kinesiology, University of Texas at Arlington, Arlington, TX, USA

*Correspondence:

Marco Brotto

Marco.brotto@uta.edu

Abstract

Skeletal muscles play key roles in maintaining the homeostasis of the musculoskeletal system. Muscles are vital mechanically, offer joint stability and dictate mechanisms of movement. Biochemically, skeletal muscle has a pivotal role in its secretory and endocrine function through the secretion of myokines. The induction of muscle damage through intra-muscular injection of 1.2% Barium Chloride in the tibialis anterior muscle caused an inflammatory, immune response. This immune response showed a significant increase in the concentration of Prostaglandin E2, and lipid mediator derivatives of the EPA and DHA signaling pathway. Muscle weakness and regeneration was confirmed through a significant decrease in grip strength at 4-days post injury that returned to control-baseline strength by 1-month post injury. The muscle weakness caused joint alterations observed in changes in the Raman spectra in the articulating cartilage and increase in the bone volume fraction in the cortical shell of the subchondral bone, detected as thickening of the subchondral bone, features that are characteristic of osteoarthritis in rodents and in humans.

Introduction

Skeletal muscle is essential to the overall health and well-being of humans. The skeletal muscle's main function is to generate force and power that enables the body to maintain posture, produce movement, and influences activity (Fronera et al., 2015). In humans, 40% of the total body weight is comprised from skeletal muscle (Fornera et al., Hardy et al., 2016). Skeletal muscle injuries account for 10 to 55 % of all sports related injuries, and 90% of those injuries are account grade I muscle injuries (Fernades et al., 2011; Maffullie et al., 2015).

Grade I mild muscle injuries are defined as effecting some of the muscle fibers, with slight edema and discomfort (Fenades et al., 2011). There are a variety of ways in which grade I muscle injuries can be modeled in small animal models these include, Cardiotoxin, Freeze Injury, Notexin, and Barium Chloride ($BaCl_2$). In a recent study conducted by Hardy et al. in 2016, it was found that $BaCl_2$ produces consistent and repeatable muscle damage that does not affect satellite cell activation. $BaCl_2$ causes muscle damage by inhibiting potassium channels causing depolarization of the sarcolemma and an intracellular calcium leak with leads to apoptosis and cell death of the muscle fiber (Jung et al., 2019; Awad et al., 2022).

The skeletal muscle plays a direct role both mechanically and biochemically in the homeostasis of the musculoskeletal system (Msk). The advanced network of tissues in the Msk communicate through release of secretory factors (Allen et al., 2008; Brotto & Bonewald, 2015; Brotto & Johnson, 2014; Dallas et al., 2013; Isaacson & Brotto, 2014; Kurek et al., 1997; Pedersen, 2013). During the muscle regeneration process an inflammatory, immune response in which is controlled by the release of pro-inflammatory molecules, such as cytokines, reactive

oxygen species (ROS), and lipid signaling mediators (LMs, i.e. leukotrienes and prostaglandins 9PGs) in which communicate with the entire Msk (Kojouharov et al., 2021).

The tibialis anterior (TA) muscle has typically been used in studies of muscle regeneration (Hardy et al., 2016; Jung et al., 2019). The TA muscle is easily identifiable and has a major role in the locomotor ability to walk and stabilize the lower limb (Mahrajar et. al., 2019). Periarticular muscle weakness causes instability of the joint and increases the mechanical load (Brandt, 2006). This makes the TA a prime candidate to induce muscle damage and explore the surrounding effects on the Msk. The instability of the joint is a prime contributor to the development of and progression of osteoarthritis (OA) seen in alteration in the subchondral bone (Poulet et al., 2014; Jia et al; Holzer et al 2020; Li et al., 2013).

There is little information on the role in which muscle regeneration plays in the homeostasis and maintenance of the surrounding joint tissue The purpose of this study was to initialize and extrapolate the systematic physiological and biomechanical changes in the joint tissues following acute muscle damage.

Methods

Animals

The experimental tests, assays and manipulations were conducted at the University of Texas at Arlington Bone Muscle Research Center, and the micro-computed tomography scan and evaluation was conducted at the University of Texas at Arlington Bone Vascular and Microcirculation Laboratory . The experiments in this study were approved by the University of Texas at Arlington Institutional Animal Care and Use Committee and conducted according to the

Institute of Laboratory Animal Research guidelines. Animal husbandry, care and use activities followed the AAALAC Guide for Care and Use of Laboratory Animals.

48 Skeletally mature, young wild mice (6 months old, C57Bl6, Charles River Laboratory) were used for these experiments. The mice were equally separated male and female into 4 groups (n=12, 6 male 6 female) corresponding to duration of experimental protocol (Control, 4-Day post injection, 7-Day post injection, and 1-month post injection). Acute inflammatory muscle damage was induced by intra-muscular (IM) injection of Barium Chloride (BaCl2). Mice in the injections group received a singular IM injection of 50 µL of 1.2% BaCl2 in the left tibialis anterior. The contralateral right limb served as the sham control and received an IM injection of 50 µL sterile saline solution. Prior to receiving the IM injections, the mice were anesthetized using isoflurane. While anesthetized the animals' weight was recorded, lower leg shaved, and then received ~30 µL of an abdominal subcutaneous injection of Buprenorphine Sustained release to modulate any pain expected following acute muscle damage. The mice recovered in a warmed cage until the righting reflux returned. Mice were housed with littermates in same experimental group, and was given moist, easily accessible chow until experimental endpoint.

Physical Strength and Activity

At the time of experiment, grip strength was measured in the animal's fore limbs, hind limbs, and all limbs. The grip strength was measured using a grip force dynamometer (BIO-GS3 grip strength test). This apparatus is a force transducer attached to a small metal grid, in which the animal can attach. In measurement of the front limb grip strength the mouse's forelimbs attach to the grid and the experimenter pulls the mouse by the base of the tail until the grip is broken. The peak force produced is interfaced and recorded through the BIO-CIS software

(Bioseb). This is repeated 3 times, and the mouse can recover before starting the next measurement. In the all- limb grip strength, all 4 limbs of the mouse can attach to the grid, and the experimenter pulls the mouse by the base of the tail until the grip is broken. The hind limb grip strength the experimenter holds the mouse by the scruff to allow only the hind limbs to attach to the grid and with the other hand pulls the mouse by the base of the tail until the grip is broken.

The mouse can fully rest and recover before the physical activity assessment in the force plate actimeter. The force plate actimeter (BASI Inc) is an animal enclosure that has 4 force transducers that measures the locomotor activity, and records the distance traveled, area, force, spatial statistics, and bouts of low mobility. The mice are individually placed in the enclosure for 3 minutes to allow for acclimation, and then physical activity is measured for 20 minutes. Data was measured at 50 points/second at 1024 point per frame for 60 frames.

After physical assessment, the mice are euthanized via cervical dislocation. The animals' weight was measured. All tissues are harvested, and flash frozen in liquid nitrogen for later experimentation.

Histology

The tibialis anterior muscle was cut in half along the horizontal midline of the muscle belly. Half of the muscle was flash frozen for Raman spectroscopy and half was placed in 10% formalin for tissue preservation. After 24 hours, the formalin fixed muscle was dehydrated through a series of increasing ethyl alcohol concentrations and embedded in paraffin. The muscle was oriented for transverse cross sections and serially sectioned for 7-μm -thick sections. The sections were stained with hematoxylin and eosin (H&E).

Targeted Lipidomics

Following our previously published quantification method (Wang et al., 2017), targeted lipidomics was performed on the serum. Briefly, 50 µl of serum was allocated and placed in an RNAase/DNAase free microcentrifuge tube. In each serum sample 5 µL of internal standard (IS) mixture stock solution (5 µg/mL for AA-d8, 2 µg/mL for DHA-d5 and EPA-d5, and 0.5 µg/mL for all the rest IS) was added, then agitated on ice and in the dark for 1 hour.

The serum was then subjected to solid phase extraction (SPE). 4 mL of ice-cold 0.1 % formic acid was added to the serum samples to protonate the LM species. The sample was loaded in preconditioned cartridge (Strata-X 33 µm polymeric reversed phase SPE cartridge). After fully loading the samples, the cartridge was washed with 0.1% formic acid (1 mL) and shortly followed by another wash with 15% (v/v) ethanol in water (1 mL) to remove excess salts. The LMs were eluted by methanol, and the dried extracts were stored at -80˚C.

All components of LC-MS/MS system are from Shimadzu Scientific Instruments, Inc. (Columbia, MD). LC system was equipped with four pumps (Pump A/B: LC-30AD, Pump C/D: LC-20AD XR), a SIL-30AC autosampler (AS), and a CTO-30A column oven containing a 2-channel six-port switching valve. The LC separation was conducted on a C8 column (Ultra C8, 150 × 2.1 mm, 3 µm, RESTEK, Manchaca, TX) along with a Halo guard column (Optimize Technologies, Oregon City, OR). The MS/MS analysis was performed on Shimadzu LCMS-8050 triple quadrupole mass spectrometer. The instrument was operated and optimized under both positive and negative electrospray and multiple reaction monitoring modes (+/− ESI MRM). Standard lipid mediators and corresponding isotope-labelled lipid mediator internal standards (IS) were purchased from Cayman Chemical Co. (Ann Arbor, MI). All

analyses and data processing were completed on Shimadzu LabSolutions V5.91 software (Shimadzu Scientific Instruments, Inc., Columbia, MD).

Raman Spectroscopy

Raman Spectroscopy (DXR; Thermo Scientific) was measured using a 780 nm excitation laser at 100mW 10x objective and a 50 μm slit for all samples. The samples were photobleached for 30 seconds prior to spectra collection, and 5 second exposure time was used for collection. 20 spectra per location was recorded between 400 and 2000 cm-1. Frozen TA muscle samples were thawed and scanned directly at the mid-point of the muscle belly at the location of injection, cartilage samples were scanned at the medial tibial plateau, and bone samples were scanned at the mid-shaft. Spectra was analyzed using the baseline correction as previously reported (Zhang et al., 2010). The spectra were normalized using standard normal variate normalization. Python code for Raman data processing is in the supplementary material.

Micro-computed tomography (μCT)

Scans were performed using a high-resolution μCT 45 (Scanco Medical). The tibia was scanned at a resolution of 15.3 μm at 55 kVp. The subchondral cortical bone shell was fully analyzed, and the following parameters were calculated: cortical bone volume (BV, mm^3), tissue volume, and bone volume fraction (BV/TV). Care was taken so that trabecular bone was not included in this analysis of the subchondral cortical bone.

Rigor and Reproductivity

To ensure the rigor and reproducibility of this study, all animals were obtained through a single provider, Charles Rivers Laboratory. All animals were of the same genetic strain, C57BL/6. The animals were maintained in an animal housing system designed and managed to protect animals from undesirable microbes. A single researcher induced muscle damage with 50

μL of 1.2% $BaCl_2$ in the left limb and injected 50 μL sterile saline in the contralateral sham right limb directly in the mid-point of the Tibialis anterior. A total of 48 mice that were equally were equally distributed between the 4 experimental groups (Control – Baseline n=12, 4 – Day n=12, 7-Day n=12, 1 – Month n=12), and each group was equally distributed for gender (male n=6, female n=6). The physical assessment, grip strength and force plate actimeter, was conducted by a single, semi-blinded researcher only knowing if the mouse received the injection and not duration post injection. All animals received the physical assessment (n=12 per group) before tissue harvesting to ensure consistency in treatment between animals in their individual groups. The assessment of the histology, lipidomics, Raman, and μCT (n=6 per group) was conducted by a blinded researcher.

Statistical Analysis

To limit the number of animals used in this study, an a priori power analysis was conducted using G*Power 3.1.9.7. It was determined to achieve 80% power for detecting a large effect at the significance criterion of $\alpha = 0.05$ a sample size of N=48 was sufficient to study the hypothesizes. We hypothesize that the $BaCl_2$ injection will induce muscle weakness that will return to baseline levels after 1 – month post injury shown by a decrease in the mean values of grip strength and physical activity levels when comparing the control – baseline animals to the time point groups post injection of $BaCl_2$. We hypothesize that there will be alterations in the joint due to the induced muscle damage shown by an increase in Lipid Mediators in the serum, alterations in the Raman Spectrum in the muscle, bone, and cartilage, as well as increases in the bone/volume fraction in the cortical shell of the subchondral bone of the injured limb. Alternatively, the null hypothesizes of this study in the physical assessment, targeted lipodomics in serum, Raman spectroscopy of muscle, bone and cartilage, and the μCT of the subchondral

bone is that there will be no significant mean differences between the control-baseline animals and different time point groups post injection of $BaCl_2$, or that there will be no significant mean differences between the sham contralateral limb compared to $BaCl_2$ injected limb indicating there is no relationship between muscle damage and the joint tissues. Data was analyzed for variance using One-way ANOVA to compare group and gender mean differences with SPPS statistical software (version 28; IBM). The Levene's test was used to determine if the variance of groups was equal. If the F statistic was ≤ 0.05, then Tukey post-hoc tests were performed to assess group differences. The significance level was set at $p \leq 0.05$. Data was visualized using Origin Pro 2022 (OriginLab) and expressed as mean ± standard deviation (M±SD).

Results

Physical Strength and Activity

There were no significant differences in body mass between groups at the initial weight or weight post injection of $BaCl_2$ (see **Table 1**). Grip strength in the front limbs showed no significant difference between groups or gender (see **Figure 1)**. The all-limb grip strength showed a highly significant decrease in peak force in the 4-day and 7-day group ($p < .001$) and a significant decrease in the one-month ($p < .009$). The grip strength was shown to rise as the 7-day group was significantly higher than the 4-day group ($p < .002$), and the 1-month was significantly higher than the 7-day ($p < .001$). This trend was consistent between genders and when the force was normalized to full body mass. The hind limb grip strength was significantly diminished in all groups compared to the control. The grip strength in the hind limbs begun to return as the 7-day and 1-month were significantly higher than the 4-day group ($p < .004$). However, there were no significant differences in hind limb grip strength in the 1-month compared to the control. The trend of diminished grip strength in the hind limbs was consistent between genders and when

normalized for full body mass. The front limb grip strength showing no significant decrease in grip strength, while the all-limb grip strength and hind limb grip strength have significant decrease illustrates the muscle damage was localized to the effected limb and did not cause systemic muscle weakness.

The acute muscle damage did not affect the locomotor and physical activity measured in the actimeter. There was no significant difference between groups in all statistically measured categories, distance traveled, area, force, bout of low mobility, spatial statistic, and focused stereotypy. (see **Figure 2**). There were no significant differences observed between genders. This shows evidence that after injury the mice were still physically active and used the effected limb.

Table 4-1: Physical Characteristics

Group		N	Age	Initial Weight	Post Weight	Injected TA	Sham TA
			(weeks)	(grams)	(grams)	(grams)	(grams)
Control - Baseline	Female	6	28 ±0.4	24.93 ±3.97	-	0.0575 ±0.005	0.0549 ±0.006
	Male	6	28 ±0.5	31.04 ±2.96	-	0.0598 ±0.005	0.0588 ±0.006
	Total	12	28 ±0.5	27.99 ±4.62	-	0.0575 ±0.005	0.0569 ±0.006
4-Day	Female	6	29 ±0.0	25.06 ±2.72	22.12 ±1.74	0.0384 ±0.008	0.0455 ±0.005
	Male	6	28 ±1.6	33.42 ±2.98	30.36 ±2.92	0.0520 ±0.005	0.0541 ±0.003
	Total	12	28 ±1.1	29.24 ±5.15	26.24 ±4.87	0.0457 ±0.009	0.0498 ±0.006
7-Day	Female	6	28 ±1.0	27.62 ±3.47	24.70 ±3.12	0.0451 ±0.008	0.0452 ±0.004
	Male	6	28 ±1.5	35.51 ±3.58	32.22 ±2.88	0.0609 ±0.015	0.0545 ±0.007
	Total	12	28 ±1.2	31.56 ±5.32	28.46 ±4.86	0.0530 +0.014	0.0498 ±0.007
1-Month	Female	6	28 ±1.0	25.07 ±5.26	26.05 ±5.67	0.0617 ±0.004	0.0453 ±0.002
	Male	6	28 ±0.4	30.03 ±4.05	31.26 ±3.78	0.0697 ±0.011	0.0529 ±0.006
	Total	12	28 ±0.7	27.55 ±5.17	28.66 ±5.34	0.0654 ±0.009	0.0491 ±0.006
Total	Female	24	28 ±0.8	25.67 ±3.87	24.45 ±3.92	0.0500 ±0.011	0.0477 ±0.006
	Male	24	28 ±1.1	32.50 ±3.86	31.22 ±3.02	0.0606 ±0.011	0.0551 ±0.006
	Total	48	28 ±1.0	29.09 ±5.15	27.84 ±4.87	0.0553 ±0.012	0.0514 ±0.007

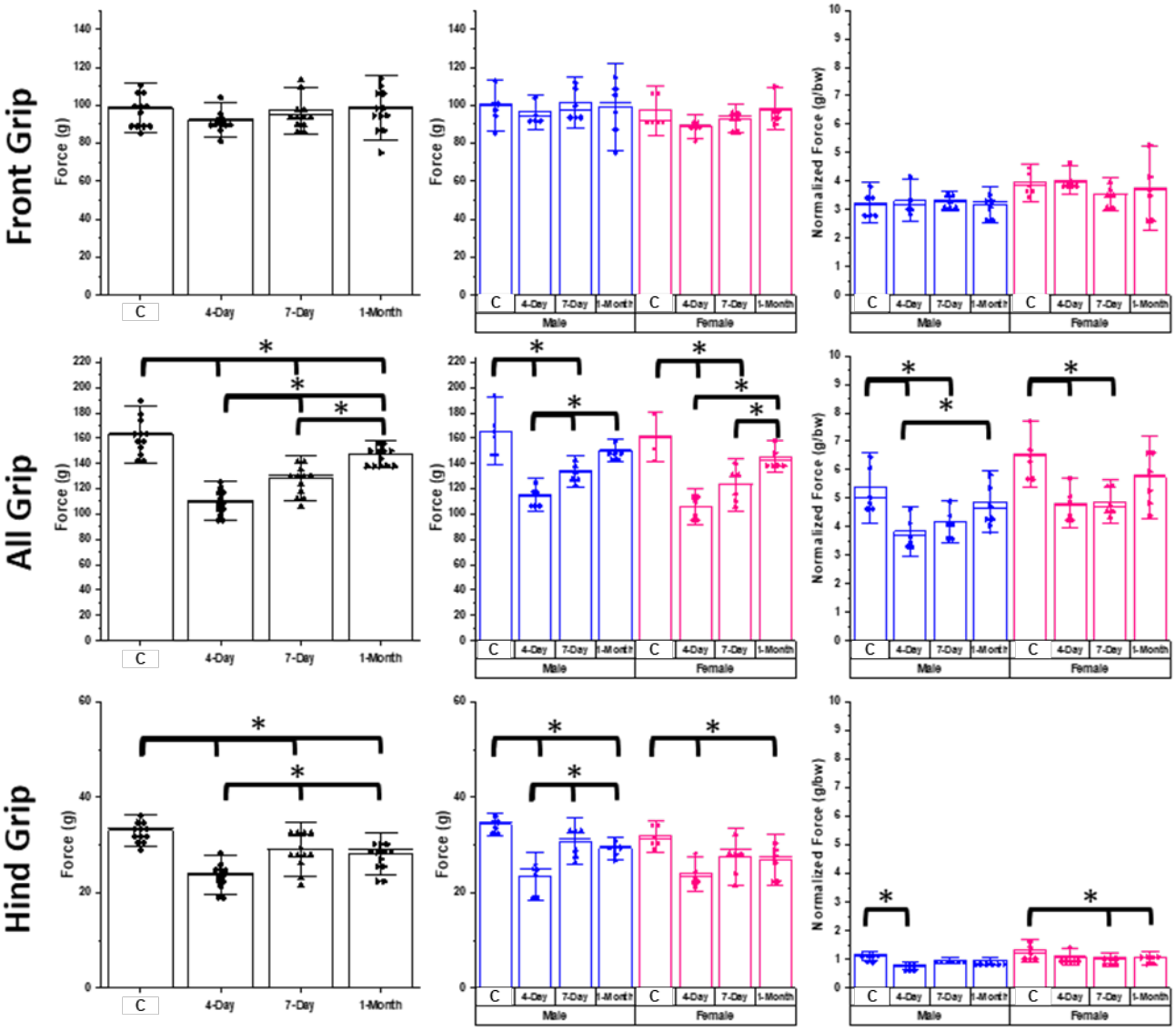

Figure 4-1: Grip strength was measured in front limbs, all limbs, and hind limbs and force production was calculated in grams. There were no significant changes in front limb grip strength between groups. The 4-Day, 7-Day and 1-Month showed significant ($p > .05$) decline in hind limb grips strength following acute muscle injury as compared to the control, and there was no significant difference between experiment time points. The 4-Day and 7-Day showed significant decline in all limb grip strength as compared to the control.

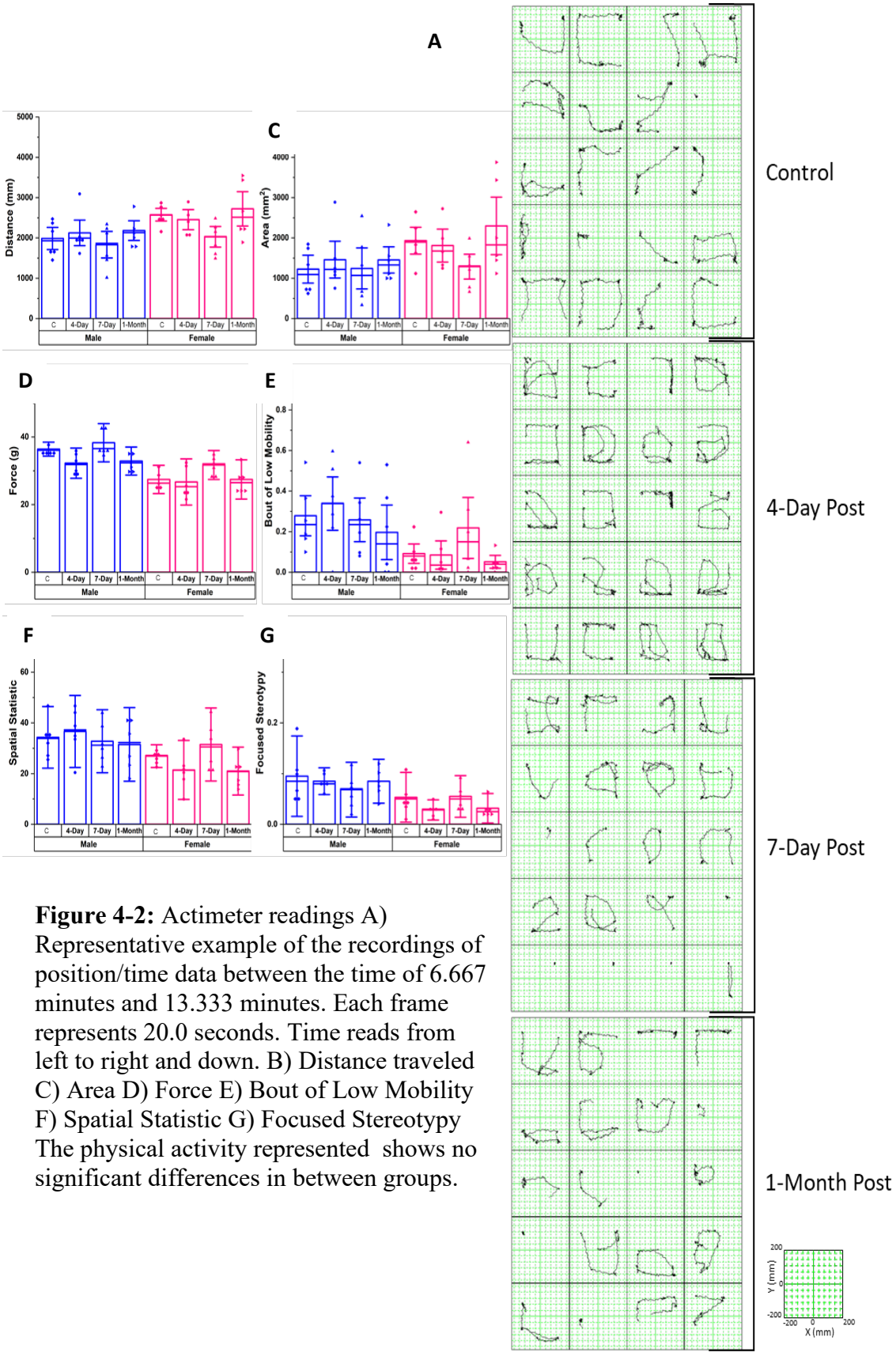

Figure 4-2: Actimeter readings A) Representative example of the recordings of position/time data between the time of 6.667 minutes and 13.333 minutes. Each frame represents 20.0 seconds. Time reads from left to right and down. B) Distance traveled C) Area D) Force E) Bout of Low Mobility F) Spatial Statistic G) Focused Stereotypy The physical activity represented shows no significant differences in between groups.

Histology

The gross morphology of the TA muscle after $BaCl_2$ injury shows at 4 – days post injury there is necrotizing and clearance of the damaged fibers along with mononuclear cells. At 7 – day post injury there are small myofiber development with a presence of mononuclear cells. At 1-month post injury the muscle is showing signs of regeneration in organized myofibers. At 1-month the myofibers are showing maturation, by having peripherally located nuclei.

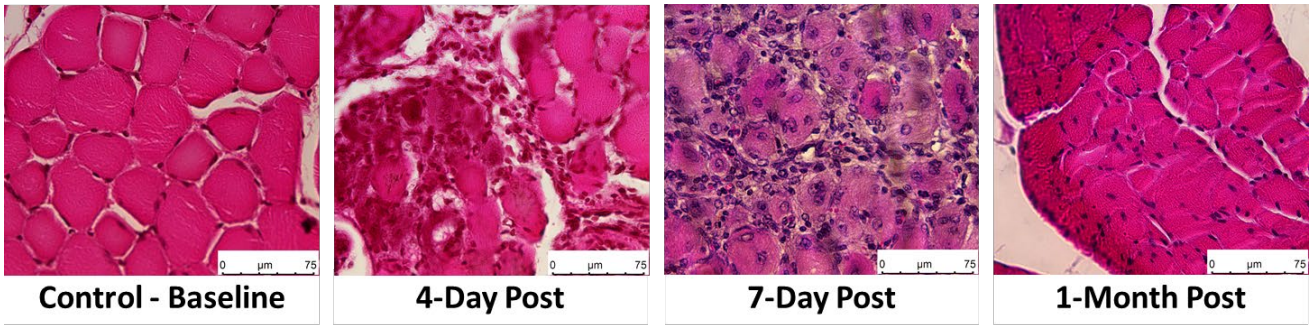

Figure 4-3: H&E stain of TA muscle cross section.

Targeted Lipidmics

Lipid signaling is essential in the role of muscle regeneration and the health of the musculoskeletal system. There were 44 LMs of 6 different lipid pathways profiled based on the LC-MS/MS analytical method in the serum (see Figure 4.). Further, there were 21 lipid mediators that were able to be quantified for their absolute concentration, based on the internal standards (see **Figure 5**.).

There were 4 LMs derived from the arachidonic acid (AA, 20:4, ω-6) that showed a trend in increasing concentration in the serum post injury, and by the 1-month time point showed

2-3 folds higher in concentration (6-keto-PGF, PGE2, PGD2, and 14,-15 DHET). PGE2 was found significantly higher at 1 month compared to the control ($p<0.05$). There were 2 LMs from the AA pathway that had a negative fold change (TXB2 and 12-HHT).

The Docosahexaenoic Acid (DHA , 22:6, ω-3) and Eicosatetraenoic acid (EPA 20:5, ω-3) are ω-3 polyunsaturated fatty acid (PUFA). The profiling of the DHA and EPA pathway showed remarkably high fold change at 1-month post injury as compared to the control. LMs in the EPA that showed 3 – 4 folds increase are 12-HEPE, 15-HEPE, 18-HEPE. The LMs in the DHA pathway that 3- 4 folds increase are 16-HDoHE, 17- HDoHE, 13- HDoHE, 14- HDoHE, and 11-HDoHE. In the quantification of the absolute concentration 8- HDoHE showed 2.8 fold increase at 1-month post injury. There was no significant change in the ratio of concentration between ω-6 PUFAS and ω-3 PUFAS as shown in AA/EPA, AA/DHA, and AA/(EPA+DHA).

In the linoleic acid pathway (LA, 18:2 ω-6), quantification of the LMs revealed that 13-HODE that there was an increase of 4.8 folds increase at the 1-month time period. 13-HODE was elevated throughout the time of injury, and at 4-days post injury there was a 3.9 fold increase in concentration.

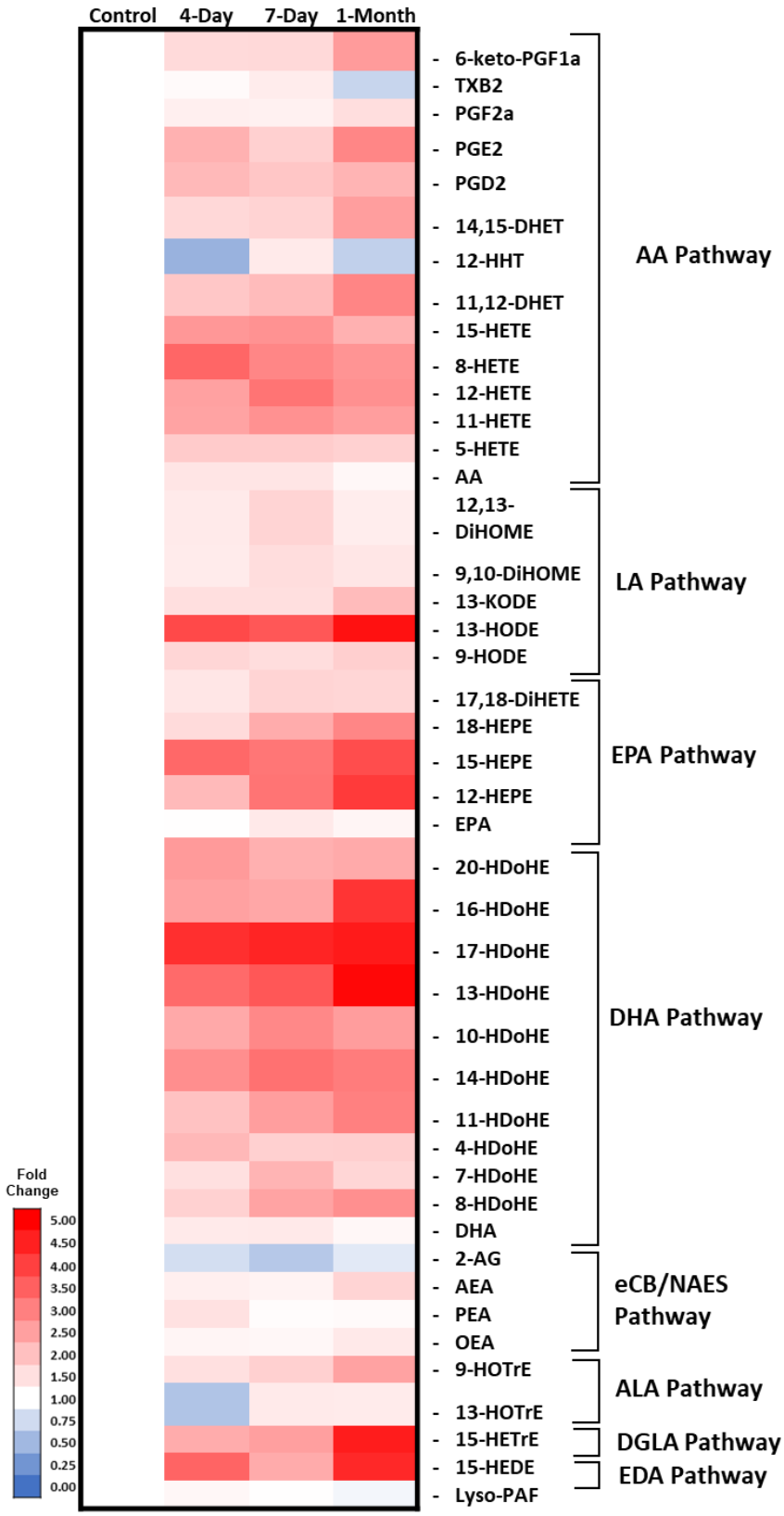

Figure 4-4: Heatmap of fold change of LMs profile compared to control

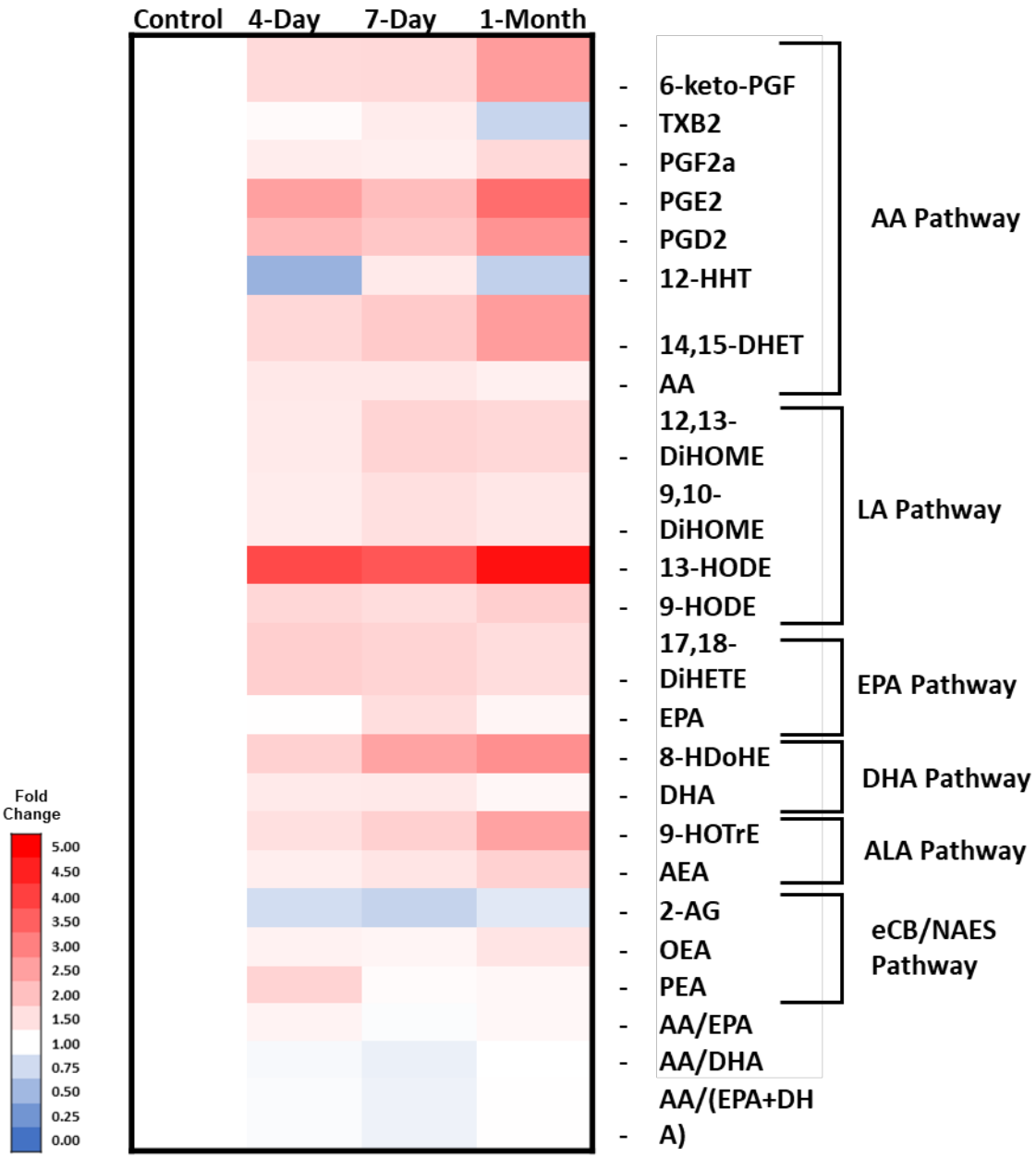

Figure 4-5: Heatmap of fold change of LMs concentration compared to Control

Raman Spectroscopy

Characterization of the muscle, cartilage, and bone by Raman Spectroscopy is given in figures 6, 7, and 8 respectively. The TA muscle was scanned at the mid-point of the muscle belly directly at the sight of injury. After 4-days post injury the Amide III (1242 cm^{-1}) height increased, while the peak height of the CH_2 deformation (1447 cm^{-1}) decreased along with the

peak Amide I (1660 cm^{-1}). The peak height of Amide III decreased back to the baseline control level at 1-month post injury. The peak height of CH_2 Deformation and Amide I increased back to baseline control levels at 1-month. The changes in peak height of Amide III, CH_2 deformation, and Amide I reveal the changes in collagen type I organization during muscle damage and recovery (Stani et al., 2021; Vidal et al., 2011) . At 4-Day's post injury the organization of the muscle is at it's lowest along with the highest amount of disruption in collagen. As the muscle recovers with the regeneration of myofibers and clearance of mononuclear cells the organization of collagen returns to baseline control levels. There were no detected alterations in proline (936 cm^{-1}) and phenylalanine (1003 cm^{-1}) between groups this shows that throughout injury there is no impairment in the ability for protein synthesis which is vital for regeneration (Maria Plesia et al., 2021; Wu et al., 2011). The Raman spectrum produced from the control, 4 – day, 7 – day, and 1 – month resembles the path of muscle regeneration.

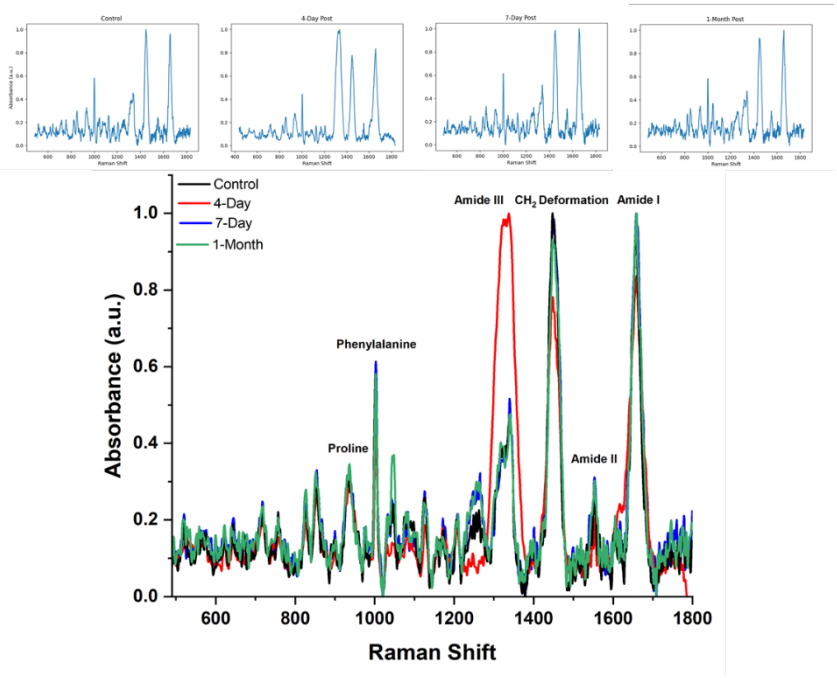

Figure 4-6: Raman Spectroscopic graphs for TA muscle.

The cartilage was scanned in the mid-point of the medial tibial plateau. The peak assignments were consistent with the previous studies (Pezzotti et al., 2022; Albro et al., 2018; Takahashi et al., 2014; Dehring et al., 2006; Lim et al., 2011). In a time dependent manner the peak intensity of Amide I (1660 cm^{-1}) and CH_2 Deformation (1447 cm^{-1}) decreased when compared to the baseline control of the articular cartilage. The decrease in peak height of Amide I and CH_2 deformation is indicative of the loss integrity of the articular cartilage due to the structure of the collagen (Lim et al., 2011; Pezzotti et al., 2021; Gaifulina et al., 2021) of As the mouse articular cartilage is thinner as compared to the thickness of human cartilage there is a higher spectral overlap with the underlying tibia bone shown in the peak of $\nu_1PO_4^{3-}$ at 959 cm^{-1}, which is indicative of bone mineral (Esmonde-White et al., 2014).

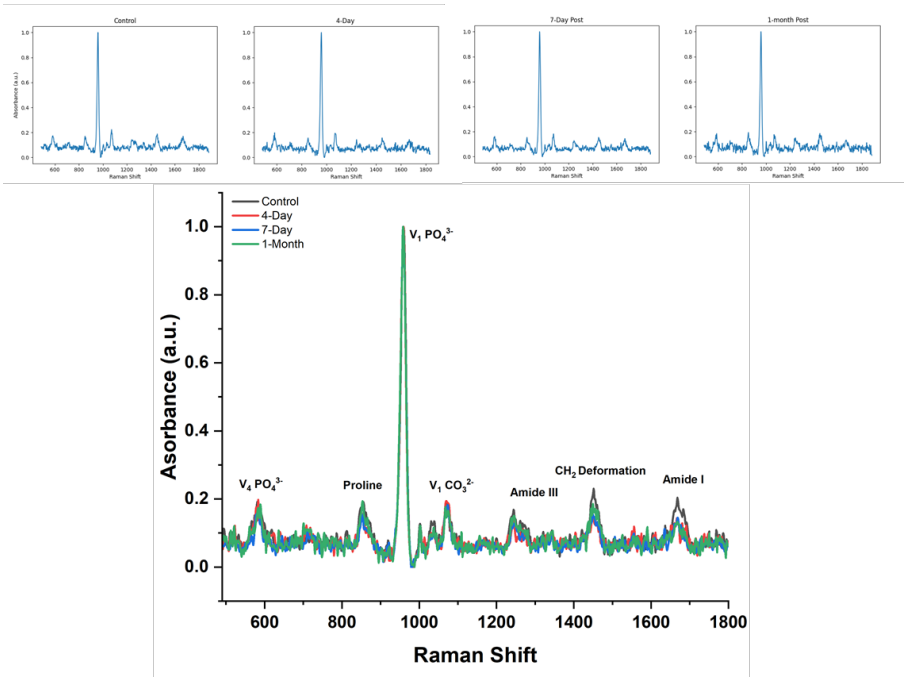

Figure 4-7: Raman Spectroscopic graphs of cartilage on the medial tibial plateau.

The Raman spectrum of the bone scanned at the mid-shaft of the tibia was scanned as a control to demonstrate that the $BaCl_2$ is localized to the injected muscle and does not cause alterations to the integrity of the mid-shaft of the tibia. The Raman spectra produced a consistent spectrum across the control, 4-Day, 7-Day, and 1-Month for both, the left injected limb with

$BaCl_2$ and the contralateral right sham limb (see Figure 8). The relative peak assignments of $\nu_1PO_4^{3-}$ at 959 cm^{-1}, $\nu_2PO_4^{3-}$ at 430 cm^{-1}, Amide I at 1660 cm^{-1}, Amide III at 1242 cm^{-1} is indicative of mature, healthy bone mineral (Mandair et al., 2015; Morris et al., 2011). This shows that the mid-shaft of the tibia does not have changes in the functional groups or chemical structure throughout the acute muscle injury.

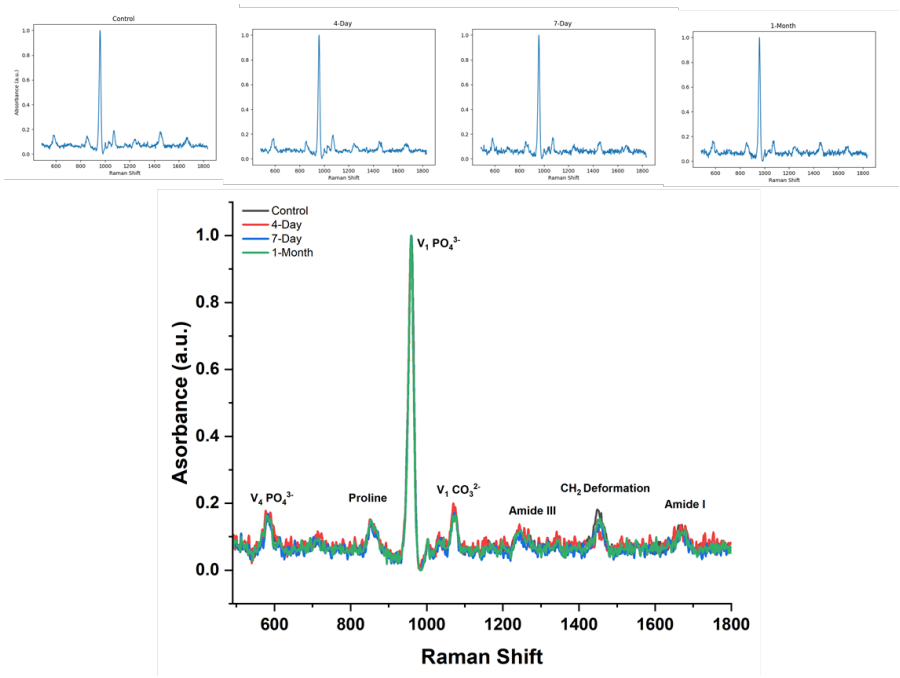

Figure 4-8: Raman Spectroscopic graphs of the mid-shaft cortical bone of the tibia.

Subchondral bone modifications

The cortical shell of the subchondral bone of the $BaCl_2$ injected limb showed to have a have and significant increase in bone volume fraction (BV/TV) as compared to the contralateral sham limb after 7 days and 1 month post injury (see **Figure 8**; $p<0.05$). There was a non-significant increase in bone volume fraction after 4-days of injury ($p<0.053$). There was no significant differences found in the cortical bone volume (mm^3) between the contralateral sham and the $BaCl_2$ injected limb (4-day: Injected 1.524±0.78, Sham 1.322±0.78; 7-Day: Injected 1.611±0.078, Sham 1.326±0.78; 1-Month injected 1.476±0.78, Sham1.248±0.095: ±Standard

error). Cortical bone thickness maps were generated to visualize the displacement of the thickness profile (see **Figure 8.B**).

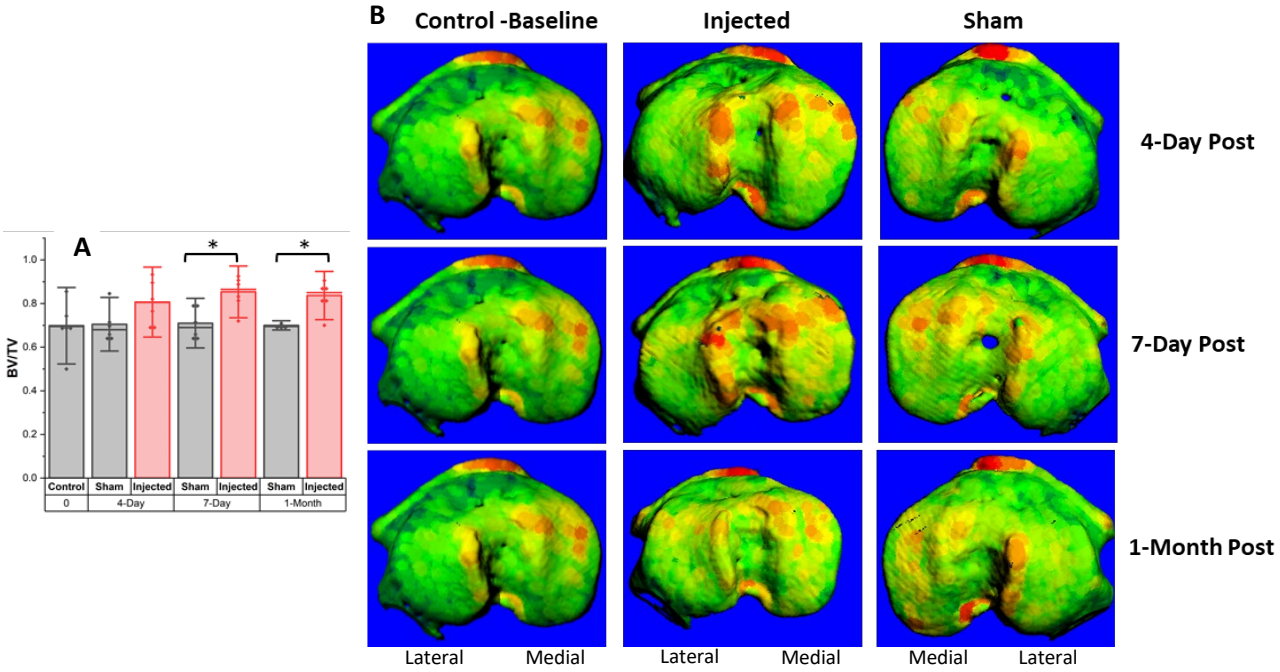

Figure 4-9: A) Bone volume fraction (BV/TV) B)Thickness profile map of the cortical bone shell of the subchondral bone of the tibia.

Discussion

The morphological changes observed in the TA muscle post $BaCl_2$ injury are consistent with the previous studies (Mortan et al. 2019; Jung et al., 2019; Hardy et al., 2016). The $BaCl_2$ inhibits the potassium ion channels causing a depolarization of the sarcolemma triggering an influx of intracellular calcium which leads is apoptosis and cell death (Morton et al., 2019). The cellular death than inspires an acute inflammatory immune response to initiate the repair and remodeling. The immune response in muscle regeneration for mild to moderate injuries similar to $BaCl_2$ has been described in Kojouharov et al 2021. It is shown that in the initial phase of muscle damage, the destructive phase is dominated by the influx of Peripheral Mononuclear Monocytes (PMNs) for phagocytosis of the muscle debris (Kojoruharov et al., 2021; Järvinen, et

al., 2014). The destructive phase can be shown in the four – days post injury to the TA (see **Figure 3**.; Hardy et al., 2016). At 7-days post injury of $BaCl_2$ the muscle has transitioned into the remodeling and repair phase in which PMNs have attracted and activated the satellite cells to proliferate and begin to differentiate into new muscle fibers. This is driven by LMs from the EPA and DHA pathway (Korjoruharov et al., 2021; McGlory et al., 2019). At 1-month post injury the muscle is in the final stages of repair, in which the new muscle fibers are beginning to mature and reach full recovery after injury.

In our target lipidomics it was found that the concentration of Prostaglandin E2 (PGE2) was significantly increased in the serum 1-month post injury of $BaCl_2$ and had elevated levels at 4- and 7-days post injury. This is a vital LM in maintaining the health and function of the muscle (Ho et al., 2017; Lui et al; 2016; Awad et al., 2022). PGE2 has been shown to influence the muscle protein turnover and cause the muscle-specific stem-cells vital for regeneration to expand (Lui et al., 2016; Ho et al., 2017). In-vitro we have shown that supplementation of PGE2 promotes skeletal muscle regeneration (Awad et al., 2022). However, while PGE2 is necessary for skeletal health, it has been shown that PGE2 plays a role in the development and pain in OA (Jiang et al., 2022). PGE2 acts via the EP4 receptor in osteoclast, and in the subchondral bone mediates osteoclastogenesis. Recently it was found that through the knock-out of the EP4 receptor in osteoclasts inhibits the disease progression of OA (Jiang et al., 2022).

The targeted lipidomics follows closely to the inflammatory and immune response in muscle damage a regeneration described in Kojoruharov et al., 2021. We have shown that the ω-3 PUFAs, EPA and DHA LM derivatives increase in concentration through the process of muscle regeneration. ω-3 PUFAs have an anti-inflammatory and antioxidant effect and have a beneficial role in improving muscle recovery (Ochi et al., 2018). DHA and EPA promote muscle

regeneration through improved satellite cell activation (de Carvalho et al. 2017). DHA has been shown to promote mitochondrial biogenesis in skeletal muscle (Chen et al., 2022). While, EPA has been shown to enhance skeletal muscle hypertrophy, and modulates glucose metabolism (Siriguleng et al., 2021). In bone it has been found that DHA and EPA supplementation increases the bone mineral density, accelerates the bone mineral apposition, and alters the microstructure of the trabecular bone (Fu et al., 2020). The linoleic acid metabolite 13-hydroxyoctadecadienoic acid (13-HODE) was elevated throughout the duration of injury, this is a beneficial effect as it has been shown in preventing muscle atrophy and can modulate the activation of PMNs (Lee et al., 2022; van de Velde et al., 1994).

The grip strength of the mouse followed the trend of muscle regeneration. In the all-limb and hind limb grip strength. It was shown that there was an initial muscle weakness caused by the muscle damage at the 4 -day period, and the strength of the mice began to recover over time. There were no alterations in the front limb grip strength indicating that the muscle weakness was localized to the hind limb. A limitation to the grip strength is that in the hind limb grip strength both limbs are exerting a force, and the injured limb may receive beneficial force production from the sham contralateral limb. The animals remained physically active across all experimental groups. This is indicative that the affected limb was still used, and the acute injury was not great enough to affect the locomotor pattern of the mice. Further studies will need to be conducted to find if there were any compensatory gait patterns or any alterations in the mechanical loading of the hind limb after muscle damage and the process of regeneration.

The Raman spectroscopy analyses of the TA muscle support the muscle damage and regeneration seen in our histological analysis (see **Figure 3**). The acute muscle damage occurred by the $BaCl_2$ injection showed disorganization of the collagen at 4 - days post injection that was

resolved by 1 – month indicating muscle regeneration. The articular cartilage demonstrated alterations in the composition of collagen that is suggestive of cartilage degeneration (Lim et al; 2011; Albro et al., 2018). Further, experimentation and processing will need to be conducted to determine the degree chemical alterations occurred in the articular cartilage. The Raman spectra of the tibia showed no evidence of alterations, which shows that the $BaCl_2$ had no effect on the mid-shaft of the bone.

Modifications in the bone volume fraction of the subchondral bone have been indicative of joint damage and the progression of OA (Wegner et al., 2019; Wang et al., 2005; Poulet et al., 2014; Jia et al; Holzer et al 2020; Li et al., 2013). The muscle damage caused from the IM injection of $BaCl_2$ has been shown to have caused muscle weakness in measurements of grip strength. This weakness creates instability in the knee joint and induces a greater load on the subchondral bone. Which has been confirmed previously that muscle weakness, caused by botulinum toxin type-A induced joint damage and the onset of OA in rabbits (Youssef et al., 2009). The bone volume fraction (BV/TV) after injury was increased in the injured limb compared to the contralateral control at day 7- and 1-month post injury. These findings are indicative of changes of the subchondral bone and evidence of joint damage (Lajeunesse et al., 2003; Jolzer et al., 2020; Li et al., 2013). Further analyzation of the displacement of the cortical thickness on the medial and lateral tibial plateau needs to be conducted. However, in visualization the medial tibial plateau shows higher areas of cortical bone thickness as compared to the lateral tibial plateau.

Limitations of the Study

Due to the lack of previous research, this study marks the novel conceptualization of the disease mechanisms in which acute muscle injury has detrimental effects to the joint, and the

potential onset and development of OA. The findings of this study have to be seen in light of some limitations, which include the histological characterization of articular cartilage. To provide full confirmation of the disease progression and state of OA, histological analyzation of the articular cartilage using the OARSI scale is needed in future studies. In our preliminary data of articular cartilage stained with SafraninO/Fast green, there is a time dependent increase in cartilage damage seen in the affected limb. This damage is consistent with the alterations of mechanical loading and instability of the limb (Wegner et al., 2019; Stiffel et al., 2020; Tsubosaka et al., 2020; Zaki et al., 2021). However, the increase in bone volume fraction and the alterations in cartilage Raman spectrum is confirmation that there are alterations occurring in the joint that are similar to the pathophysiology of disease development in OA in both rodents and in humans. The bone/volume fraction showing a significant increase as compared to the contralateral sham limb, shows evidence of subchondral bone modification and potential sclerosis, further thickness analysis of the cortical bone as detected in the medial to lateral plateau thickness ratio and trabecular bone analysis will provide further information on the mechanical loading pattern of the joint. To confirm the origin of the LMs in serum targeted lipidomics in the muscle are needed. This will provide further information on the mechanisms of skeletal muscle regeneration, and the ratio in which the LMs are translocated in the serum and give evidence of the musculoskeletal – cross communication occurring biochemically after muscle damage. The statistical analysis was conducted using one-way ANOVA, and further examination finding the relationship between multiple variables using either a MANOVA or multiple linear regression is needed to fully understand how all factors of muscle damage are communicating to affect the joint. Limiting the number of animals used is of high importance however, as this research continues increasing the sample size would increase the accuracy of the

results and may reveal correlations that are otherwise missed. A single bout of mild to moderate muscle damage caused by $BaCl_2$ was used in this study, further experimentation needs to be done in examining continuous muscle weakness and repetitive injury. This can be conducted by multiple time point injections to mimic the results of continuous wear and tear through time. Skeletally mature, young mice were used for this study in which the muscle regeneration process is not inhibited as in aging (Carosio et al., 2011). Further experiments using aged models are necessary to understand the mechanisms of joint damage on aged, diminished muscle regeneration.

Conclusion

This study serves as a novel launching point in understanding the systemic effects of muscle damage. It is shown that $BaCl_2$ effectively causes localized muscle damage and weakness that returns within 1 month after injury. The muscle damage elucidates an inflammatory, immune response to initiate muscle regeneration. During muscle regeneration there are elevated pro and anti-inflammatory LMs in the serum that are vital to the skeletal muscle regeneration process. Along with their healing aspects in muscle, these LMs also have a potential role in the regulation and maintenance of the subchondral bone. There are indications of alterations in the joint tissue, as seen in the subchondral bone and articular cartilage. The subchondral bone had an increased bone volume fraction which is indicative of joint damage and may lead to the onset progression of OA. Further studies need to be conducted to determine the full scope on the degree of joint degradation has occurred after muscle damage.

References

Albro, M.B., Bergholt, M.S., St-Pierre, J.P. *et al.* Raman spectroscopic imaging for quantification of depth-dependent and local heterogeneities in native and engineered cartilage. *npj Regen Med* **3**, 3 (2018). https://doi.org/10.1038/s41536-018-0042-7

Allen, D. L., Cleary, A. S., Speaker, K. J., Lindsay, S. F., Uyenishi, J., Reed, J. M., Madden, M. C., & Mehan, R. S. (2008). Myostatin, activin receptor IIb, and follistatin-like-3 gene expression are altered in adipose tissue and skeletal muscle of obese mice. *American Journal of Physiology-Endocrinology and Metabolism*, 294(5), E918–E927. https://doi.org/10.1152/ajpendo.00798.2007

Awad, K., Moore, L., Huang, J., Mo, C., Wang, Z., Brotto, L., & Brotto, M. (2022). PGE2 and WNT3a Promote Skeletal Muscle Regeneration after Barium Chloride Damage In-vitro. The FASEB Journal, 36.

Brandt, K. D. (2006). Yet more evidence that osteoarthritis is not a cartilage disease. *Annals of the Rheumatic Diseases*, *65*(10), 1261–1264. https://doi.org/10.1136/ard.2006.058347

Bielajew, B.J., Hu, J.C. & Athanasiou, K.A. Collagen: quantification, biomechanics and role of minor subtypes in cartilage. *Nat Rev Mater* **5**, 730–747 (2020). https://doi.org/10.1038/s41578-020-0213-1

Brotto, M., & Bonewald, L. (2015). Bone and muscle: Interactions beyond mechanical. *Bone*, *80*. https://doi.org/10.1016/j.bone.2015.02.010

Brotto, M., & Johnson, M. L. (2014). Endocrine Crosstalk Between Muscle and Bone. *Current Osteoporosis Reports*, *12*(2). https://doi.org/10.1007/s11914-014-0209-0

Carosio, S., Berardinelli, M. G., Aucello, M., & Musarò, A. (2011). Impact of ageing on muscle cell regeneration. Ageing research reviews, 10(1), 35–42. https://doi.org/10.1016/j.arr.2009.08.001

Chen, W., Chen, Y., Wu, R. *et al.* DHA alleviates diet-induced skeletal muscle fiber remodeling via FTO/m^{6}A/DDIT4/PGC1α signaling. *BMC Biol* 20, 39 (2022). https://doi.org/10.1186/s12915-022-01239-w

Dallas, S. L., Prideaux, M., & Bonewald, L. F. (2013). The Osteocyte: An Endocrine Cell … and More. *Endocrine Reviews*, *34*(5), 658–690. https://doi.org/10.1210/er.2012-1026

de Carvalho, S. C., Hindi, S. M., Kumar, A., & Marques, M. J. (2017). Effects of omega-3 on matrix metalloproteinase-9, myoblast transplantation and satellite cell activation in dystrophin-deficient muscle fibers. *Cell and tissue research*, *369*(3), 591–602. https://doi.org/10.1007/s00441-017-2640-x

Dehring KA, Smukler AR, Roessler BJ, Morris MD. Correlating Changes in Collagen Secondary Structure with Aging and Defective Type II Collagen by Raman Spectroscopy. *Applied Spectroscopy*. 2006;60(4):366-372. doi:10.1366/000370206776593582

Esmonde-White K. Raman Spectroscopy of Soft Musculoskeletal Tissues. *Applied Spectroscopy*. 2014;68(11):1203-1218. doi:10.1366/14-07592

Ferguson, E. J., Seigel, J. W., & McGlory, C. (2021). Omega-3 fatty acids and human skeletal muscle. *Current opinion in clinical nutrition and metabolic care*, *24*(2), 114–119. https://doi.org/10.1097/MCO.0000000000000723

Fernandes, T. L., Pedrinelli, A., & Hernandez, A. J. (2015). MUSCLE INJURY - PHYSIOPATHOLOGY, DIAGNOSIS, TREATMENT AND CLINICAL

PRESENTATION. Revista brasileira de ortopedia, 46(3), 247–255. https://doi.org/10.1016/S2255-4971(15)30190-7

Frontera, W. R., & Ochala, J. (2015). Skeletal muscle: a brief review of structure and function. Calcified tissue international, 96(3), 183–195. https://doi.org/10.1007/s00223-014-9915-y

Fu, M., , Tian, Y., , Zhang, T., , Zhan, Q., , Zhang, L., , & Wang, J., (2020). Comparative study of DHA-enriched phosphatidylcholine and EPA-enriched phosphatidylcholine on ameliorating high bone turnover *via* regulation of the osteogenesis-related Wnt/β-catenin pathway in ovariectomized mice. *Food & function*, *11*(11), 10094–10104. https://doi.org/10.1039/d0fo01563f

Gaifulina, R., Nunn, A. D., Draper, E. R., Strachan, R. K., Blake, N., Firth, S., ... & Dudhia, J. (2021). Intra-operative Raman spectroscopy and ex vivo Raman mapping for assessment of cartilage degradation. *Clinical Spectroscopy*, *3*, 100012.

Hardy, D., Besnard, A., Latil, M., Jouvion, G., Briand, D., Thépenier, C., Pascal, Q., Guguin, A., Gayraud-Morel, B., Cavaillon, J.-M., Tajbakhsh, S., Rocheteau, P., Chrétien, F., 2016. Comparative Study of Injury Models for Studying Muscle Regeneration in Mice. PLOS ONE 11, e0147198.. doi:10.1371/journal.pone.0147198

Ho, A. T. V., Palla, A. R., Blake, M. R., Yucel, N. D., Wang, Y. X., Magnusson, K. E. G., Holbrook, C. A., Kraft, P. E., Delp, S. L., & Blau, H. M. (2017). Prostaglandin E2 is essential for efficacious skeletal muscle stem-cell function, augmenting regeneration and strength. Proceedings of the National Academy of Sciences of the United States of America, 114(26), 6675–6684. https://doi.org/10.1073/pnas.1705420114

Holzer, L. A., Kraiger, M., Talakic, E., Fritz, G. A., Avian, A., Hofmeister, A., Leithner, A., & Holzer, G. (2020). Microstructural analysis of subchondral bone in knee

osteoarthritis. *Osteoporosis international : a journal established as result of cooperation between the European Foundation for Osteoporosis and the National Osteoporosis Foundation of the USA*, *31*(10), 2037–2045. https://doi.org/10.1007/s00198-020-05461-6

Järvinen, T. A., Järvinen, M., & Kalimo, H. (2014). Regeneration of injured skeletal muscle after the injury. *Muscles, ligaments and tendons journal*, *3*(4), 337–345.

Jia, H., Ma, X., Wei, Y., Tong, W., Tower, R.J., Chandra, A., Wang, L., Sun, Z., Yang, Z., Badar, F., Zhang, K., Tseng, W.-J., Kramer, I., Kneissel, M., Xia, Y., Liu, X.S., Wang, J.H.C., Han, L., Enomoto-Iwamoto, M. and Qin, L. (2018), Loading-Induced Reduction in Sclerostin as a Mechanism of Subchondral Bone Plate Sclerosis in Mouse Knee Joints During Late-Stage Osteoarthritis. Arthritis Rheumatol, 70: 230-241. https://doi.org/10.1002/art.40351

Jiang, W., Jin, Y., Zhang, S., Ding, Y., Huo, K., Yang, J., Zhao, L., Nian, B., Zhong, T. P., Lu, W., Zhang, H., Cao, X., Shah, K. M., Wang, N., Liu, M., & Luo, J. (2022). PGE2 activates EP4 in subchondral bone osteoclasts to regulate osteoarthritis. *Bone research*, *10*(1), 27. https://doi.org/10.1038/s41413-022-00201-4

Jung, H. W., Choi, J. H., Jo, T., Shin, H., & Suh, J. M. (2019). Systemic and Local Phenotypes of Barium Chloride Induced Skeletal Muscle Injury in Mice. Annals of geriatric medicine and research, 23(2), 83–89. https://doi.org/10.4235/agmr.19.0012

Kojouharov, H. V., Chen-Charpentier, B. M., Solis, F. J., Biguetti, C., & Brotto, M. (2021). A simple model of immune and muscle cell crosstalk during muscle regeneration. *Mathematical biosciences*, *333*, 108543. https://doi.org/10.1016/j.mbs.2021.108543

Kim, N., Kang, M. S., Nam, M., Kim, S. A., Hwang, G. S., & Kim, H. S. (2019). Eicosapentaenoic Acid (EPA) Modulates Glucose Metabolism by Targeting AMP-Activated Protein Kinase (AMPK) Pathway. *International journal of molecular sciences*, *20*(19), 4751. https://doi.org/10.3390/ijms20194751

Kurek, J. B., Bower, J. J., Romanella, M., Koentgen, F., Murphy, M., & Austin, L. (1997). The role of leukemia inhibitory factor in skeletal muscle regeneration. *Muscle & Nerve*, *20*(7), 815–822. https://doi.org/10.1002/(SICI)1097-4598(199707)20:7<815::AID-MUS5>3.0.CO;2-A

Lajeunesse, D., Massicotte, F., Pelletier, J. P., & Martel-Pelletier, J. (2003). Subchondral bone sclerosis in osteoarthritis: not just an innocent bystander. Modern rheumatology, 13(1), 7–14. https://doi.org/10.3109/s101650300001

Lee, M. H., Lee, J. H., Kim, W. J., Kim, S. H., Kim, S. Y., Kim, H. S., & Kim, T. J. (2022). Linoleic Acid Attenuates Denervation-Induced Skeletal Muscle Atrophy in Mice through Regulation of Reactive Oxygen Species-Dependent Signaling. *International journal of molecular sciences*, *23*(9), 4778. https://doi.org/10.3390/ijms23094778

Li, G., Yin, J., Gao, J., Cheng, T.S., Pavlos, N.J., Zhang, C., Zheng, M.H., 2013. Subchondral bone in osteoarthritis: insight into risk factors and microstructural changes. Arthritis Research & Therapy 15, 223.. doi:10.1186/ar4405

Lim, N. S., Hamed, Z., Yeow, C. H., Chan, C., & Huang, Z. (2011). Early detection of biomolecular changes in disrupted porcine cartilage using polarized Raman spectroscopy. *Journal of biomedical optics*, *16*(1), 017003. https://doi.org/10.1117/1.3528006

Liu, S. Z., Jemiolo, B., Lavin, K. M., Lester, B. E., Trappe, S. W., & Trappe, T. A. (2016). Prostaglandin E2/cyclooxygenase pathway in human skeletal muscle: influence of muscle fiber type and age. Journal of applied physiology (Bethesda, Md. : 1985), 120(5), 546–551. https://doi.org/10.1152/japplphysiol.00396.2015

Maffulli, N., Del Buono, A., Oliva, F., Giai Via, A., Frizziero, A., Barazzuol, M., Brancaccio, P., Freschi, M., Galletti, S., Lisitano, G., Melegati, G., Nanni, G., Pasta, G., Ramponi, C., Rizzo, D., Testa, V., & Valent, A. (2014). Muscle Injuries: A Brief Guide to Classification and Management. Translational medicine @ UniSa, 12, 14–18.

Maharaj, J. N., Cresswell, A. G., & Lichtwark, G. A. (2019). Tibialis anterior tendinous tissue plays a key role in energy absorption during human walking. *The Journal of experimental biology*, *222*(Pt 11), jeb191247. https://doi.org/10.1242/jeb.191247

Mandair, G. S., & Morris, M. D. (2015). Contributions of Raman spectroscopy to the understanding of bone strength. *BoneKEy reports*, *4*, 620. https://doi.org/10.1038/bonekey.2014.115

Manitta, L., Labrune, M., Olive, L., Fayolle, C., & Berteau, J. P. (2022). Subchondral bone alterations in a novel model of intermediate post traumatic osteoarthritis in mice. *Journal of Biomechanics*, 142, 111233-111233. https://doi.org/10.1016/j.jbiomech.2022.111233

Maria Plesia, Oliver A. Stevens, Gavin R. Lloyd, Catherine A. Kendall, Ian Coldicott, Aneurin J. Kennerley, Gaynor Miller, Pamela J. Shaw, Richard J. Mead, John C. C. Day, and James J. P. Alix *ACS Chemical Neuroscience* 2021 *12* (10), 1768-1776 DOI: 10.1021/acschemneuro.0c00794

McGlory, C., Calder, P. C., & Nunes, E. A. (2019). The Influence of Omega-3 Fatty Acids on Skeletal Muscle Protein Turnover in Health, Disuse, and Disease. *Frontiers in nutrition*, *6*, 144. https://doi.org/10.3389/fnut.2019.00144

Morris, M. D., & Mandair, G. S. (2011). Raman assessment of bone quality. *Clinical orthopaedics and related research*, *469*(8), 2160–2169. https://doi.org/10.1007/s11999-010-1692-y

Morton, A. B., Norton, C. E., Jacobsen, N. L., Fernando, C. A., Cornelison, D. D. W., & Segal, S. S. (2019). Barium chloride injures myofibers through calcium-induced proteolysis with fragmentation of motor nerves and microvessels. Skeletal muscle, 9(1), 27. https://doi.org/10.1186/s13395-019-0213-2

Ochi, E., & Tsuchiya, Y. (2018). Eicosapentaenoic Acid (EPA) and Docosahexaenoic Acid (DHA) in Muscle Damage and Function. *Nutrients*, *10*(5), 552. https://doi.org/10.3390/nu10050552

Pedersen, B. K. (2013a). Muscle as a Secretory Organ. In *Comprehensive Physiology* (pp. 1337–1362). Wiley. https://doi.org/10.1002/cphy.c120033

Pezzotti, G., Zhu, W., Terai, Y., Marin, E., Boschetto, F., Kawamoto, K., & Itaka, K. (2022). Raman spectroscopic insight into osteoarthritic cartilage regeneration by mRNA therapeutics encoding cartilage-anabolic transcription factor Runx1. *Materials today. Bio*, *13*, 100210. https://doi.org/10.1016/j.mtbio.2022.100210

Poulet, B., De Souza, R., Kent, A.V., Saxon, L., Barker, O., Wilson, A., Chang, Y.-M., Cake, M., Pitsillides, A.A., 2015. Intermittent applied mechanical loading induces subchondral bone thickening that may be intensified locally by contiguous articular cartilage lesions. Osteoarthritis and Cartilage 23, 940–948.. doi:10.1016/j.joca.2015.01.012

Rehan Youssef, A., Longino, D., Seerattan, R., Leonard, T., & Herzog, W. (2009). Muscle weakness causes joint degeneration in rabbits. *Osteoarthritis and Cartilage*, *17*(9), 1228–1235. https://doi.org/10.1016/j.joca.2009.03.017

Stani, C., Vaccari, L., Mitri, E., & Birarda, G. (2020). FTIR investigation of the secondary structure of type I collagen: New insight into the amide III band. Spectrochimica acta. Part A, Molecular and biomolecular spectroscopy, 229, 118006. https://doi.org/10.1016/j.saa.2019.118006

Siriguleng, S., Koike, T., Natsume, Y., Jiang, H., Mu, L., & Oshida, Y. (2021). Eicosapentaenoic acid enhances skeletal muscle hypertrophy without altering the protein anabolic signaling pathway. *Physiological research*, *70*(1), 55–65. https://doi.org/10.33549/physiolres.934534

Takahashi, Y., Sugano, N., Takao, M., Sakai, T., Nishii, T., & Pezzotti, G. (2014). Raman spectroscopy investigation of load-assisted microstructural alterations in human knee cartilage: Preliminary study into diagnostic potential for osteoarthritis. *Journal of the mechanical behavior of biomedical materials*, *31*, 77–85. https://doi.org/10.1016/j.jmbbm.2013.02.014

van de Velde, M. J., Engels, F., Henricks, P. A., & Nijkamp, F. P. (1994). 13-HODE inhibits the intracellular calcium increase of activated human polymorphonuclear cells. *Journal of leukocyte biology*, *56*(2), 200–202. https://doi.org/10.1002/jlb.56.2.200

Vidal, B.deC., & Mello, M. L. (2011). Collagen type I amide I band infrared spectroscopy. Micron (Oxford, England : 1993), 42(3), 283–289. https://doi.org/10.1016/j.micron.2010.09.010

Wang, Z., Bian, L., Mo, C., Kukula, M., Schug, K. A., & Brotto, M. (2017). Targeted quantification of lipid mediators in skeletal muscles using restricted access media-based trap-and-elute liquid chromatography-mass spectrometry. *Analytica Chimica Acta*, *984*. https://doi.org/10.1016/j.aca.2017.07.024

Wang, Y., Wluka, A.E. & Cicuttini, F.M. The determinants of change in tibial plateau bone area in osteoarthritic knees: a cohort study. *Arthritis Res Ther* **7**, R687 (2005). https://doi.org/10.1186/ar1726

Wu, G., Bazer, F. W., Burghardt, R. C., Johnson, G. A., Kim, S. W., Knabe, D. A., Li, P., Li, X., McKnight, J. R., Satterfield, M. C. (2011) Proline and hydroxyproline metabolism: implications for animal and human nutrition. *Amino Acids 40* (4), 1053– 1063, DOI: 10.1007/s00726-010-0715-z

Yu, D., Xu, J., Liu, F., Wang, X., Mao, Y., & Zhu, Z. (2016). Subchondral bone changes and the impacts on joint pain and articular cartilage degeneration in osteoarthritis. Clinical and experimental rheumatology, 34(5), 929–934.

Zhang, Z. M., Chen, S., & Liang, Y. Z. (2010). Baseline correction using adaptive iteratively reweighted penalized least squares. *The Analyst*, *135*(5), 1138–1146. https://doi.org/10.1039/b922045c

Zhu, J., Zhu, Y., Xiao, W., Hu, Y., & Li, Y. (2020). Instability and excessive mechanical loading mediate subchondral bone changes to induce osteoarthritis. *Annals of translational medicine*, *8*(6), 350. https://doi.org/10.21037/atm.2020.02.103

Supplementary Material

Raman Processing Python Code

Raman.py

://github.com/StatguyUser/BaselineRemoval/commit/6310a0bb142b26808db43943d4c445498a117313

```
from BaselineRemoval import BaselineRemoval
from RamanFilter import RamanFilter
import numpy as np
import sys
from matplotlib import pyplot as plt
from sklearn import preprocessing
from scipy import signal
from scipy.signal import find_peaks
import csv

#Intialize the file and name
filepath =  #insert file path
filename = #File name
ID = #Sample Identifier
signalMin = 400 # Minumum Cut off of X-signal
signalMax = 1800 # Maximum Cut off of X-signal
ta = RamanFilter(filepath, filename, ID, signalMin,signalMax )
polynomial_degree = 2    # only needed for Modpoly and IModPoly algorithm

#Call filtering of signal
baseObj = BaselineRemoval(ta.y)
ta.mPoly = baseObj.ModPoly(polynomial_degree)
ta.iPoly = baseObj.IModPoly(polynomial_degree)
ta.zhangFit = baseObj.ZhangFit()
ta.normFit = ((ta.zhangFit - np.min(ta.zhangFit)) / (np.max(ta.zhangFit) - np.min(ta.zhangFit)))
#ta.FilteredData= ta.normFit.tolist() #normalized data into list form

# save output to CSV file
np.savetxt(#Insert user file path m%s.csv' %(ID), [ta.x, ta.normFit], delimiter=',',fmt="%.6f")
#header= 'Raman Shift, Absourbance', comments="")x,y,z equal sized 1D arrays
```

```
#Ploting of all filters
ta.plot_original()
ta.plot_filtered()
ta.plot_zhang_fit()
ta.plot_norm_fit()


#Normalized data is shifted to left by mininum cut off - reshift data
ta.zeros = np.zeros(signalMin)
ta.zeroedNorm = np.concatenate((ta.zeros, ta.normFit), axis=-1)

#Adding Normalized plus dead signal
plt.plot(ta.zeroedNorm)
plt.title("with zeros in front")
plt.ylabel("Absorbance (a.u.)")
plt.ylim(0,1.25)
plt.xlabel("Raman Shift")
plt.show()


#Find the multiple peaks on the normalized array
peaks, _ = find_peaks(ta.zeroedNorm , height=0.1)#set height of 0.1 to ignore noise can be
adjusted
peaks_list=list(peaks)
#print(peaks_list)

#Find the promience of the each peak
promin = signal.peak_prominences(ta.zeroedNorm , peaks)[0]
promin_list = list(promin)
contur_height = ta.zeroedNorm[peaks] - promin


#Find the witdth of each peak
half_peak_res=signal.peak_widths(ta.zeroedNorm , peaks, rel_height=0.5)
half_width_list = list(half_peak_res[0])
full_peak_res=signal.peak_widths(ta.zeroedNorm , peaks, rel_height=1)
full_width_list = list(full_peak_res[0])

#the left and right starting points for each peak at baseline
left_full = list(full_peak_res[2])
right_full = list(full_peak_res[3])
```

```
#Plot Normalized signal with identified peaks with promenices and resolution
plt.plot(ta.zeroedNorm)
plt.title('Peaks - xline - half and full res')
plt.ylabel("Absorbance (a.u.)")
plt.xlabel("Raman Shift")
plt.plot(peaks, ta.zeroedNorm[peaks], "*")
plt.plot(np.zeros_like(ta.zeroedNorm) , "--", color="green")
plt.vlines(x=peaks, ymin=contur_height, ymax=ta.zeroedNorm[peaks])
plt.hlines(*half_peak_res[1:], color="C4")
plt.hlines(*full_peak_res[1:], color="C5")
plt.xlim(signalMin,signalMax)
plt.show()


#dictionarys of known peaks

Muscle = {"Proline, Glucose, Proteins": 920,
        "Proline, Hydorxyproline, proteins (a-helix)":936,
        "Hydoroxyproline, Proline, Valine, Protiens, Hydroxyapatite, Cartenoids":952,
        "Thymine, Uracil, Typtophan, Protieins": 984,
        "Phenylalanine (phenyl ring breathing mode), Proteins":990,
        "Phenylalanine (phenyl ring breathing mode), Proteins":1003,
        "Trypohan, proteins":1015,
        "Poline, protiens":1042,
        "Lipids, Phospholipids, Tyrptophan, Nucleic acids":1078,
        "Uracil, Nucleic Acids, protiens, Lipids":1102,
        "Trptophan, Valine, Protiens, Glucose, Lipids, Phospholipids":1124,
        "Tyrosine, Phenylalanine, Proteins": 1169,
        "Tyrosine, Phenylalanine, Hydroxyproline, Proteins": 1204,
        "Proteins, Amide III (β-sheet)":1242,
        "Proteins, Amide III(α - helix),Tyrosine, Tryptophan, Proline,Proteins, Fatty
Acids,Phospholipids, Lipids": 1272,
        "Proteins, Amide III (α-helix)": 1340,
        "Valine, Proline, Tryptophan Proteins, Phospholipids,Guanine": 1318,
        "Tryptophan, Valine, Proline, Proteins, Adenine, Guanine Nucleic acids": 1332,
        "Saccharide, Adenine, Thymine, Guanine": 1376,
        "Cholesterol, Phospholipids,Fatty acids, Triglycerides, Lipids, Proteins": 1435,
        "CH2 Deformation": 1450,
        "Proline, Tryptophan, Proteins, Deoxyribose, Cytosine, Guanine, Adenine, Nucleic acids":
1464,
        "Cytosine, Adenine, Guanine":1513,
        "Tryptophan, Proteins, Amide II":1552,
        "Proteins, Amide I(α - helix),Phospholipids, Lipids": 1665,
```

```
        "Phospholipids": 1750}

Bone ={"v4PO43": 550,
       "Proline": 830,
       "v1PO43": 957,
       "v1PO43": 960,
       "Phenyalanine": 1003,
       "v3PO43": 1035,
       "v3PO43": 1048,
       "Proteoglycan": 1060,
       "v1CO32": 1070,
       "v3PO43": 1076,
       "v(C-O-C)": 1176,
       "Tyrosine, hydroxyproline": 1204,
       "Amide III": 1242,
       "Amide III": 1272,
       "Lipid Band": 1300,
       "Amide III": 1340,
       "pentosidine": 1365,
       "proteoglycan": 1375,
       "CH2 Deformation": 1450,
       "Phenyalinine": 1609,
       "Amide I": 1660,
       "Amide I": 1690}

Cartilage = {"v1PO43": 957,
       "v1PO43": 960,
       "Phenyalanine": 1003,
       "v3PO43": 1035,
       "v3PO43": 1048,
       "Proteoglycan": 1060,
       "v1CO32": 1070,
       "v3PO43": 1076,
       "v(C-O-C)": 1176,
       "Tyrosine, hydroxyproline": 1204,
       "Amide III": 1242,
       "Amide III": 1272,
       "Lipid Band": 1300,
       "Amide III": 1340,
       "pentosidine": 1365,
       "proteoglycan": 1365,
       "CH2 Deformation": 1450,
       "Phenyalinine": 1609,
```

```
      "Amide I": 1650,
      "Amide I": 1690}

#Identify if signal contains known peaks
#return overlapping peaks

#protect Peak list
f_peaks=peaks_list

#error range in raman shifiting plus or minus 3 points
MinusPeaks = []
PlusPeaks=[]
PlusPeaks2= []
PlusPeaks3=[]
MinusPeaks2=[]
MinusPeaks3=[]
for i in range(len(f_peaks)):
   PlusPeaks.append(f_peaks[i] + 1)
   PlusPeaks2.append(f_peaks[i] + 2)
   PlusPeaks3.append(f_peaks[i] + 3)
   MinusPeaks.append(f_peaks[i] - 1)
   MinusPeaks2.append(f_peaks[i] - 2)
   MinusPeaks3.append(f_peaks[i] - 3)
#print(MinusPeaks3)
#print(MinusPeaks2)
#print(MinusPeaks)
#print(peaks_list)
#print(PlusPeaks)
#print(PlusPeaks2)
#print(PlusPeaks3)


#Compare peaks to known list
Peak_List = list(Muscle.values())
#creat output array of values
OutPeaks = []
OutDic={} #peak_name{[location, prom, full, half, area]}}
for key,value in Muscle.items():
   if value in peaks_list:
      o = value
      oo = key
      op= peaks_list.index(value)
      oprom = promin[op]
```

```
    op_full= full_width_list[op]
    op_half = half_width_list[op]
    op_left = int(left_full[op])
    op_right = int(right_full[op])
    op_area = np.trapz(ta.zeroedNorm[op_left : op_right])
    o_dict = {oo:[o, oprom,op_full, op_half, op_area] }
    o_dict = {oo: [o,op_area]}
    OutDic.update(o_dict)
    OutPeaks.append(o)
elif value in PlusPeaks:
    p = value
    p2= value - 1
    pp = key
    ppp = peaks_list.index(p2)
    pprom = promin[ppp]
    pp_full = full_width_list[ppp]
    pp_half = half_width_list[ppp]
    pp_left = int(left_full[ppp])
    pp_right = int(right_full[ppp])
    pp_area = np.trapz(ta.zeroedNorm[pp_left : pp_right])
    p_dict = {pp: [p, pprom, pp_full, pp_half, pp_area]}
    p_dict = {pp: [p, pp_area]}
    OutDic.update(p_dict)
    OutPeaks.append(p)
elif value in MinusPeaks:
    n = value
    n2= value + 1
    nn = key
    npp = peaks_list.index(n2)
    nprom = promin[npp]
    np_full = full_width_list[npp]
    np_half = half_width_list[npp]
    np_left = int(left_full[npp])
    np_right = int(right_full[npp])
    np_area = np.trapz(ta.zeroedNorm[np_left : np_right])
    n_dict = {nn: [n, nprom, np_full, np_half, np_area]}
    n_dict = {nn: [n,np_area]}
    OutDic.update(n_dict)
    OutPeaks.append(n)
elif value in PlusPeaks2:
    s = value
    s2= value-2
    ss = key
```

```
    sp = peaks_list.index(s2)
    sprom = promin[sp]
    sp_full = full_width_list[sp]
    sp_half = half_width_list[sp]
    sp_left = int(left_full[sp])
    sp_right = int(right_full[sp])
    sp_area = np.trapz(ta.zeroedNorm[sp_left : sp_right])
    s_dict = {ss: [s, sprom, sp_full, sp_half, sp_area]}
    s_dict = {ss: [s,sp_area]}
    OutDic.update(s_dict)
    OutPeaks.append(s)
elif value in MinusPeaks2:
    m = value
    m2= value + 2 # reverse the error signal
    mm = key
    mp = peaks_list.index(m2)
    mprom = promin[mp]
    mp_full = full_width_list[mp]
    mp_half = half_width_list[mp]
    mp_left = int(left_full[mp])
    mp_right = int(right_full[mp])
    mp_area = np.trapz(ta.zeroedNorm[mp_left : mp_right])
    m_dict = {mm: [m, mprom, mp_full, mp_half, mp_area]}
    m_dict = {mm: [m, mp_area]}
    OutDic.update(m_dict)
    OutPeaks.append(m)
elif value in PlusPeaks3:
    q = value
    q2= value -3  # reverse the error signal
    qq = key
    qp = peaks_list.index(q2)
    qprom = promin[qp]
    qp_full = full_width_list[qp]
    qp_half = half_width_list[qp]
    qp_left = int(left_full[qp])
    qp_right = int(right_full[qp])
    qp_area = np.trapz(ta.zeroedNorm[qp_left : qp_right])
    #q_dict = {qq: [q, qprom, qp_full, qp_half, qp_area]}
    q_dict = {qq: [q, qp_area]}
    OutDic.update(q_dict)
    OutPeaks.append(q)
elif value in MinusPeaks3:
    l = value
```

```
        l2= value +3 # reverse the error signal
        ll = key
        lp = peaks_list.index(l2)
        lprom = promin[lp]
        lp_full = full_width_list[lp]
        lp_half = half_width_list[lp]
        lp_left = int(left_full[lp])
        lp_right = int(right_full[lp])
        lp_area = np.trapz(ta.zeroedNorm[lp_left : lp_right])
        l_dict = {ll: [l, lprom, lp_full, lp_half, lp_area]}
        l_dict = {ll: [l, lp_area]}
        OutDic.update(l_dict)
        OutPeaks.append(l)

#Look at output dictionary
print(OutDic)

#Plot Overlaping Peaks
plt.plot(ta.zeroedNorm)
plt.title('Overlapping Peaks')
plt.ylabel("Absorbance (a.u.)")
plt.ylim(0,1.25)
plt.xlabel("Raman Shift")
for i in range(len(OutPeaks)):
    plt.plot(OutPeaks[i], ta.zeroedNorm[OutPeaks[i]], "*")
    plt.text(OutPeaks[i], (ta.zeroedNorm[OutPeaks[i]]* (1.5+.01)), OutPeaks[i], fontsize=8)
plt.xlim(signalMin,signalMax)
plt.show()


print ("finished")
```

RamanFilter.py

```
import numpy as np

from matplotlib import pyplot as plt


class RamanFilter:

    def __init__(self, filepath, filename, ID, signalMin, signalMax):

        fn = filepath + filename

        data_load = np.genfromtxt(fn, delimiter=",")
```

```
    Smin = signalMin
    Smax = signalMax
    self.name = ID
    self.x = data_load[Smin:Smax, 0]
    self.y = data_load[Smin:Smax, 1]
    self.mPoly = np.zeros(np.size(self.x))
    self.iPoly = np.zeros(np.size(self.x))
    self.zhangFit = np.zeros(np.size(self.x))

def plot_original(self):
    plt.title(self.name)
    plt.ylabel("Absorbance (a.u.)")
    plt.xlabel("Raman Shift")
    plt.plot(self.x, self.y)
    plt.show()

def plot_filtered(self):
    plt.title(self.name)
    plt.ylabel("Absorbance (a.u.)")
    plt.xlabel("Raman Shift")
    plt.plot(self.x, self.mPoly, label="mPoly")
    plt.plot(self.x, self.iPoly, label="iPoly")
    plt.plot(self.x, self.zhangFit, label="Zhang Fit")
    plt.legend()
    plt.show()

def plot_zhang_fit(self):
    plt.title('Zhang Fit of ' + self.name)
```

```
    plt.ylabel("Absorbance (a.u.)")
    plt.xlabel("Raman Shift")
    plt.plot(self.x, self.zhangFit)
    plt.show()

def plot_norm_fit(self):
    plt.title(self.name)
    plt.ylabel("Absorbance (a.u.)")
    plt.xlabel("Raman Shift")
    plt.plot(self.x, self.normFit)
    plt.show()
```

CHAPTER 5

Conclusion

Musculoskeletal disorders (MSkD) are broad enveloping term that covers a range of debilitating disorders, such as Osteoarthritis, Osteopenia, Sarcopenia, Tendonitis, Myopathies, and muscle weakness (National Academics of Science, 2020). Osteoarthritis (OA) is one of the leading MsKDs, and the most common of joint disorders (Glyn-Jones et al., 2015; Kontzias, 2020; National Academies of Sciences, 2020). OA is classically described as a chronic joint arthropathy that is characterized in disruption of the articular cartilage and in the subchondral bone (Glyn-Jones et al., 2015; Poulet et al., 2014; Jia et al., 2018; Holzer et al 2020; Li et al., 2013).

Mouse models are an efficient way to model the mechanisms of disease state of OA. In Chapter Two, we found that from 2019 to December 2022 there were 7 different types of methodologies to induce OA. Those approaches were both surgical and non-surgical. The most common method was surgical induction via destabilization of the medial meniscus (DMM). This surgical approach closely resembles the onset and progression of post-traumatic OA (PTOA). This model increases the mechanical stress on the posterior femur and central tibia (Leahy et al., 2015; Shu et al., 2016; Haase et al. 2019; Wang et al., 2014; Das Neves Borges et al., 2017). In the non-surgical methodologies, load-induced OA was the most common. Load induced OA is a non-invasive methodology that closely resembles the manifestation post-traumatic OA. (Wegner et al., 2019). Both surgical and load induced methodologies the on set of OA begins 1-2 weeks post induction (Tsubosaka et al., 2020; Haase et al., 2019; Tsuchiya et al., 2020, Wegner et al., 2019). Each of the models have their advantages and disadvantages in understanding the mechanisms of OA. All but one model, the aging model, of the currently used methodologies in inducing OA demonstrate induction of OA through direct joint and articular cartilage injury. This is a gap in the current literature as, OA is a multifactorial disease, with risk factors including age,

obesity, history of injury, and genetic disposition. Each of these mechanisms of plays a vital role in the onset and progression of disease. Without modeling other mechanisms of disease induction the full understanding of the pathophysiology will not be complete and the development of new therapies and treatment protocols could be attenuated.

In relation to developing new animal models, the need for development of new biomarkers in OA research is high as the incidence of disease continues to rise (Glyn-Jones et al., 2015). In Chapter 3, we systematically searched the literature on the RNA sequencing of synovial tissues in patients with OA. The synovium is a pivotal joint tissue in maintaining the health of the joint. It was found that there was 8 differently expressed genes (DEGs). These genes were: MMP13, MMP1, MMP2, APOD, IL6, TNFAIP6, FCER1G, and IGF1. Each of these correspond with the inflammatory pathway and the regulation of the extracellular matrix. Two of the DEGs were shown to overlap in 4 out of the 5 included studies, MMP13 and IL6. MMP13 is a member of the Matrix Metallopeptidase family. MMP13 when it becomes a mature protease cleaves type II collagen (Garnero 2007; Salerno et al. 2020; O'Leary et al. 2016). This degradation of collagen is a hallmark of OA development.. Interleukin-6 (IL6) is a pro-inflammatory cytokine, which has been shown to disrupt the extracellular matrix and induces MMP13 (Wiegertjes et al. 2020; Laavola et al 2018). These 8 DEGs, and especially the MMP13 and IL6, are prime candidates for molecular targets in understanding the mechanisms of disease. In future research, IL6 and MMP13 will be analyzed in their potential role in in joint degeneration in response to muscle damage.

Muscle weakness and atrophy has been characterized to accompany the manifestation and progression of OA, due to low physical activity and disuse (Brandt, 2006). However, we showed that skeletal muscle damage caused by a single intra-muscular injection of 1.2% Barium

Chloride ($BaCl_2$) had alterations in the articulating cartilage and in the cortical shell of the subchondral bone.

The muscle damage was confirmed through histological cross sections that was consistent with previous findings (Hardy et al., 2016; Jung et al., 2019). Muscle weakness and regeneration of strength was confirmed by a significant decrease in all limb and hind limb grip strength after muscle injury that time dependently rose. The physical activity assessment from the actimeter showed that there were no significant changes in the distance traveled, area measured, or force produce. This is indicative that the muscle injury was not a severe injury, in which the animal was not able to use the limb. In the future, locomotor and pain assessments can be done to assess the gait and loading changes occurring on the hind limb. The alterations in the joint tissue measured by the bone volume fraction are consistent with previous finding in which there was instability in the knee joint (Wang et al., 2005; Poulet et al., 2014; Jia et al; Holzer et al 2020; Li et al., 2013). In future studies, the trabecular bone and analyzation of the difference between the medial and lateral tibial plateau thickness will show the complete pattern of load distribution of the joint.

The alterations in the joint tissue may not seem to be a long time, as the manifestation of OA in humans after injury such as an ACL takes approximately 5 years (Cinque et al., 2017). In relation one day for a mouse is the equivalent to about 176 days for a human (Dutta et al., 2016). Our experimental time points of 4-Day, 7-Day, 1-Month was equivalent to ~2 years, . ~3.4 years, and ~14.5 respectively in humans.

Overall, this novel study on analyzing the physical morphological, biochemical adaptations on the joint tissue, showed that a single bout of skeletal muscle damage can be a primary causation to the alterations of the joint and have potential onset of OA. This research

marks a launching point in fully understanding the mechanisms in which muscle damage effects the entirety of the joint. Future research in identifying the molecular signaling pathway, will provide an expanded approach to understanding the musculoskeletal cross-communication. Expanding this research will provide molecular targets to develop new therapies. Transgenic mice will allow for precise analyzation of the pathophysiology of disease, both in muscle damage and in OA.

References

Brandt, K. D. (2006). Yet more evidence that osteoarthritis is not a cartilage disease. *Annals of the Rheumatic Diseases*, *65*(10), 1261–1264. https://doi.org/10.1136/ard.2006.058347

Dutta, S., & Sengupta, P. (2016). Men and mice: Relating their ages. Life sciences, 152, 244–248. https://doi.org/10.1016/j.lfs.2015.10.025

Das Neves Borges, P., Vincent, T. L., & Marenzana, M. (2017). Automated assessment of bone changes in cross-sectional micro-CT studies of murine experimental osteoarthritis. *PLoS ONE,* 12(3), 1–22. http://10.0.5.91/journal.pone.0174294

Cinque, M. E., Dornan, G. J., Chahla, J., Moatshe, G., & LaPrade, R. F. (2018). High Rates of Osteoarthritis Develop After Anterior Cruciate Ligament Surgery: An Analysis of 4108 Patients. *The American journal of sports medicine*, *46*(8), 2011–2019. https://doi.org/10.1177/0363546517730072

Garnero, Patrick. 2007. "Chapter 8 - Biochemical Markers of Osteoarthritis." In Osteoarthritis, edited by Leena Sharma and Francis Berenbaum, 113–30. Philadelphia: Mosby. https://www.sciencedirect.com/science/article/pii/B9780323039291500136.

Glyn-Jones, S., Palmer, A. J. R., Agricola, R., Price, A. J., Vincent, T. L., Weinans, H., & Carr, A. J. (2015). Osteoarthritis. *The Lancet,* 386(9991), 376–387. DOI: 10.1016/S0140-6736(14)60802-3

National Academies of Sciences, Engineering, and Medicine; Health and Medicine Division; Board on Health Care Services; Committee on Identifying Disabling Medical Conditions Likely to Improve with Treatment. Selected Health Conditions and Likelihood of Improvement with Treatment. Washington (DC): National Academies Press (US); 2020

Apr 21. 5, Musculoskeletal Disorders. Available from: https://www.ncbi.nlm.nih.gov/books/NBK559512/

Haase, T., Sunkara, V., Kohl, B., Meier, C., Bußmann, P., Becker, J., Jagielski, M., von Kleist, M., & Ertel, W. (2019). Discerning the spatio-temporal disease patterns of surgically induced OA mouse models. *PLoS ONE*, 14(4), 1–19. http://10.0.5.91/journal.pone.0213734

Holzer, L. A., Kraiger, M., Talakic, E., Fritz, G. A., Avian, A., Hofmeister, A., Leithner, A., & Holzer, G. (2020). Microstructural analysis of subchondral bone in knee osteoarthritis. *Osteoporosis international : a journal established as result of cooperation between the European Foundation for Osteoporosis and the National Osteoporosis Foundation of the USA*, *31*(10), 2037–2045. https://doi.org/10.1007/s00198-020-05461-6

Jia, H., Ma, X., Wei, Y., Tong, W., Tower, R.J., Chandra, A., Wang, L., Sun, Z., Yang, Z., Badar, F., Zhang, K., Tseng, W.-J., Kramer, I., Kneissel, M., Xia, Y., Liu, X.S., Wang, J.H.C., Han, L., Enomoto-Iwamoto, M. and Qin, L. (2018), Loading-Induced Reduction in Sclerostin as a Mechanism of Subchondral Bone Plate Sclerosis in Mouse Knee Joints During Late-Stage Osteoarthritis. Arthritis Rheumatol, 70: 230-241. https://doi.org/10.1002/art.40351

Laavola, M., Leppänen, T., Hämäläinen, M., Vuolteenaho, K., Moilanen, T., Nieminen, R., Moilanen, E., 2018. IL-6 in Osteoarthritis: Effects of Pine Stilbenoids. Molecules 24, 109. doi:10.3390/molecules24010109

Li, G., Yin, J., Gao, J., Cheng, T.S., Pavlos, N.J., Zhang, C., Zheng, M.H., 2013. Subchondral bone in osteoarthritis: insight into risk factors and microstructural changes. Arthritis Research & Therapy 15, 223.. doi:10.1186/ar4405

Poulet, B., De Souza, R., Kent, A.V., Saxon, L., Barker, O., Wilson, A., Chang, Y.-M., Cake, M., Pitsillides, A.A., 2015. Intermittent applied mechanical loading induces subchondral bone thickening that may be intensified locally by contiguous articular cartilage lesions. Osteoarthritis and Cartilage 23, 940–948.. doi:10.1016/j.joca.2015.01.012

Salerno, Anna, Kyla Brady, Margot Rikkers, Chao Li, Eva Caamaño-Gutierrez, Francesco Falciani, Ashley W. Blom, Michael R. Whitehouse, and Anthony P. Hollander. 2020. "MMP13 and TIMP1 Are Functional Markers for Two Different Potential Modes of Action by Mesenchymal Stem/Stromal Cells When Treating Osteoarthritis." STEM CELLS, July. https://doi.org/10.1002/stem.3255.

Wang, Q., Pan, X., Wong, H. H., Wagner, C. A., Lahey, L. J., Robinson, W. H., & Sokolove, J. (2014). Oral and topical boswellic acid attenuates mouse osteoarthritis. *Osteoarthritis & Cartilage*, 22(1), 128–132. https://doi.org/10.1016/j.joca.2013.10.012

Wang, Y., Wluka, A.E. & Cicuttini, F.M. The determinants of change in tibial plateau bone area in osteoarthritic knees: a cohort study. *Arthritis Res Ther* **7**, R687 (2005). https://doi.org/10.1186/ar1726

Wegner, A. M., Campos, N. R., Robbins, M. A., Haddad, A. F., Cunningham, H. C., Yik, J. H. N., Christiansen, B. A., & Haudenschild, D. R. (2019). Acute Changes in NADPH Oxidase 4 in Early Post-Traumatic Osteoarthritis. *Journal of Orthopaedic Research* : Official Publication of the Orthopaedic Research Society, 37(11), 2429–2436. https://doi.org/10.1002/jor.24417

Wiegertjes, R., Van De Loo, F.A.J., Blaney Davidson, E.N., 2020. A roadmap to target interleukin-6 in osteoarthritis. Rheumatology 59, 2681–2694. doi:10.1093/rheumatology/keaa248